Passive Microwave Remote Sensing of Extreme Weather Events Using NOAA-18 AMSUA and MHS

Sid-Ahmed Boukabara, *Senior Member, IEEE*, Fuzhong Weng, and Quanhua Liu

***Abstract*—The ability to provide temperature and water-vapor soundings under extreme weather conditions, such as hurricanes, could extend the coverage of space-based measurements to critical areas and provide information that could enhance outcomes of numerical weather prediction (NWP) models and other storm-track forecasting models, which, in turn, could have vital societal benefits. An NWP-independent 1D-VAR system has been developed to carry out the simultaneous restitutions of atmospheric constituents and surface parameters in all weather conditions. This consistent treatment of all components that have an impact on the measurements allows an optimal information-content extraction. This study focuses on the data from the NOAA-18 satellite (AMSUA and MHS sounders). The retrieval of the precipitating and nonprecipitating cloud parameters is done in a profile form, taking advantage of the natural correlations that do exist between the different parameters and across the vertical layers. Stability and the problem's ill-posed nature are the two classical issues facing this type of retrieval. The use of empirically orthogonal-function decomposition leads to a dramatic stabilization of the problem. The main goal of this inversion system is to be able to retrieve independently, with a high-enough accuracy and under all conditions, the temperature and water-vapor profiles, which are still the two main prognostic variables in numerical weather forecast models. Validation of these parameters in different conditions is undertaken in this paper by comparing the case-by-case retrievals with GPS-dropsondes data and NWP analyses in and around a hurricane. High temporal and spatial variabilities of the atmosphere are shown to present a challenge to any attempt to validate the microwave remote-sensing retrievals in meteorologically active areas.**

***Index Terms*—Atmospheric sounding, data assimilation, dropsonde, hurricane, microwave remote sensing, retrieval algorithm.**

I. Introduction

PASSIVE microwave data measured in meteorologically active areas carry a wealth of information on the hydrometeors as well as on the temperature and water-vapor profiles. The assimilation of these space-based measurements, in either geophysical or radiometric form, could help the numerical weather prediction (NWP) models in the analysis and forecast stages by giving information about actual cloud and precipitation, thus reducing the spin-up problem that usually impacts the beginning of the forecast period [1]. The effect of the hydrometeors on the brightness temperatures measured by the microwave sensors may be negligible, significant, or something in between depending on the spectral region considered and on the type and intensity of the precipitation, making these millimeter-wave sensors an ideal tool to probe the active areas. This effect also depends, in certain cases, on the thermodynamic temperature as this changes the dielectric properties and, therefore, the absorption of the water, and on the atmospheric water vapor, above and within the active area, as this has a screening effect on the sensitivity to cloudy layers, all of which advocate for having a consistent treatment of the atmospheric profiles of temperature, water vapor, and hydrometeors. For this purpose, a physical retrieval algorithm has been developed based on a radiance assimilation-type technique to invert simultaneously the vertical profiles of temperature, water vapor, nonprecipitating cloud, and liquid and frozen precipitating hydrometeor parameters. The surface boundary layer is also treated dynamically by including the surface-emissivity spectrum and the skin temperature as part of the control-parameter vector. Optionally, the inversion of surface pressure could also be triggered under certain conditions, otherwise obtained from the background (fixed value). The information content in the radiances is however limited. This is alleviated by performing the retrieval in a mathematically reduced space which stabilizes the retrieval significantly. However, stability of the retrieval does not eliminate the null space: existence of multitude solutions that fit equally well the radiances. In other words, including the hydrometeors in the retrieved state vector increases the number of degrees of freedom in the solution-finding process. It is important to note that these degrees of freedom are also due to the limited number of channels available. Adding hypothetical channels would theoretically put additional constraints on the solution finding and reduce these degrees of freedom.

This null space is the main reason why the stated goal of this study is primarily the sounding of temperature and humidity and, to a lesser degree, the surface sensing under extreme weather events. The cloud and precipitating parameters are part of the retrieval process mainly to absorb the effects they have on the raw measurements.

The microwave sensors AMSU and MHS onboard NOAA-18, which contain a combination of semiwindow and sounding channels, will be used to test this retrieval algorithm.

Manuscript received June 1, 2006; revised February 8, 2007. The views expressed here are those of the authors and do not necessarily represent those of the National Oceanic and Atmospheric Administration.

S.-A. Boukabara is with the I.M. Systems Group, Inc. at NOAA/NESDIS/STAR, Camp Springs, MD 20746 USA (e-mail: Sid.Boukabara@noaa.gov).

F. Weng is with NOAA/NESDIS/STAR, Camp Springs, MD 20746 USA (e-mail: Fuzhong.Weng@noaa.gov).

Q. Liu is with QSS Group Inc. at NOAA/NESDIS/STAR, Camp Springs, MD 20746 USA (e-mail: Quanhua.Liu@noaa.gov).

Color versions of one or more of the figures in this paper are available online at http://ieeexplore.ieee.org

Digital Object Identifier 10.1109/TGRS.2007.898263

Note that the approach will sometimes be purposefully labeled assimilation and sometimes retrieval across the remainder of this paper. Assimilation of radiances amounts indeed to a retrieval, the retrieved parameters being the control parameters. The difference resides in the reliance on an existing analysis used as first guess and background to which the retrievals are constrained (or assimilated). But, it is important to state at this stage that no NWP information is used in this system (forecast or analysis). As will be described later, the background constraints will be built offline based on climatology. On the radiance level, all channels are used simultaneously in order to obtain a retrieval that satisfies all measurements together. This study should be viewed as an attempt to treat the whole geophysical state vector, including hydrometeors in a consistent fashion, but relying on the radiometric signal only, as we do not use the cloud/convective schemes either to generate hydrometeors from the temperature and the water vapor as other studies chose to do [5], [9], [27]. Nonprecipitating cloud and hydrometeors are thus treated from a pure radiometric-signal stand, just like the water vapor, temperature, emissivity, and skin temperature.

The next section reviews the previous studies that dealt with assimilating rain-impacted microwave measurements either within an NWP context or not, followed by Section III describing the retrieval system used in this paper. The latter also briefly describes the different components used within the 1D-VAR system, including the forward radiative operator. Section IV focuses on describing the instrumental configuration, while Section V takes a look at the expected performances in a simulation setting. Section VI deals with describing the real data that we will be using, including the GPS-dropsondes, and lays out the validation results.

II. Review of Rainy Data Assimilation and Retrieval

Microwave-based assimilation of radiance measurements is not new; NWP centers have routinely or experimentally assimilated the clear-sky radiometric data as well as the microwave-retrieved products and have more recently directly assimilated the radiances measured in cloudy and precipitating conditions [5], [9], [30].

Microwave measurements have also been used extensively for the retrieval of cloud, rain, and other precipitating parameters, either with relatively simple regression-based algorithms or with more physically based algorithms, similar to those used in NWP assimilation. Numerous sensors have been used for measuring cloud and precipitation: SSM/I, TRMM/TMI, AMSU/MHS, and AMSR-E are among them [13], [17], [48]. Improvements have recently been made in this field of assimilating the cloud- and rain-impacted microwave radiances into NWP models as well as in the microwave remote sensing of cloud and hydrometeor parameters. These two problems are, in fact, similar in nature. The former (NWP assimilation) attempts to fit the impacted radiances by adjusting the temperature and water-vapor profiles and, along the way, generates the cloud/hydrometeor parameters (usually, by incorporating the cloud and convective schemes). The latter (hydrometeors retrieval) is based also on finding the hydrometeors (or integrated amount) that fit the radiances either through an Look-Up-Table (LUT) search or through a variational technique and, along the way, need to account, somehow, for the temperature and water-vapor profiles. The physical inversion approach was found to be superior in retrieving quantities (such as rainfall rate) using the regression-based algorithms. One obvious reason is that a physical retrieval can adapt dynamically to the particular circumstance and is more likely to distinguish the precipitation signal from the water vapor and temperature signals. We exclusively focus on the physical approaches in this review.

A. *Classification via Handling the Ill-Posed Nature*

The inversion of cloudy/rainy radiances into the geophysical space is a notoriously ill-posed problem. Several physical approaches have been tried in the past to add external constraints and, therefore, stabilize the problem. Some approaches are based on precomputation of hydrometeor profiles and their corresponding radiances. The retrieval, thus, becomes a residual minimization procedure which aims at finding the closest precomputed profile to match the measurements [17], [31], [44]. Others rely on the NWP forecast outputs and associated cloud and convective schemes to constrain the temperature and water vapor as well as their relationship to the cloud and hydrometeor parameters [5], [9], [26], [27], [35]. As mentioned earlier, the present study employs the empirically orthogonal-function (EOF) decomposition technique to all vertical profiles, including the hydrometeors as well as to the surface emissivity vector, in order to constrain the inversion problem. The use of background covariances, which are computed offline and independently from the NWP forecast data, constitutes an additional constraint to the problem, in addition to introducing physical consistency between the retrieved parameters.

B. *Bayesian Approach*

Tassa *et al.* [44] developed a Bayesian algorithm to retrieve surface precipitation and cloud profiles over the ocean. The training is done using a combination of outputs from a mesoscale microphysical model and a 3-D radiative transfer model (RTM). This method is similar to that adopted by Evans *et al.* [11], Kummerow *et al.* [17], and Marzano *et al.* [28]. In these algorithms, the retrieval is done by selecting, among the precomputed profiles, those that minimize the residuals with the measurements at hand. This strongly depends on the cloud/radiation database and does not account for the local variabilities of temperatures, water-vapor profiles, and surface emissivity that could equally impact the brightness temperatures. This method typically applies to the cloudy/rainy conditions. The clear-sky case is screened out in the preprocessing stage. Preclassification of precipitating events based on the nature (stratiform/convective) or intensity (moderate/intense) is usually performed. In [45], the important parameters that do impact the brightness temperatures, but are not part of the searched parameters, are used to generate a sensitivity matrix which is used as an upper threshold limit to the residual minimization process. These factors include size distribution, density, shape, and phase for the hydrometeors. This matrix could also be used in variational analyses but was not in that study. Di Michele *et al.* [31] developed a Bayesian retrieval algorithm named Bayesian algorithm for microwave precipitation retrieval (BAMPR) that they compared to the Goddard profiling (GPROF) algorithm. Despite the similar approaches between the retrieval approaches, they found that their results differ, and those differences were attributed mainly to the training datasets and the cloud classification.

C. 1D-VAR Approach

Eyre [12] used a variational technique (labeled equivalently estimation-theory solution) for atmospheric sounding which he applied to the microwave and infrared data from TIROS Operational Vertical Sounder (TOVS). Besides temperature and moisture, cloud amount and top pressure were also retrieved. Surface pressure, temperature, and emissivity were also allowed to vary. A damping term was introduced in the solution for certain parameters to stabilize the retrieval process after an oscillatory behavior was noticed. This consisted of a diagonal matrix with unity values except for those parameters causing the instability, amounting to an effective reduction of their variances. Eyre [12] studied the effect of assuming a single layer cloud model by simulating the mixed clouds. He found that the system was able to find an effective cloud amount and vertical location to compensate for the mixed cloud nature. It is interesting to highlight that he reported also that the effects of the effective cloud-parameter retrieval had little impact on the temperature and humidity profiles.

The standard use of 1D-VAR algorithms for the inversion of microwave data relies on using a background covariance matrix. This was shown to have limitations in the case of cloud and rain, as their variances will inevitably be large which would amount to an absence of constraint [37], [38]. In this latter study, a physical retrieval of moisture, cloud, wind speed, and rain was applied to SSM/I, and a spatial smoothing was adopted, attributing the horizontal variability exclusively to cloud structures.

In their 1996 study, Phalippou *et al.* introduced a 1D-VAR algorithm for the clear and cloudy skies for an SSM/I configuration and highlighted its potential for the NWP. It later became operational at ECMWF. The integrated amount of cloud liquid was made to vary as a scaling factor for the retained vertical structure (the output of the ECMWF cloud scheme was assumed). This approach cannot easily be extended to sounding configurations as the cloud structure severely alters the vertical weighting functions [21]. Moreover, the absorption of the cloud is also dependent, through the dielectric constant, on the temperature of the cloudy layer [50] which places some importance on the location of the cloud within the vertical temperature profile. An error in the temperature location is likely to translate into an error in the resulting liquid total amount. Chevallier *et al.* [7] demonstrated the proof of concept of a 1D-VAR algorithm that could be used to assimilate clouds data. A fast RTM was developed along with its adjoint operator. It was applied to the advanced TOVS data. Deblonde and English [8] also used a variational algorithm for the cloudy but nonprecipitating conditions, similar to that of [36], except that an alternative method was tested where the total-water-content profile was retrieved and, then, split into humidity and liquid using an empirical function. A higher rate of divergence was reported using this approach particularly in the clear-sky cases, but improved temperature retrieval performances were found using this method in cloudy skies.

Liu and Weng [21] more recently proposed a multistep variational algorithm that retrieved temperature, moisture, and cloud profiles in all-weather conditions. NCEP forecasts were used as background, and regression-based algorithms were used to produce the first guess for temperature and humidity profiles. Surface wind and pressure were also taken from the NCEP-forecast data. The integrated amount of cloud liquid was found to be consistent with the original value but that the profile presented differences due to the limited information content. To constrain the problem and make the retrieval more stable, hydrometeor profiles were modeled in an oversimplified fashion. The present study could be viewed as an upgrade to the study of Liu and Weng where the stability and information-content issues are handled through the EOF decomposition which also removed the need to have a multistep approach.

D. 1D-VAR + Cloud Models Approach

Cloud models have started recently to become part of the 1D-VAR schemes to force consistency between the temperature and humidity profiles on one hand and the cloud and other hydrometeor profiles on the other hand. Direct measurements of brightness temperatures in rainy conditions started being assimilated, first, at ECMWF [5] where low-frequency SSM/I channels were assimilated and, then, experimentally at MSC [9]. The first step in these two stage approach (1D-VAR + 4DVAR) consists of a 1D-VAR algorithm that incorporates moist physical schemes in its forward operator, which computes the hydrometeor profiles (cloud, ice, rain, and snow) from the profiles of temperature and water vapor.

Moreau *et al.* [35] developed a 1D-VAR algorithm to retrieve the rain profiles with ECMWF model outputs used to produce the first guess for temperature and humidity and a cloud/convective scheme used to relate them to hydrometeors. However, frozen hydrometeors were excluded in their experiment which was mitigated by the choice of low-frequency channels only.

Moreau *et al.* [34] compared the performances of two 1D-VAR-based retrievals of temperature and humidity profiles from the passive TRMM and SSM/I data measured in rainy areas. The first uses classically retrieved rainfall rate as input, while the second uses directly the brightness temperatures. Both use, besides an RTM, simplified convective and large-scale condensation parameterization. They found that problems with the convergence arise when background precipitation is generated through convection and not by large-scale processes.

Bauer *et al.* [3] studied the performances of the cloud retrieval using the European Global Precipitation Mission configuration. They used the ECMWF short-term forecast profile of temperature and humidity for the initialization of the first guess. The hydrometeor first guess and background combines the temperature and humidity profiles with cloud and convective model schemes, following a similar approach implemented in [35]. In their study, surface emissivity and temperature were fixed to climatologic values and not part of the control vector. The temperature and water vapor were not part of the control vector either, as the purpose was to assess the accuracy of hydrometeor retrieval only. For this reason, the forward operator consisted of an RTM only (no convective or cloud scheme). Deblonde *et al.* [9] incorporated the ECMWF approach into the Canadian 1D-VAR assimilation system of the SSM/I retrieved rainfall rates or brightness temperatures. The resulting integrated water-vapor amount is assimilated in a 4DVAR assimilation scheme.

E. On the Use of Cloud and Convective Schemes in 1D-VAR

For it to work in a 1D-VAR context, the cloud and convective schemes employed need to be simplified and made less nonlinear which raises the question of their accuracy. Their adjoint model needs also to be developed and incorporated. This can be computed analytically (usually, for the simplified schemes) or by finite difference (usually, for the full moist physical schemes). The RTM would need to be coupled with the cloud schemes, and therefore, their uncertainties need to be accounted for. Deblonde *et al.* [9] questioned the usefulness of using a deep-convection scheme for the assimilation of cloudy/rainy radiances because of its high nonlinearity. The equivalent error was found to have a very large spread in cases where deep convection dominated. The inputs also need to be simplified as cloud models do normally depend also on time trends of radiation and vertical diffusion produced by the dynamical and other physical processes. In the same study, it was highlighted that using shallow convective scheme to produce cloud water content in the 1D-VAR actually degraded the comparison with the algorithm of Weng and Grody [46]. It was further shown that the deep convective scheme deteriorated the fit between the modeled and observed brightness temperatures, which shows that the cloud model schemes are far from being accurate, and their corresponding errors need to be accounted for in the 1D-VAR assimilation when used, along with the RTM errors. Contrary to RTMs, cloud models are very different and produce nonsimilar results in most cases. If these differences and impacts of linearization and simplifications are accounted for, the resulting errors that a 1D-VAR must use might amount to not constraining the retrieval. Moreover, cloud schemes have been documented to be sometimes locally biased, in need of tuning, and are by no means accurate in their relationship between the temperature (T) and humidity (Q) profiles on one hand and the cloud (C) and hydrometeor (H) profiles on the other. Their use carries a set of uncertainties that would need to be accounted for in the error covariance matrix, which would defeat, at least partially, the purpose of using them as a means to constraint the retrieval.

III. Retrieval/Assimilation System

A. Suggested Approach

In this paper, we have adopted an approach that relies exclusively on the direct-impact signatures of hydrometeors on the brightness temperatures. The natural correlations between the cloud and hydrometeor parameters are included in the system, through the development of a covariance matrix that puts constraints on the independence of these parameters, between themselves across the layers as well as between the parameters. Separate retrievals treating parameters independently cannot, for obvious reasons, ensure that these retrieved parameters will be consistent, all at once, with the measured radiances [37], [38]. For this reason, in the approach adopted, all channels, including window and sounding channels, are used simultaneously in order to retrieve all parameters together. The use of sounding channels was shown to present many advantages in precipitation probing, including their lesser sensitivity to surface emittance and their ability to slice the cloud profile vertically [3].

The effects of clouds could potentially improve the temperature retrieval of the cloudy layer rather than degrade it, due to the increased absorption in that layer and, therefore, increased sensitivity. Eyre [12] argues that retrievals that remove the effects of clouds in preprocessing stages only degrade the retrievals. This all-channel–all-parameter approach allows an optimal extraction of information from the measurements. It is also beneficial to use all channels together with sensitivity to a wider range of precipitation amount [1] rather than a selective channel set. The retrieval of cloud and hydrometeors in a profile form presents some nice features, including avoiding in carrying the cloud top and thickness in the state vector which usually presents some instability, when these values cross the vertical-level boundaries. It can also provide information about the multilayer nature of the cloud. Frozen and liquid profiles are both retrieved in profile form, which means that at any given layer, it is possible that we could get a mixture of these phases. This, of course, would assume that we have enough radiometric signal to distinguish them without ambiguity. With this approach: 1) Reliance on a moist physics model to relate the temperature and water vapor to the cloud and hydrometeor profiles is avoided, which allows 2) saving time by using only the RTM to project the geophysical space into the radiance space; 3) derivatives are all computed through the RTM adjoint, and no derivation of the cloud model is needed with its additional cost; 4) measurement errors, which are essential for the 1D-VAR, need only to be estimated for the instrumental noise and the RTM uncertainty. Uncertainties associated with the cloud physics modeling are therefore avoided; 5) dependence of the resulting retrievals on NWP-specific information (forecast) and/or convection scheme is also avoided. It is recognized that the cause-to-effect type of relationship between the T and Q profiles on one hand and the C and H profiles on the other is no longer hard coded through a cloud scheme coupled with the RTM such as in the studies aforementioned. These constraints are however indirectly present, although loosely, through the background covariance matrix to ensure consistency, the same way that the temperature layers are being constrained to produce a physically realistic temperature profile overall without a direct scheme that relates each layer temperature to the others. This mechanism can take advantage of known relationships between the hydrometeor formation and the nonatmospheric variables. We emphasize that the retrieved cloud and hydrometeor profiles should be viewed as an effective product that, radiometrically, represent the effects of a conglomerate of parameters that have been reported to have significant impacts on brightness temperatures. These include the following:

1) beam-filling effect;
2) shape of the particles and droplets;
3) their orientation;
4) their density;
5) volume mixture rate of liquid and frozen matters;
6) particle size distribution;
7) vertical distribution of all of the above [6];
8) 3-D cloud and rain effects or nonvalidity of plane-parallel assumption;
9) differences between the air temperature and the frozen/liquid water phases temperatures.

Using these effective profiles in the retrieval is a result of the recognition that we cannot realistically claim to be able to retrieve accurately so many parameters with the available number of channels, without too heavily relying on the external data. We will call this handling of precipitation parameters, for the purpose of retrieving temperature and humidity, a *precip-clearing* procedure, as it effectively amounts to clearing the effects of these precipitation parameters from the retrievals of temperature and moisture profiles. We emphasize that this *precip-clearing* is highly nonlinear as it accounts for the effects of precipitation, not at the radiance level, but by accounting for the hydrometeors themselves as part of the retrieved state vector within the retrieval iterations.

B. Description

The 1D-VAR system used in this paper is labeled the microwave integrated retrieval system (MIRS). The retrieval of the precipitating and nonprecipitating cloud parameters is done in a profile form as said before, along with the temperature and humidity profiles. A 100-layer pressure grid is used ranging from 1050 to 0.1 mbar. Layers below the surface are disabled before the retrieval is triggered and do not play any role. The humidity, cloud, and hydrometeor parameters are actually retrieved in the natural logarithm space. This has the advantages of 1) avoiding the nonphysical negative values and 2) making their probability density functions (pdfs) more Gaussian, which is a necessary mathematical condition, as will be described later. To alleviate the limited information content available in the instruments at hand, the inversion is performed in a reduced eigenvalue space as mentioned before, which makes the retrieval process stable and mathematically consistent; the number of EOFs used in the retrieval is less or equal to the number of channels available.

C. Mathematical Basis

The mathematical basis of MIRS is a proven and widely used variational approach described in [39]. We will briefly review it here for the purpose of showing that it is valid in precipitating conditions as well. We will follow the probabilistic approach as it will highlight the only three important assumptions made for this type of retrievals, namely, the local linearity of the forward problem, the Gaussian nature of both the geophysical state vector and the errors associated with the forward model and the instrument noise, and finally, that the measurements and the forward operator are nonbiased to each other. It is important to keep in mind that the variational, Bayesian, optimal estimation theory, and maximum probability are all the same solutions (if the same assumptions are made), although reached through different paths. The following will link the probabilistic approach to the variational solution which seeks to minimize a cost function. Intuitively, the retrieval problem amounts in finding the geophysical vector X which maximizes the probability of being able to simulate the measurement vector Y^{m} using X as an input and using Y as the forward operator. This translates mathematically into maximizing $P(X|Y^{\mathrm{m}})$.

The Bayes theorem states that the joint probability $P(X,Y)$ could be written as

$$P(X,Y) = P\left(Y|X\right) \times P(X) = P\left(X|Y\right) \times P(Y).$$

Therefore, the retrieval problem amount to maximizing

$$P(X|Y^{\mathrm{m}}) = \frac{P\left(Y^{\mathrm{m}}|X\right) \times P(X)}{P(Y^{\mathrm{m}})}.$$

X is assumed to follow a Gaussian distribution

$$P(X) = \exp\left[-\frac{1}{2}(X - X_0)^T \times B^{-1} \times (X - X_0)\right]$$

where X_0 and B are the mean vector (or background) and covariance matrix of X, respectively. Ideally, the probability $P(Y^{\mathrm{m}}|X)$ is a Dirac-Delta function with a value of zero except for X. Modeling errors and instrumental noises all influence this probability. For simplicity, it is assumed that the pdf of $P(Y^{\mathrm{m}}|X)$ is also a Gaussian function with $Y(X)$ as the mean value (i.e., the errors of modeling and instrumental noise are nonbiased), which could be written as

$$P(Y^{\mathrm{m}}|X) = \exp\left[-\frac{1}{2}\left(Y^{\mathrm{m}} - Y(X)\right)^T \times E^{-1} \times \left(Y^{\mathrm{m}} - Y(X)\right)\right].$$

E is the measurement and/or modeling error covariance matrix. Maximizing $P(X|Y^{\mathrm{m}})$ is a minimization of $-\log(P(X|Y^{\mathrm{m}}))$ which could be computed from the previous equations as

$$J(X) = \left[\frac{1}{2}(X - X_0)^T \times B^{-1} \times (X - X_0)\right] + \left[\frac{1}{2}\left(Y^{\mathrm{m}} - Y(X)\right)^T \times E^{-1} \times \left(Y^{\mathrm{m}} - Y(X)\right)\right].$$

$J(X)$ is called the cost function which we want to minimize. The first right term J_{b} represents the penalty in departing from the background value (*a priori* information), and the second right term J_{r} represents the penalty in departing from the measurements. The solution that minimizes this two-term cost function is sometimes referred to as a constrained solution. The minimization of this cost function is also the basis for the variational analysis retrieval. In theory, one could also find another optimal cost function for a non-Gaussian distribution and nonlinear problems. It is just not as a straightforward problem. The solution that minimizes this cost function is easily found by solving for

$$\frac{\partial J(X)}{\partial X} = J^{'}(X) = 0$$

and assuming local linearity around X, which is generally a valid assumption if there is no discontinuity in the forward operator

$$Y(X_0) = Y(X) + K[X_0 - X].$$

K, in this case, is the Jacobian or derivative of Y with respect to X. This results into the following departure-based solution:

$$\begin{aligned}(X - X_0) &= \Delta X \\ &= \left\{(B^{-1} + K^T E^{-1} K)^{-1} K^T E^{-1}\right\} \\ &\quad \times \left[Y^{\mathrm{m}} - Y(X_0)\right].\end{aligned}$$

If the previous equations are ingested into an iterative loop, each time assuming that the forward operator is linear, we end up with the following solution to the cost-function minimization process:

$$\Delta X_{n+1} = \left\{\left(B^{-1} + K_n^T E^{-1} K_n\right)^{-1} K_n^T E^{-1}\right\} \\ \times \left[(Y^{\mathrm{m}} - Y(X_n)) + K_n \Delta X_n\right]$$

where n is the iteration index. The previous solution could be rewritten in another form after matrix manipulations

$$\Delta X_{n+1} = \left\{B K_n^T \left(K_n B K_n^T + E\right)^{-1}\right\} \\ \times \left[(Y^{\mathrm{m}} - Y(X_n)) + K_n \Delta X_n\right].$$

The latter is more efficient as it requires the inversion of only one matrix. At each iteration n, we compute the new optimal departure from the background given the derivatives as well as the covariance matrices. This is an iterative-based numerical solution that accommodates moderately nonlinear problems or/and parameters with moderately non-Gaussian distributions. This approach to the solution is generally labeled under the general term of physical retrieval and is also employed in the NWP assimilation schemes along with the horizontal and temporal constraints. The whole geophysical vector is retrieved as one entity, including the temperature, moisture, and hydrometeor atmospheric profiles as well as the skin surface temperature and emissivity vector, ensuring a consistent solution that fits the radiances.

D. Forward Model

This type of inversion of cloudy/rainy radiances supposes the use of a forward operator that can simulate the multiple scattering effects due to ice, rain, snow, graupel, and cloud liquid water at all microwave frequencies and generate the corresponding Jacobians for all atmospheric and surface parameters. The forward operator used in this paper is the community RTM (CRTM) developed at the Joint Center for Satellite Data Assimilation (JCSDA) [47]. CRTM produces radiances as well as Jacobi, for all geophysical parameters. It is valid in clear, cloudy, and precipitating conditions. Derivatives are computed using K-matrix developed by tangent linear and adjoint approaches. This is ideal for retrieval and assimilation purposes. The different components of CRTM briefly are the optical-path-transmittance (OPTRAN) fast atmospheric absorption model [29], the NESDIS microwave emissivity model [20], and the advanced doubling adding radiative transfer solution for the multiple-scattering modeling [22].

E. Covariance Matrix and Background

The covariance matrix plays an important role in variational algorithms. Lopez [23] estimated an error covariance matrix of cloud and rain from the French global model ARPEGE. Chevallier *et al.* [7] simply defined an empirical covariance matrix of clouds with large errors. Moreau *et al.* [35] used the regular covariance matrix of temperature and humidity which they convolved with moist convection and large-scale condensation schemes to produce an ensemble of rain water and cloud profiles. This covariance was computed for each grid point. In this paper, the part of the covariance matrix B related to temperature and humidity is based on a set of globally distributed radiosondes (known as the NOAA-88 set) containing more than 8000 individual profiles, mostly over islands. The impact of using a different covariance has not been tested, but we expect that a more representative dataset could improve the retrieval performances. The exact formula used to compute these covariances is given as

$$\sigma_{ij}^2 = \frac{1}{N}\sum_{i=1}^{N}\sum_{j=1}^{N}(x_i - \overline{x_i}) \times (x_j - \overline{x_j})$$

where σ_{ij} is one of the elements of the matrix corresponding to row i and column j. N is the number of profiles used, and $\overline{x}$ is the average value along the row or along the column.

The part related to the cloud parameters is, for practical reasons, also built independently offline. These statistics are generated from a multitude runs (three time-consecutive fields) based on the fifth generation mesoscale model (MM5) simulations, corresponding to hurricane Bonnie (1998), with 4-km resolution and 23 vertical levels, which are extrapolated to the internal pressure grid of MIRS (100 layers).

The ability of these runs to represent the hydrometeors' global variability is not fully established, but this is believed to be accurate enough for the case of hurricanes and tropical storms. Impact studies (not shown) were also performed and showed that the system is able to reach convergence (therefore, a radiometric solution) in many conditions that are independent from the set that was used to generate these covariances. Given the high dimensionality of the covariance matrix, it is technically not feasible to include the actual values of this matrix in this paper. The matrix file is however readily available to interested parties. The background is coming from the same climatology used for building the covariance matrix, not from the NWP forecasts. Because the climatology we used is neither geographically nor time varying, the background fields are simply a mean value computed from a set of NOAA radiosondes in the case of the nonprecipitating parameters and from a number of MM5 runs for the precipitating parameters. These average background values are used everywhere, which means that the background field (to use data-assimilation terminology) is a constant field with only one value: the mean climatic value.

F. EOF Decomposition

The retrieval in MIRS is performed in EOF space through projections back and forth, at each iteration, between the original geophysical space and the reduced space. This method has been routinely used in operational centers as a standard transform approach of control variables [24]. It has also been used in the context of retrieval of trace gases, sounding, and surface properties [20], [33], [43], [49]. Applying it in the context of our 1D-VAR retrieval is therefore not very original except may be for its extension to cloud and precipitation profiles which is, to our knowledge, new. Only a limited number of eigenvectors/eigenvalues are kept in this reduced space. The selection of how many EOFs to use for each parameter is somehow subjective but depends on the number of channels available that are sensitive to that parameter. Other approaches exist such as in [36], which suggested an objective way of choosing which parameters will be included in the control parameters, using the ratio between the background covariance matrix and the *a posteriori* covariance (ratio of diagonal elements). This ratio, however, depends on the Jacobian which is only known at the end of the iterative process, unless the problem is purely linear (not the case when cloud and precipitation as well as the high-frequency channels are involved). Advantages of performing the retrieval in EOF space are the following: 1) handling the strong natural correlations that sometimes exist between parameters which usually create a potential for instability (or oscillation) in the retrieval process (small pivot), which is reduced significantly by performing the retrieval in an orthogonal space and 2) time saving by manipulating and inverting smaller matrices. The projection in EOF space is performed by diagonalizing the *a priori* covariance matrix

$$B \times L = L \times \Theta$$

where L is the eigenvector matrix, which is also called the transformation matrix, and Θ is the eigenvalue diagonal matrix which contains the independent pieces of information. The retrieval could therefore be performed using the original matrices B, ΔX, K_n as stated before (retrieval in original space), or, alternatively, it could be done using the matrices/vectors Θ, $\overline{\Delta X}$, $\overline{K_n}$ (retrieval in reduced space). The transformations back and forth between the two spaces are done using the transformation matrix L. It is important to note that, at this level, no errors are introduced in these transformations. It is merely a matrix manipulation. However, the advantage of using the EOF space is that the diagonalized covariance matrix and its corresponding transformation matrix could be truncated to keep only the most informative eigenvalues/eigenvectors. By doing so, we are bound to retrieve only the most significant features of the profile and leaving out the fine structures. How much truncation depends on how much information the channels contain. In the AMSU configuration, six EOFs are used for temperature, four for humidity and surface emissivity, one for skin temperature, one for nonprecipitating cloud, and two for both rain and frozen precipitation (a total of 20).

G. Convergence Criterion and Other Important Details

Several criteria have been reported for deciding on the convergence of variational methods, among which are the following: 1) testing that the increment of the parameter values at a given iteration is less than a certain threshold (usually, a fraction of the associated error of that particular parameter); or 2) testing that the cost-function $J(X)$ decrease is less than a preset threshold; or 3) checking that the obtained geophysical vector X at a given iteration produces radiances that fit the measurements within the noise level impacting the radiances. We have chosen the last criterion as it maximizes the radiance signal extraction. A convergence criterion based on $J(X)$, while mathematically correct, would produce an output that carries more ties to the background and, therefore, would be more inclined to present artifacts due to it. The convergence criterion adopted is when

$$\varphi^2 = \left\lfloor (Y^{\mathrm{m}} - Y(X))^T \times E^{-1} \times (Y^{\mathrm{m}} - Y(X)) \right\rfloor \leq N$$

where N is the number of channels used for the retrieval process. This mathematically means that the convergence is declared reached if the residuals between the measurements and the simulations at any given iteration are less or equal than one standard deviation of the noise that is assumed in the radiances.

Note that fitting the radiances within the noise level is necessary but not a sufficient condition. We should note here that the convergence criteria do not alter the balance of weights given to the radiances (or to the background) in the cost function that the 1D-VAR minimizes.

The evolution of the humidity profile is monitored for supersaturation in the iterative process. A maximum of 130% relative humidity is allowed. Currently, it is set in an *ad hoc* fashion at each step. This has the potential to steer nonlinearly the convergence from its mathematical path and should, in general, be avoided, but our experience has shown that this has not increased the divergence rate in a significant way.

H. Rationale for Precip-Clearing

By *precip-clearing*, we mean the inclusion of cloud and hydrometeor profiles in the retrieval state vector, not so much for the sake of their retrieval (whose accuracy is hindered by the significant null space as mentioned before) but to account for all their effects on the radiances, as well as to account for the effects of those related parameters that are not varied in the retrieval process and instead assumed constant inside the radiative transfer operator. This allows a more accurate retrieval of the other parameters, namely, the temperature and humidity profiles and the surface parameters. This is driven essentially by the limited number of channels available or, mathematically speaking, the limited number of EOFs affordable, which translates into a lack of sensitivity to fine vertical structures. The integrated values of the cloud and hydrometeor parameters (roughly represented by one or two EOFs) are however deemed accurate from simulation runs.

IV. Instrumental Configuration

In this paper, we will focus on the imaging/sounding channels of the NOAA-18 microwave sensors AMSU and MHS. This platform was launched on May 21, 2005. The main purpose of the microwave sensors is the atmospheric sounding of temperature and moisture, but other products are being produced routinely that include the rain rate, ice water path, land surface temperature and emissivity, cloud liquid amount, and total precipitable water [13], [21]. AMSU has two modules (A-1 and A-2) with channels operating at centimeter and millimeter wavelengths corresponding to frequencies ranging from 23.8 to 89 GHz and thirty scan positions per scanline. MHS on the other hand probes at millimetric frequencies between 89 and 183 GHz with a higher spatial resolution (90 scan positions per scanline). AMSU and MHS channels are unpolarized at nadir and mix-polarized off-nadir. Both sensors have a cross-track swath, scanning angles between nadir and 48.33°, corresponding to zenith angles reaching 58°.

V. Assessment of the Performances in Simulation

This section deals with the simulation results aimed at assessing the performances of the retrieval system in clear and cloudy/rainy conditions. This assessment is hard to do using the real data due to the lack of certainty about the true measure of the geophysical state. Because the system is applied in all conditions, we want first to assess its performances in the clear-sky conditions. We, then, want to know what is the advantage (if any) of using a multiple-scattering model rather than a pure absorption model. These questions will be answered in the following two subsections for an individual profile. The AMSU/MHS configuration is used. The radiances are first simulated using the forward model described in Section III-D, then the retrieval is applied after randomly impacting the radiances by a Gaussian noise whose standard deviation corresponds to the advertised NedT of the respective channels. These values were found to be consistent with those computed from the real data using the methodology of Mo [32]. In both cases, the simulated radiances were performed with a nadir-looking configuration. The background data used for these simulated retrievals are the same as used previously in Section III-E.

A. Assessment in Nonprecipitating Conditions

Fig. 1 shows the evolution of the retrieved parameters during the iterative process for a single profile where neither cloud

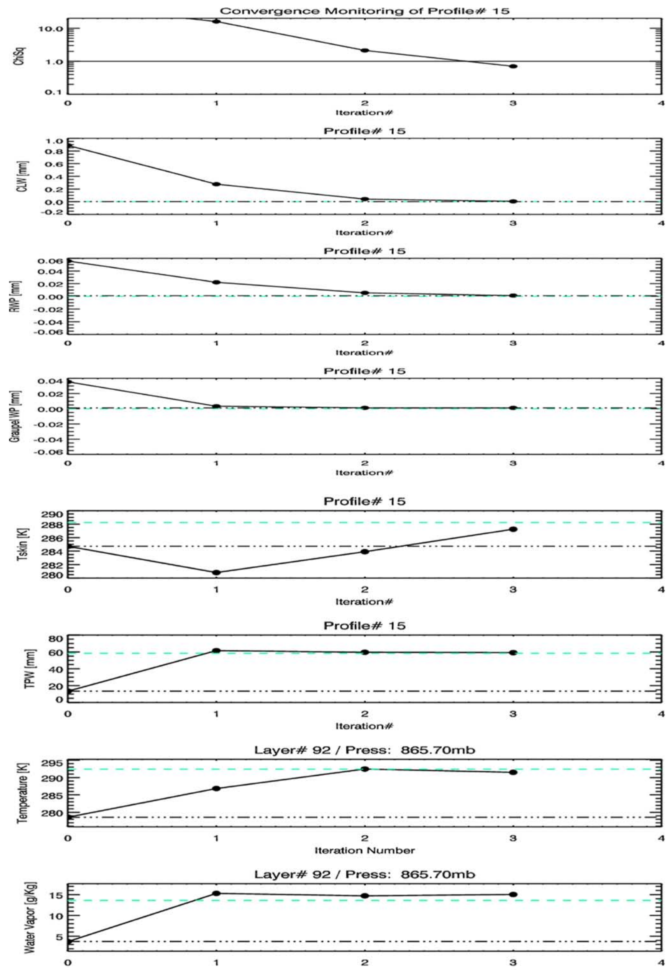

Fig. 1. Evolution of a sample of the retrieved state vector during the iterative process for an individual profile. The parameters monitored are (from top to bottom) the convergence metric, the vertically integrated cloud amount, the rain water path, the graupel-size ice amount, the skin temperature, the total precipitable water, the atmospheric temperature in layer corresponding to a pressure of 865 mbar, and, finally, the water-vapor mixing ratio in the same layer. The solid line is the retrieved quantity, the dashed line represents the truth, and the dotted-dashed line corresponds to the first guess and background values.

nor precipitation was included. It shows that the retrieved parameters are all reaching the true value within three iterations. The convergence metric is plotted in the top panel, showing that the measurements were fitted within the noise level. The first guess for the cloud and hydrometeors was chosen to be nonzero, and the values reached in the final iteration were all zero, as expected. This gives us confidence that the system will produce cloud-free retrievals when applied to the truly clear-sky cases. Even if this is shown for one particular profile only, it was tested under other configurations, and similar results were obtained (not shown here).

B. Assessment in Precipitating Conditions

Figs. 2 and 3 show the retrieval of one cloudy and rainy profile from an MM5 output run using two approaches. The radiances have been fully impacted by the extinction (absorption and scattering) effect of cloud, rain, and ice droplets during the forward simulation. The first approach (Fig. 2) consisted

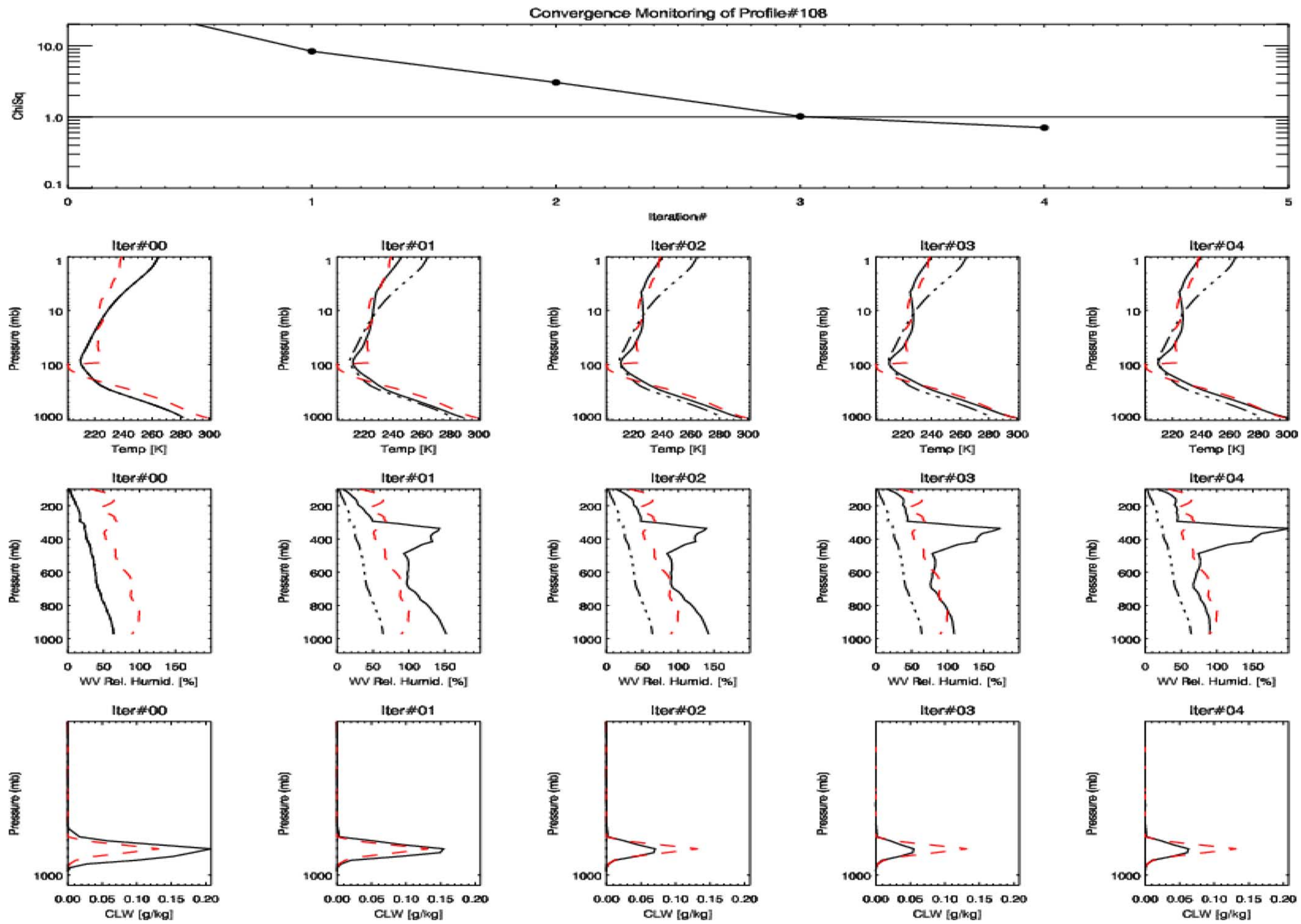

Fig. 2. Evolution, iteration-by-iteration of (from top to bottom) convergence metric, vertical profiles of temperature, moisture, and cloud amount. This is a cloudy/rainy sky (dashed lines represent true values), and the retrieval (represented by solid lines) was made assuming a purely absorbing RTM (multiple scattering turned off). Dotted-dashed lines represent the first guess and background.

of assuming that only absorption is happening; therefore, only temperature, moisture, and nonprecipitating cloud amount are retrieved, and the multiple scattering is turned off in the forward operator of the 1D-VAR. The major effect this has on the retrieval is the significant amount of supersaturation that the water vapor is experiencing to compensate for the effect of scattering, up to 200% relative humidity. This phenomenon is consistent with the previous studies that actually took advantage of this feature to estimate the amount of ice in the profile by looking at the water-vapor profile [19]. Note that this particular profile has perfectly converged within four iterations. The same radiances are inverted in Fig. 3, but, this time, by turning the scattering on, the rain and the graupel-size ice are both retrieved simultaneously with temperature, moisture, and cloud liquid amount. We notice that the water-vapor supersaturation is much reduced. There is a sort of *precip-clearing* of the radiances that allows a better retrieval of the moisture profile. The temperature profile is not much altered. The apparent discontinuity in the original temperature profile is because it is a combination of an MM5-produced profile up to 100 mbar (so that temperature, cloud, and hydrometeors are consistent) and climatology above that level. Despite the nonphysical transition of the original temperature profile at 100 mbar, which is simulated in the radiances, the retrieval is able to accommodate to a certain extent, given the shape of the background that constrains its departures. This is an example of how the variational technique is balancing *a priori* information and radiance-provided information. We also notice the degree of nullspace; the hydrometeors are not reaching the true values, and yet, the retrieval has converged within three iterations. This demonstrates that with the degrees of freedom at hand, one needs more independent radiances to constrain the problem. As a reminder, our primary goal here is to sound temperature and moisture in the cloudy/precipitating conditions, not so much the sounding of hydrometeors themselves. The integrated amounts, however, are expected to be reasonably accurate.

VI. Validation Using GPS-Dropsondes

Microwave imaging and sounding data from the NOAA-18 satellite were used to validate the retrieval system described previously in both clear cases as well as under extreme weather conditions, in the eye and within the eyewall of hurricane Dennis in the summer of 2005. This was done by comparing the retrievals of temperature and humidity profiles to the measurements made by GPS-dropsondes. Before the retrieval is performed, the brightness temperatures of the two sensors are collocated and corrected of any bias when compared to

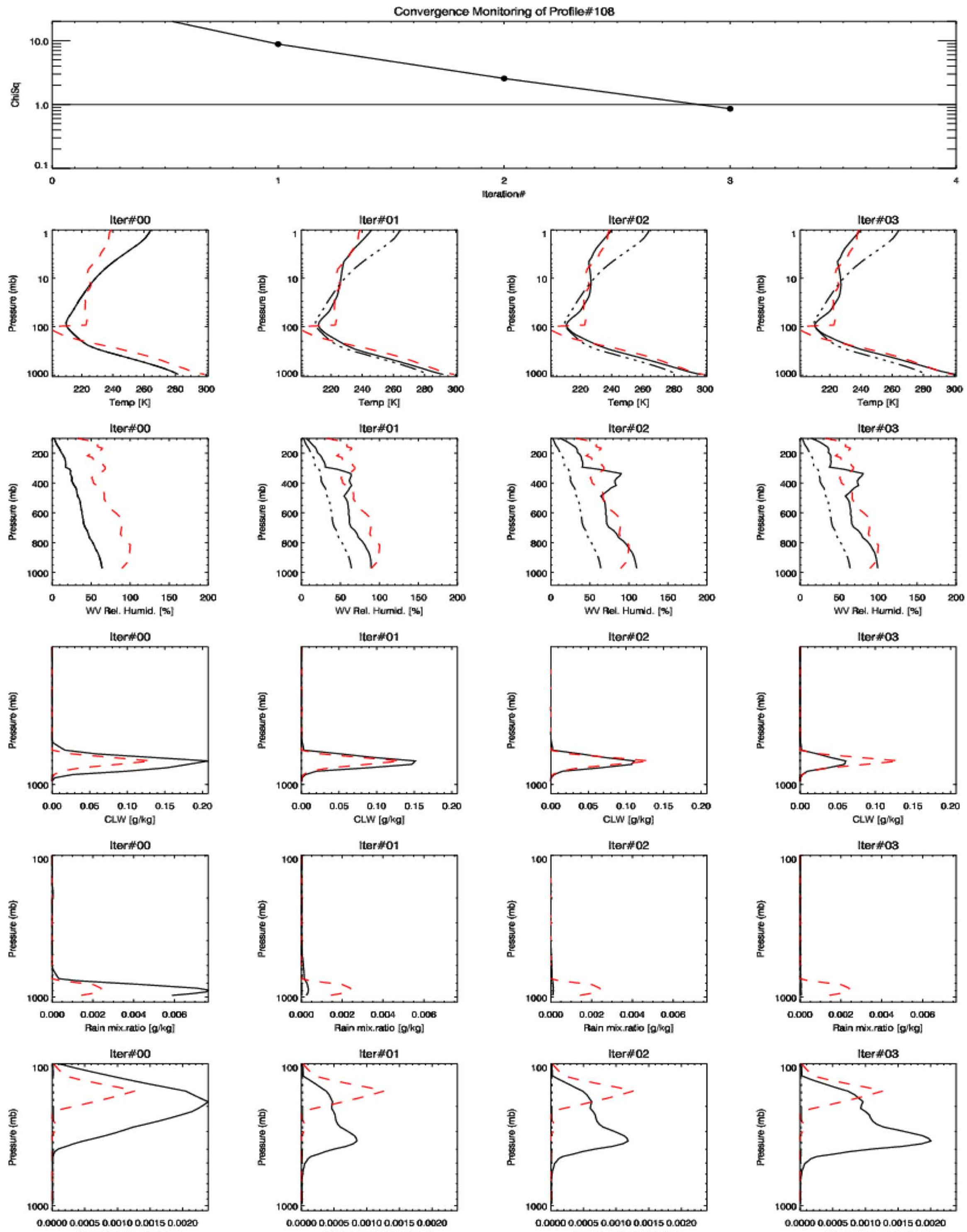

Fig. 3. Same as Fig. 2, except that the vertical profiles of rain and graupel-size ice are added. This is a cloudy/rainy sky (dashed lines represent true values), and the retrieval (represented by solid lines) was made with the full RTM where multiple-scattering effects are accounted for. The supersaturation of water vapor is much reduced compared to Fig. 2. The apparent discontinuity in the original temperature profiles is caused by their combination of the MM5-produced profiles up to 100 mbar and climatology above that level.

the forward-model simulations. The collocation is done in two different ways: 1) An averaging is performed of 3×3 MHS footprints to fit the AMSU spatial coverage (low resolution) or 2) assume the AMSU footprint valid within all the subpixel MHS footprints (high resolution). In this latter case, the subpixel heterogeneity is computed from the MHS footprints and translated into the AMSU channels but only for those that are sensitive to the same geophysical parameters, namely, channels 23.8, 31.4, 50.3, and 89 GHz. The bias removal is performed by simulating the brightness temperatures over ocean using the NCEP Global Data Assimilation System (GDAS) analyses as inputs. These biases were found to be scan dependent.

The instrumental/modeling error covariance matrix E is also built partly during this process by using the variances of the same comparisons. These variances are subjectively scaled down to account for the uncertainties in the GDAS inputs and collocation errors. The diagonal elements (in standard deviation, in Kelvin) of the modeling error matrix E for the AMSU+MHS channels (from #1 to #20) are the following: 1.9, 1.7, 1.2, 0.6, 0.3, 0.2, 0.3, 0.4, 0.4, 0.3, 0.8, 0.0, 0.0, 0.0, 2.1, 2.2, 1.4, 1.6, 1.3, and 1.1. Channels 12, 13, and 14 peak above the maximum altitude reported by GDAS, so the comparison to GDAS simulation is not terribly meaningful, therefore, the variances for these channels were deemed unreliable, and the channels were disabled. These modeling errors are used on top of the instrumental errors (NEDT values) which are computed exclusively from the raw AMSU/MHS Level-1B data, which are available from NOAA using the approach of [32]. For window channels, modeling errors are dominant over instrumental errors. These values are slightly lower than those found in the previous studies [9], [36]. They allow, however, a stable convergence in most cases. Note that these modeling errors are computed over ocean in the clear-sky conditions. The same values are used over the cloudy/rainy conditions.

A. Dropsondes Data

It is critical that one gets a clear sense of how accurate the so-considered truth measurements are before interpreting any differences between them and the retrievals. In our case, measurements are made in the cloudy/rainy conditions (typically, during hurricanes and tropical storms) by high-velocity descending GPS-dropsondes. They were obtained from the Hurricane Research Division (HRD), Miami, FL, where they were quality-controlled using the Hurricane Analysis and Processing System. They operate at altitudes up to 24 km with a descent time of about 12 min. The measurements are made every half second which allows a high vertical resolution. Along with the temperature and moisture, the vertical wind-speed profile is also measured by using the GPS-based Doppler signal, which is down to 4–10 m above the surface. The validation of these dropsondes was assessed by a comparison with standard radiosondes, radars, buoys as well as by a human visualization of clouds for the saturation check. For a full description of these measurements, see [16]. In their study, the inherent accuracy of the temperature measurement was assessed to be 0.2 °C, but a lag error correction exceeding 1 °C was applied for layers above 500 mbar. The humidity accuracy was assessed to be less than 5%, but up to 15% dry bias correction was sometimes applied (S. Feuer, personal communication, 2006). As for the wind, an accuracy of 0.5–2 m/s was estimated.

B. Limitations of the Validation in Extreme Weather Events

Traditional approach in validating the retrievals by statistical comparison with ground-truth data collected around the measurement's time/space location is not optimal in the case of hurricane conditions. The main reason is the fast-moving features involved. A category 2 storm, for instance, has an average forward speed of 30 mi/h (or 48 km/h), therefore, even if the storm features are all the same, a displacement caused by a collocation criterion of 2 h would cause a 90-km shift (~6 scanlines of MHS). For illustration, Fig. 4 shows the effect of a modest shift of three scanlines on a field of brightness temperatures, assuming the geometry of the depicted storm did not change between the shifted and the nonshifted fields. The differences between the shifted and nonshifted fields reach very high values that could make the comparison meaningless.

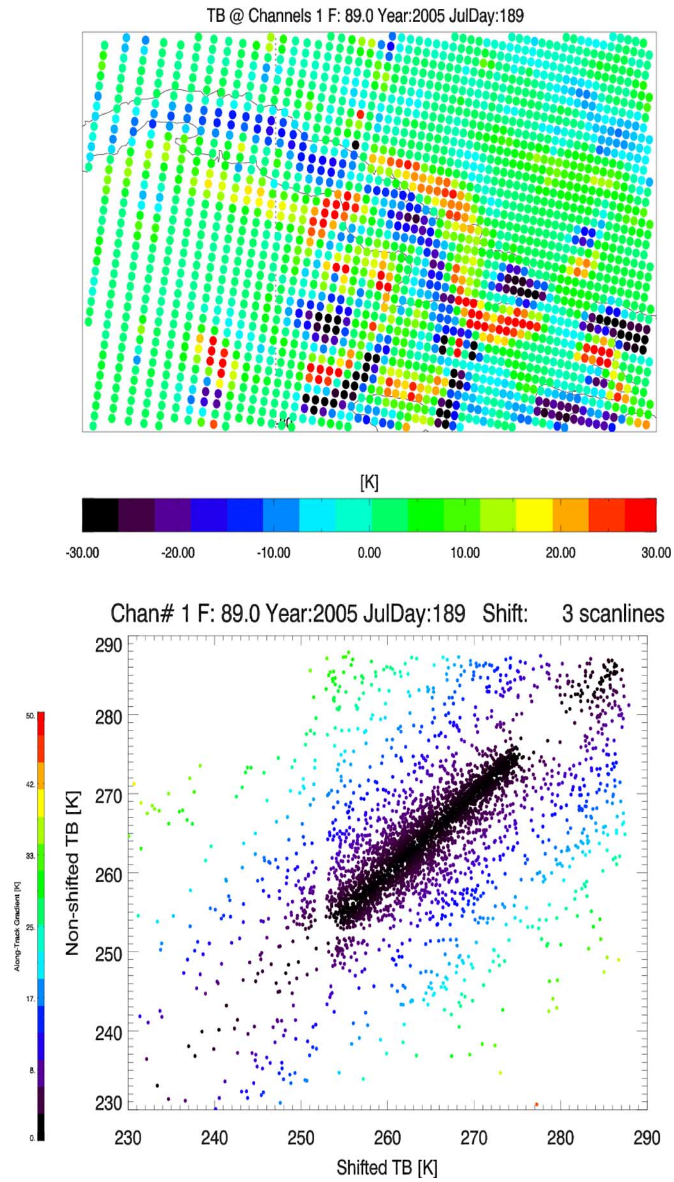

Fig. 4. Impact of shifting the field of brightness temperature by three scanlines (here 89-GHz channel) that is measured during July 2005 hurricane Dennis to simulate the effect of collocation errors in time and space. The map represents the difference of the two fields (shifted and nonshifted). In the scatterplot, the colors are modulated by the heterogeneity of the original TBs field. The darker the dot is, the smoother is the area around the measurement. Areas where the field is very heterogeneous, (green-red dots on lower panel), have differences exceeding 30 K.

In reality, it is even worse: storm intensifies, fades down, hydrometeor structures change, particles form/fall, the shift is multidirectional, etc. Collocation errors are therefore expected to be dominant in very active areas. Very strict criteria must therefore be used for the validation of hydrometeor retrieval

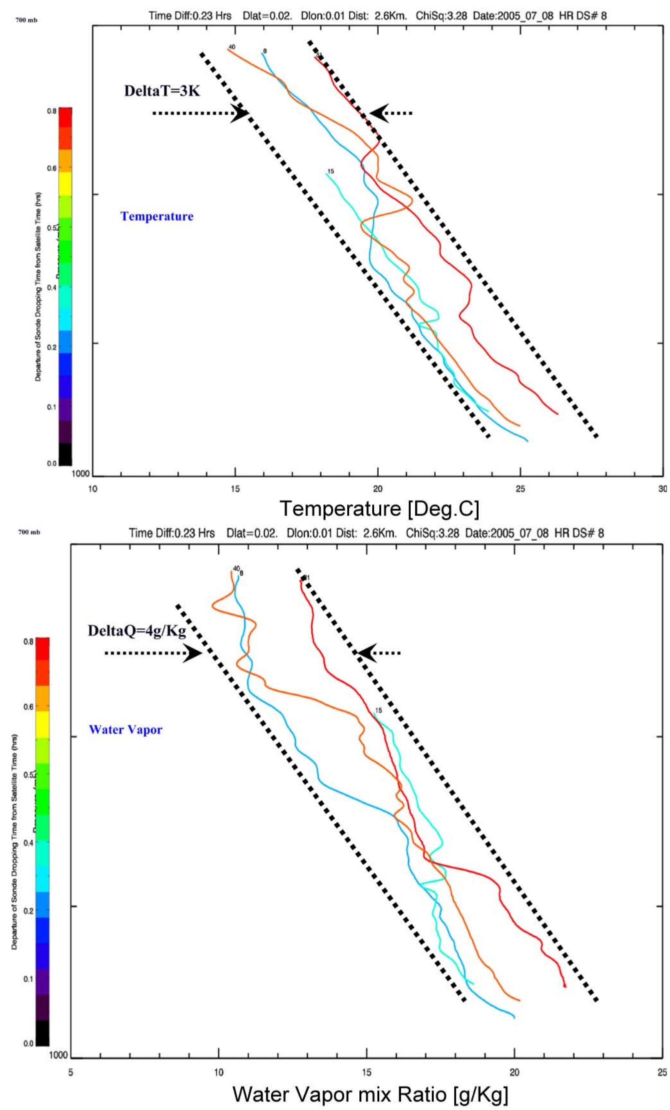

Fig. 5. Intravariability of dropsonde measurements in terms of temperature and moisture profiles, which are made within an average of 10 min from each other and within a radius of 10 km. Note that the descent time is roughly 12 min.

given their highly changing nature. Additionally, atmospheric temperature in the rain and cloud might be different from the air temperature. Sinkevich and Lawson [41] performed an assessment of the accuracy of temperature measurements in convective clouds and reported that temperature-excess amount between in-cloud and out-of-cloud areas depends on the stage of the life of the cloud and varied between 0.2 °C and up to 8 °C over ocean. Over land, an even greater temperature excess was noticed. For all these reasons, there is a need to have an almost perfect collocation in these active conditions, in order for the comparison to be meaningful. Stringent time and space criteria must therefore be used, which obviously dramatically reduces the total number of coincident collocations. This, in turn, renders the empirical assessment statistically meaningless at best or practically unfeasible at worst. Note that the tight time and space collocation must be between coincident satellite measurements, hurricane events, and ground truth such as dropsondes.

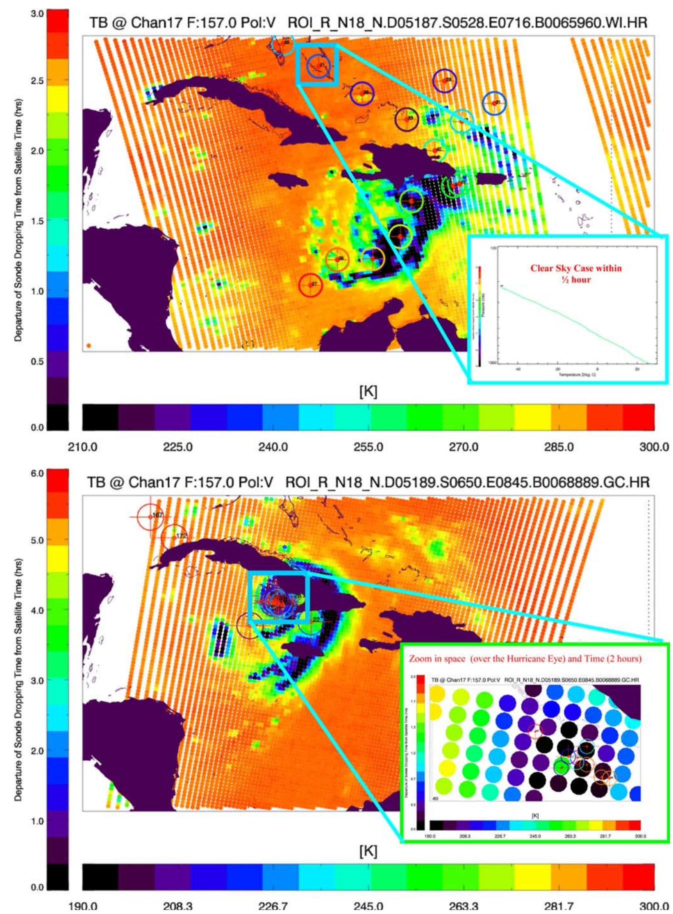

Fig. 6. Field of 157-GHz brightness temperatures taken during hurricane Dennis on (top) July 6, 2005 and (bottom) July 8, 2005. Overlaid are the circles centered around the location where the GPS-dropwindsonde was launched from the aircraft. The horizontal color bar refers to the brightness-temperature value. The vertical color bar represents the difference between the satellite-measurement time and the sonde launch time. Collocations highlighted in the upper and lower panels will serve as the validation in clear and precipitating conditions, respectively.

Fig. 5 shows the measurements of four dropsondes that were launched within the core of the hurricane (within and around the eye) with an average of 10-min interval and within 10 km distance. Differences in temperature up to 4 K and in moisture mixing ratio of up to 4 g/kg are noticed. These differences are inherent to collocation–coregistration. Although this is an almost perfect collocation between the dropsondes themselves (no retrieval involved), because the hurricane active features are moving fast, even a few minute interval and a few kilometer distance can make the sensor (in this case, the ground measurement) see a different signal. The descent time is by itself a limiting factor. By the time the dropsonde descends, it might be sampling the different parts of vertical profiles that are significantly different. The verticality of the retrieved and the ground-measured profiles is also an issue and adds to the overall uncertainty. The dropsonde presents the potential of drifting, while the retrieved profile's verticality depends on the viewing angle of the measurements where it was extracted from. If these latter are nadir viewing, then the retrieved profile is vertical. If, however, the channels are off-nadir viewing, then the retrieved profiles are slant. This clearly puts an upper limit to the expectations that one can have when comparing the retrievals with

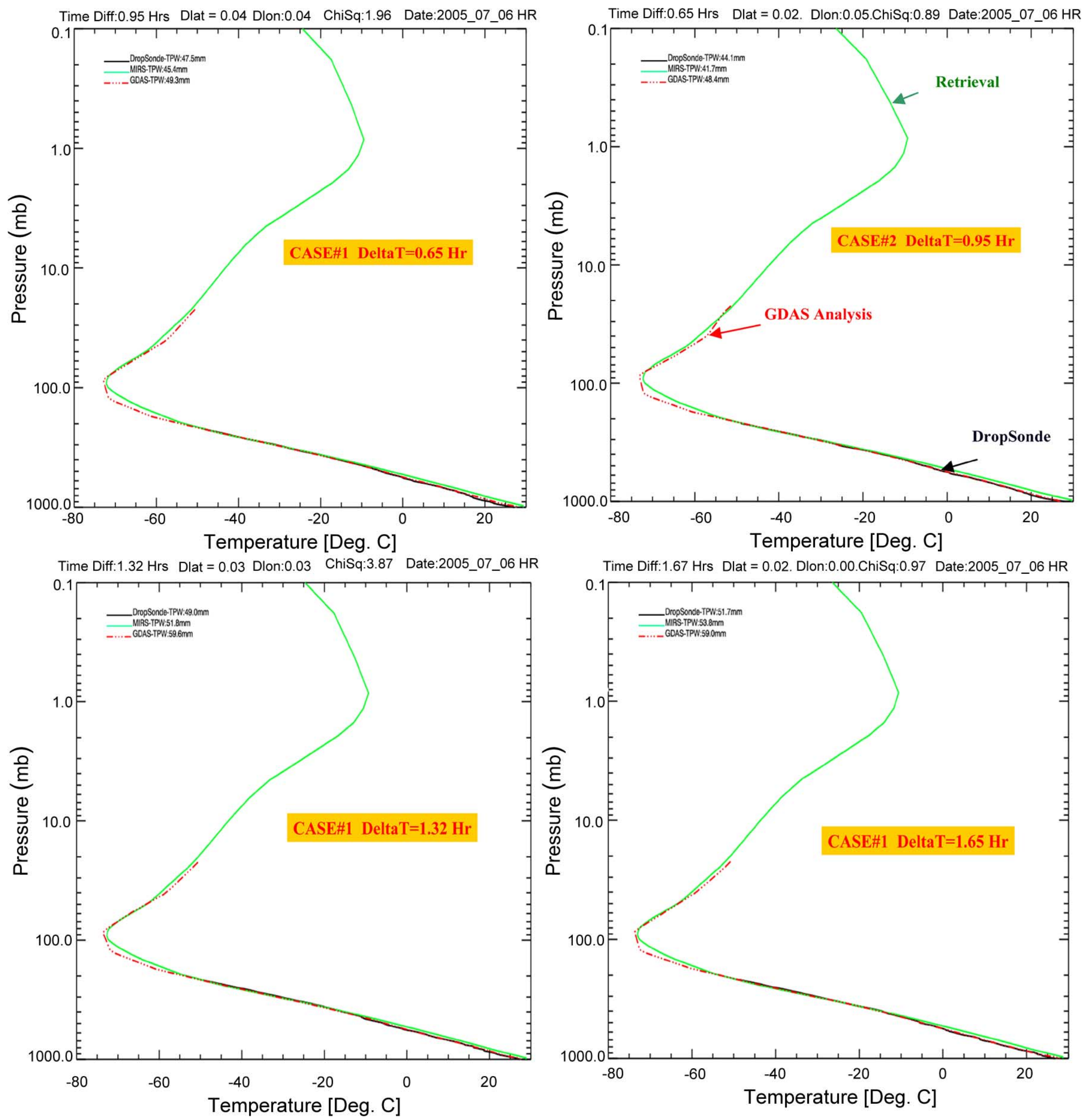

Fig. 7. Individual comparisons between dropsondes, MIRS retrievals, and GDAS. Note that all three have different pressure grids and different cloud tops. The four dropsondes represented have different time differences. The collocations are outside the inner core of the hurricane, as shown in Fig. 6 (upper panel).

the dropsonde measurements. Another type of limitation that one should be aware of is what other studies called representativeness error which relates to the fact that dropsonde measurements are point measurement and do not necessarily represent what the sensor is measuring within the field of view. This latter is around 15 km for MHS, at nadir, but more than 45 km wide at certain off-nadir viewing positions. Unfortunately, the number of dropsondes collocated with satellite measurements is limited, and therefore, the luxury of averaging within the footprint to mitigate the representativeness errors (or around the time of the measurement) cannot be afforded.

C. Case-by-Case Validation

Given the limitations discussed previously, and for the purpose of the validation, it was critical to find the as-perfect–as-possible collocation between the satellite measurements and the GPS-dropsondes. We focused on the hurricane Dennis which occurred on July 2005. Fig. 6 shows two days of that hurricane timeframe, July 6 and 8. The field of 157-GHz MHS brightness temperature is shown because of its sensitivity to cloud, rain, and ice. The dropsonde launch location is also highlighted by circles. The color of those circles indicates how far (red) or how close (dark) in time they are from when the closest satellite measurement was taken. The upper panel contains a number of decent dropsonde/satellite collocations (in space and time) that appear free of any impact of rain or ice (seems to be the same signal as the surface background). These will serve for the validation of our retrievals in a clear-sky condition. The lower panel on the other hand presents some interesting cases of dropsondes in the eye and within the eyewall of the hurricane (see close-up figure) that are very close in time to the satellite measurements. These will serve for the validation of the retrievals in the extreme conditions.

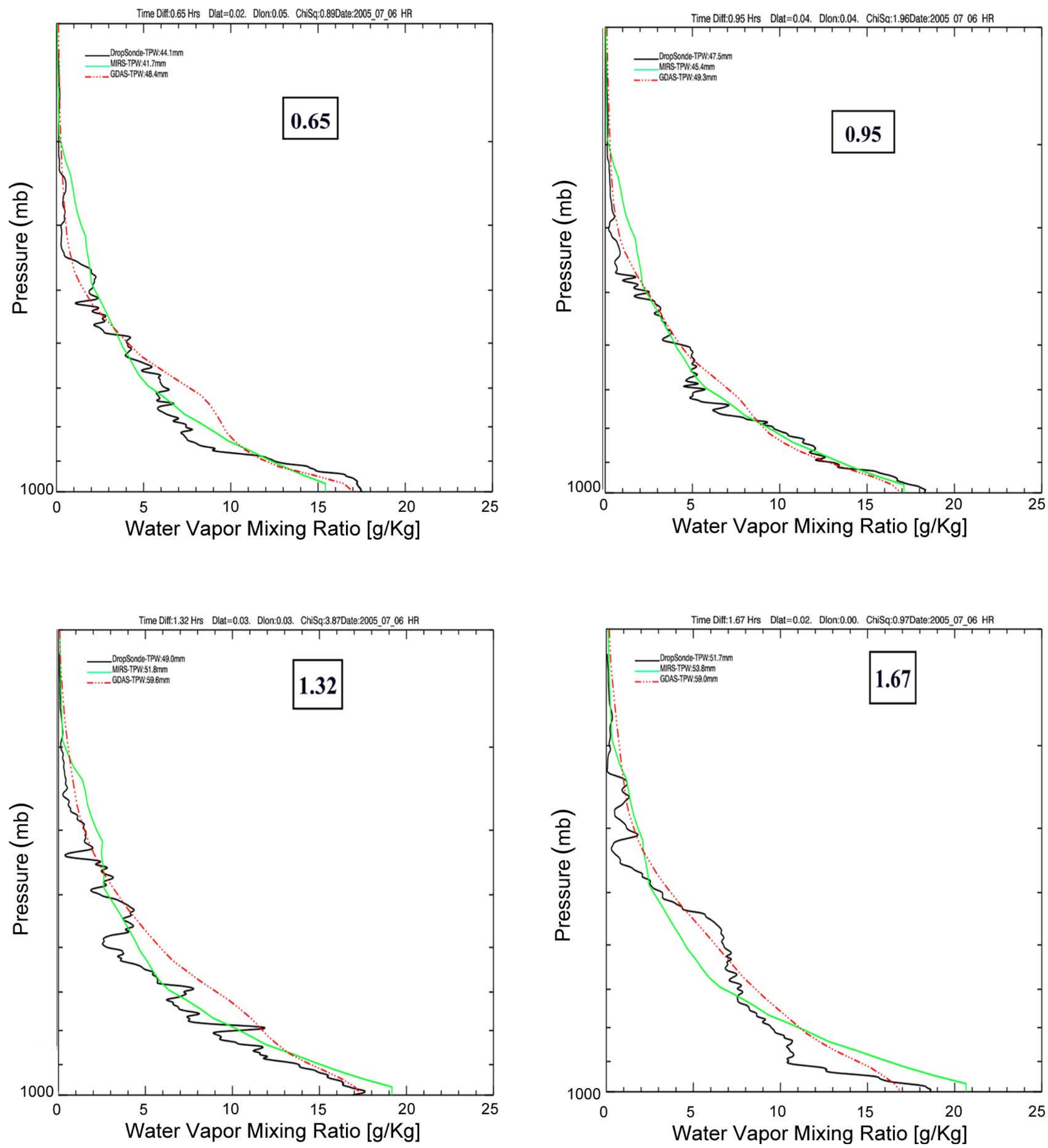

Fig. 8. Same as the previous figure, except that the water-vapor retrievals are represented. Retrievals were performed at the higher spatial resolution (MHS). Differences are higher when the retrieval is done at the lower resolution (not shown). No NWP external data were used for these retrievals.

D. *Clear-Sky Conditions*

Figs. 7 and 8 show four individual dropsondes that were identified above as clear sky along with the MIRS retrievals and the GDAS analysis (included for reference). They correspond to temperature and water vapor, respectively. The time difference is highlighted in the different panels. For temperature, errors are typically less than 1 K with a maximum of 3 K in the low altitudes. Note that the retrieval goes up to 0.1 mbar, while the dropsonde for this particular aircraft goes only to 200 mbar and GDAS to 20 mbar. The relatively large differences in the lower altitude might signal that the brightness temperatures for the low-peaking and window channels have some local residual bias that is hard to remove using the global approach we used. The water-vapor comparisons show a rather good agreement between the dropsonde measurements and the retrievals, except for the fine structures that the dropsonde is able to report while the retrieval is not detecting. This is not surprising given the vertically broad weighting functions of the 183-GHz channels and the horizontal size of the radiometric pixel which covers a much wider area than that of the point measurements. The latter are sensitive to subpixel horizontal variability. It is interesting also to note that, as one might expect, differences between the retrieval and dropsonde measurements tend to increase with larger time differences (displayed in the squares inside the plots). These retrievals were performed using the high-resolution footprint matching described earlier. Tests were done to see the impact of performing the retrievals in low resolution and were found higher due to the larger representativeness error. Note that in a relative sense, the differences are within the 10%–30% margin in the vertical region between the surface and 500 mbar.

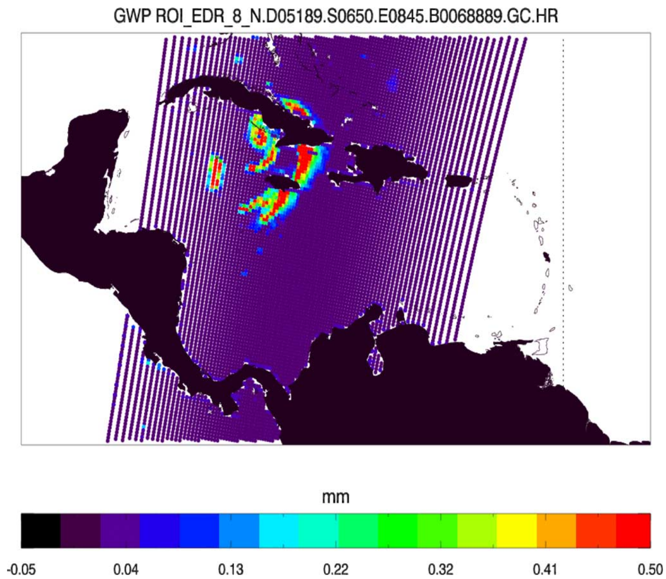

Fig. 9. Retrieval of graupel-size ice content using MIRS. Note that the output of MIRS is an actual profile. The figure above represents the vertical integration (which is performed in the postprocessing stage). Hurricane Dennis 2005 passing through the Cuba Island. Retrievals are done at MHS resolution (roughly 20 km).

E. Hurricane Conditions

Fig. 9 shows the vertically integrated graupel-size ice amount [Graupel-size ice water path (GWP)] computed from the retrieved profile. This is shown as a qualitative validation. Although the retrieval is done in profile form, the resulting integrated value displays physically plausible features and values. The retrieval corresponds to the same Dennis hurricane on July 8, 2005 (same descending orbit shown before). First, where no activity is present (from the 157-GHz brightness temperatures (TBs), the retrieval is reporting no ice or rain, even if the first guess used is actually a nonzero profile (the same used everywhere). This confirms the conclusion reached in a simulation setting (see Section V) that the system is able to produce zero amounts when the signal in the TBs indicates so, even when starting from the nonzero first guesses. Second, the large values of GWP are concentrated in the middle of the active area and decreasing gradually at the edges. One can even see that, in what seems to be the eye of the hurricane, the value of the integrated ice amount is actually very small compared to the surrounding pixels.

Figs. 10 and 11 show the comparison of MIRS retrievals to a few selected sondes that were dropped within the eye and eyewall of the hurricane. The ones closest in time and space were selected (highlighted in Fig. 6, bottom). GDAS is also represented for reference. These figures correspond to temperature and moisture, respectively. Both time difference and distance between the space-based measurement and the dropsonde are shown on the plots. Note that the vertical extent goes to 700 mbar only for this particular aircraft that dropped the sondes. GDAS and MIRS are still reporting retrievals up to 20 and 0.1 mbar. It is found that these comparisons show a rather good agreement between MIRS and the dropsondes, at least for temperature. The differences are indeed well within the intravariability of the sonde measurements themselves described previously. On top of the intravariability and the representativeness issues reported before, the vertical descent of the sonde seems to tend to drift horizontally more drastically within very active regions (see the blue curves on the figures). In contrast, the descent is almost vertical in clear-sky cases. Therefore, although the reported distance at launch location is reported to be 2.6 km for the first sonde for instance, we can see that when reaching the surface, the distance became around 10 km. Again, in fast-moving features like hurricanes, this factor could make a significant difference. For the closest collocation (less than 12 min and less than 3 km in distance), the difference in water vapor is actually also within the previously reported intravariability. When time and distance differences are larger, the moisture differences are larger. But, the errors of representativeness and the vertical drift of the sonde could at least, in part, explain the remaining differences. It is worth mentioning that NCEP GDAS does ingest the dropsonde measurements themselves within its assimilation cycle but not the rain-impacted AMSU/MHS radiances. It is interesting to notice in this case that GDAS analyses are exhibiting similar differences with the dropsondes than the MIRS retrieval does, although this latter is based solely on microwave radiances measured from AMSU and MHS.

VII. Conclusion

We have used cloud- and rain-impacted brightness temperatures in a variational retrieval, using NOAA-18 AMSU and MHS sensors. This was made possible owing to the CRTM forward model, which produces both radiances in all-weather conditions and the corresponding Jacobi for all parameters, including the cloud and hydrometeor parameters. The CRTM is incorporated into a microwave-dedicated retrieval system at NOAA/NESDIS, which is called the MIRS. The MIRS methodology described here is based on treating, in a consistent fashion, all parameters that do impact the measurements. It is also independent from the NWP-related information. The ill-posed nature of the inversion is handled through the use of the eigenvalue decomposition technique which makes the inversion very stable, and a high convergence rate is obtained. It was shown, in an ideal simulation case, that the null space is a limiting factor. This translates into cases where the retrieval process reaches a solution that satisfies the measurements, but that is different from the original in terms of hydrometeor and cloud profiles. Because of this and the limited information content of the radiances, the aim of this retrieval was essentially to target the temperature and moisture profiles as well as the surface parameters in very active regions. The hydrometeor vertical amount profiles help account for the effects they and the other parameters not accounted for explicitly, produce on the measurements (*precip-clearing*). Improvement in the cloud and hydrometeor profiling is however expected, if temperature and moisture profiles are provided externally from accurate NWP forecasts for instance. Designing the retrieval of cloud and hydrometeors in profile form presents a number of advantages, including the avoidance to account explicitly for the cloud top pressure and the cloud thickness, which could, in certain cases, cause instability or oscillation. The

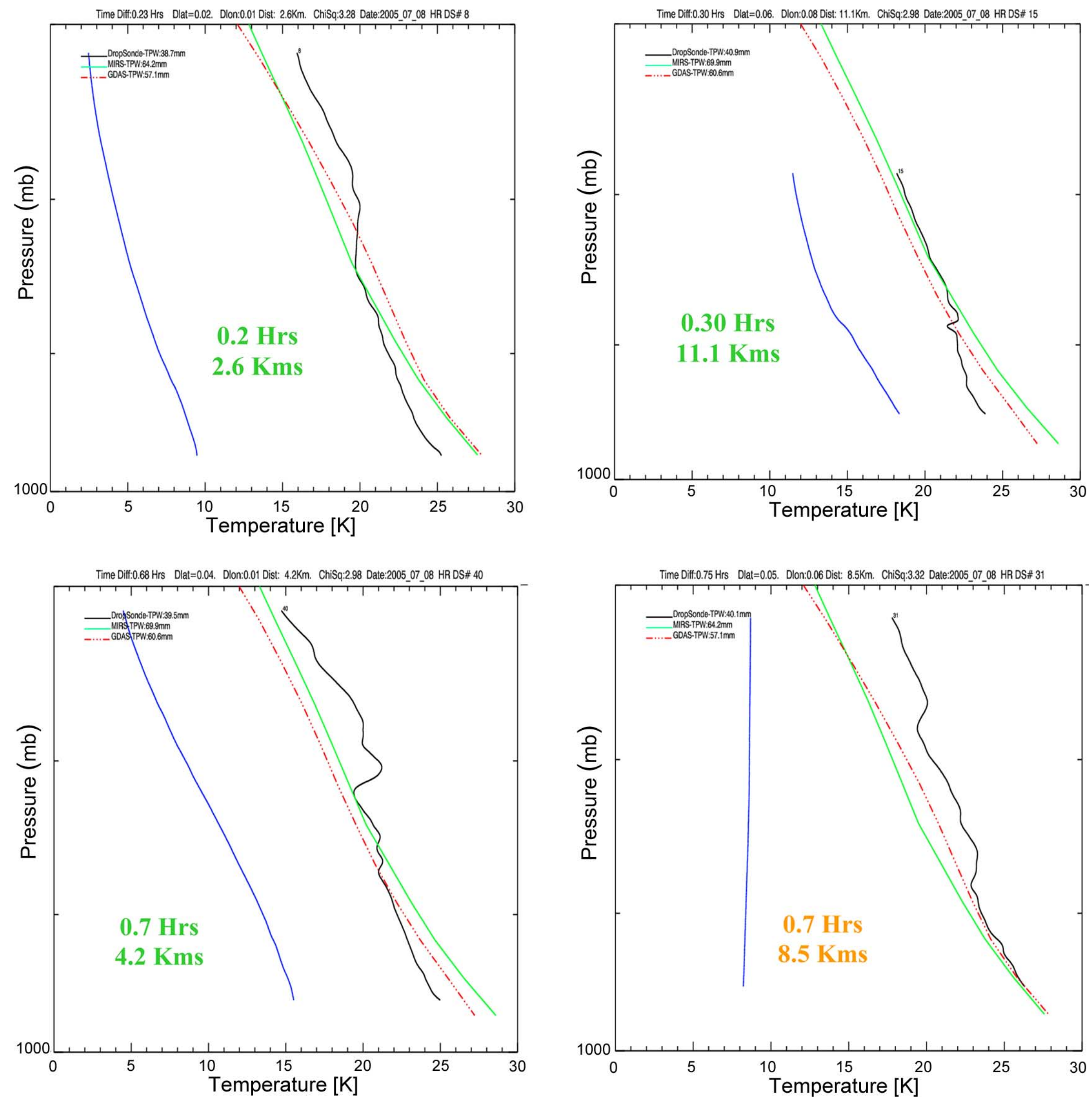

Fig. 10. Case-by-case comparison of temperature profile between 700 mbar and the surface, between (green line) MIRS retrievals, (red line) GDAS analyses, and (black line with fine vertical structures) GPS-dropsonde measurements. The blue line on the left represents the profile of the dropsonde distance drift with respect to the location of the closest satellite measurement. The collocations are within the inner core of the hurricane, as shown in Fig. 6 (lower panel).

designed system could also, in theory, give information about the multilayer nature of the clouds and mixture of phases within the cloud/precipitating layers, provided that enough information in the radiances exists. The retrieval system is used in clear, cloudy, and precipitating conditions. It was shown in simulation and confirmed with the real data that the performances, when applied to clear skies, are not degraded and that the retrieval algorithm is able to reach a zero-amount solution for all the cloud and hydrometeor parameters if the radiances indicate so.

A validation was undertaken in both clear and extremely active conditions by a controlled comparison to measurements by the aircraft GPS-dropsondes, which are taken in the vicinity of hurricane Dennis. We first showed that extreme care must be exercised when attempting validation in these weather events, as very contrasted atmospheric features are moving fast, and therefore, any collocation error in space and/or time could have enormous impact on the comparison between the retrievals and the ground-truth data. The collocation error, which is coupled with the inherent descent time of the dropsondes, thus sampling different parts of separate vertical profiles, would, in fact, be the dominant source of error. This led us to use very strict collocation criteria which, in turn, advocated doing the validation by individual comparisons rather than by computing statistical metrics. Another obvious major source of error is the representativeness error. If the same sensor is looking at different pieces of the atmosphere and this latter is very contrasted with moisture, rain, cloud, falling frozen precipitation, etc., the measurements could be very different. These differences are not due to any retrieval or calibration issues, but simply to inherent to 4-D variations of the atmosphere within the timeframe of the measurements and within the area sampled by these point measurements. Intravariability of the dropsondes themselves was assessed using four individual sondes dropped within

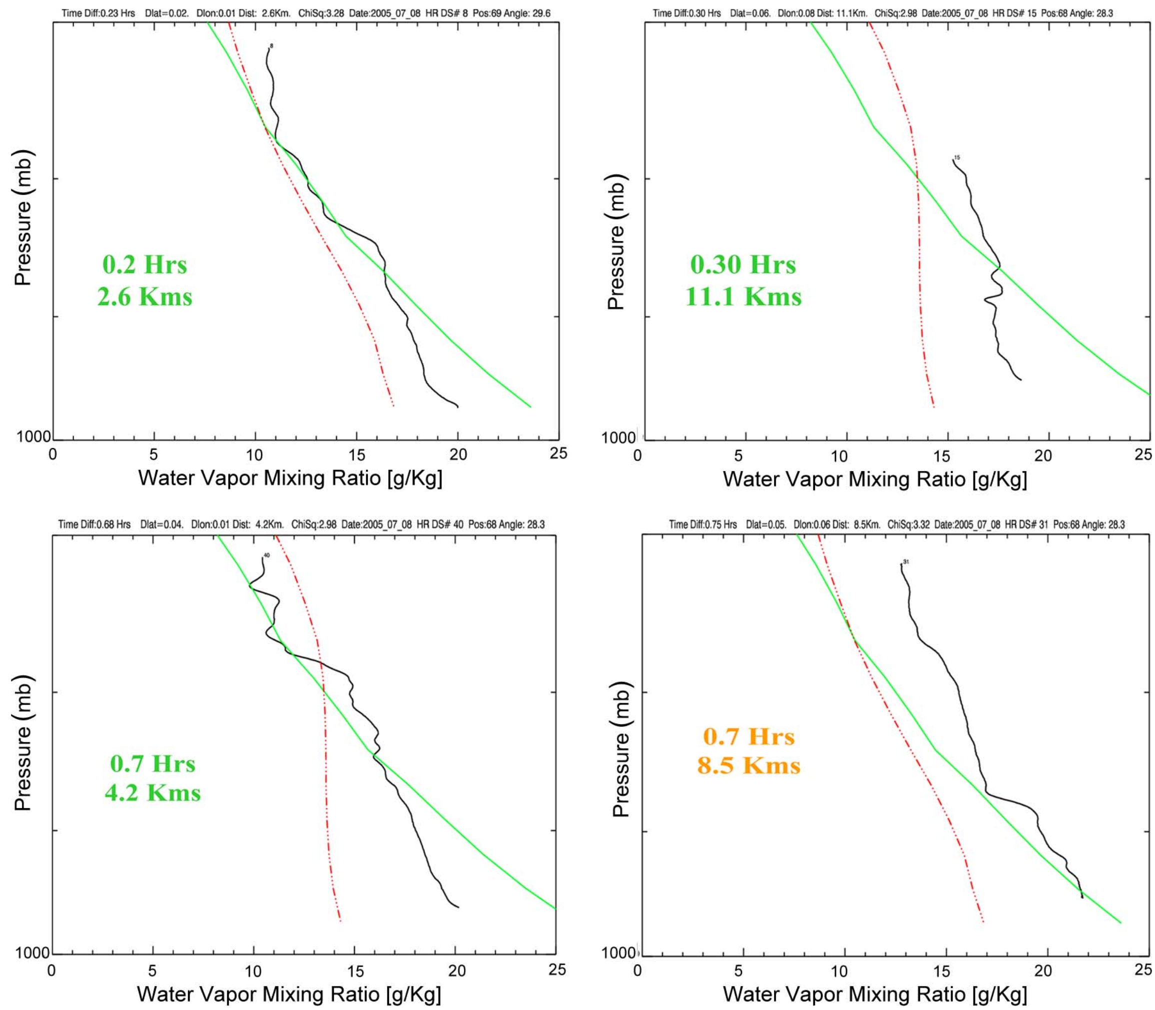

Fig. 11. Same as Fig. 10 except for the water-vapor profile.

10 min and a few kilometers from each other, which gave us an estimate of the lower limit of the differences that we must expect when validating the results.

We also hinted to the importance of the spatial resolution of the measurements which plays a key role in these active areas. To stabilize the sensor gain, the microwave radiometric measurements need to be averaged within an integration time period to reduce the noise level (NedT). This has the effect of reducing the horizontal spatial resolution. It is however acknowledged that this instrument noise is actually buried under other sources of errors such as the modeling error. It is therefore preferable from an assimilation or retrieval stand to have at least, in remote sensing of highly contrasted events (such as hurricanes and coastal boundaries), a higher horizontal spatial resolution with a higher noise rather than a lower spatial resolution with a reduced noise.

For the comparison between the MIRS retrieval and the dropsondes, we focused on two days of hurricane Dennis, corresponding to July 6 and 8, 2005. Results in the clear sky showed that the differences in temperature and water vapor were minimal. The finer vertical structures measured with the dropsondes are, for obvious reasons, not expected to be picked by the retrieval given the broad weighting functions of the sounders. The performances in the eye and the eye wall of the hurricane were shown to be largely within the intravariability of the reference measurements. These performances were comparable to those of GDAS analyses that ingested the dropsondes themselves. The MIRS-retrieved temperature and moisture profiles and the emissivity parameters, in active areas, are expected to produce positive impacts in the subsequent 4DVAR assimilations, the object of a future study. We, indeed, envision that our 1D-VAR, which considers the hydrometeor parameters as part of the retrieved vector instead of hooking it with a cloud model, could be ported into an assimilation system and used in the first part of a 1D-VAR+4DVAR assimilation process.

Acknowledgment

The authors would like to thank S. Feuer and M. L. Black from the HRD of the NOAA Atlantic Oceanographic and Meteorological Laboratory for kindly providing the dropsondes data. The authors would also like to thank the JCSDA CRTM team (Q. Liu, Y. Han, and P. Van Delst) for providing an early version of the radiative transfer model CRTM, and T. Zhu from NOAA/NESDIS for providing the MM5 runs for hurricane Bonnie.

References

[1] E. Andersson *et al.*, “Assimilation and modeling of the atmospheric hydrological cycle in the ECMWF forecasting system,” *Bull. Amer. Meteorol. Soc.*, vol. 86, no. 3, pp. 387–402, Mar. 2005.

[2] N. L. Baker, T. F. Hogan, W. F. Campbell, R. L. Pauley, and S. D. Swadley, “The impact of AMSU-A radiance assimilation in the U.S. Navy’s operational global atmospheric prediction system (NOGAPS),” Naval Research Lab., Washington, DC, NRL/MR/7530–05-8836, 2005.

[3] P. Bauer, E. Moreau, and S. Di Michele, “Hydrometeor retrieval accuracy using microwave window and sounding channel observations,” *J. Appl. Meteorol.*, vol. 44, no. 7, pp. 1016–1032, Jul. 2005.

[4] P. Bauer, E. Moreau, F. Chevallier, and U. O’Keeffe, “Multiple-scattering microwave radiative transfer for data assimilation applications,” *Q. J. R. Meteorol. Soc.*, vol. 131, no. 617, pp. 1–999, Apr. 2005.

[5] P. Bauer, P. Lopez, A. Benedetti, D. Salmond, and E. Moreau, “Implementation of 1D + 4D-VAR assimilation of microwave radiances in precipitation at ECMWF, Part I: 1D-VAR,” *Q. J. R. Soc. Meteorol.*, 2006. submitted for publication.

[6] R. Bennartz and G. W. Petty, “The sensitivity of microwave remote sensing observations of precipitation to ice particle size distributions,” *Q. J. R. Meteorol. Soc.*, vol. 40, no. 3, pp. 245–364, Mar. 2001.

[7] F. Chevallier, P. Bauer, J.-F. Mahfouf, and J. J. Morcrette, “Variational retrieval of cloud profile from ATOVS observations,” *Q. J. R. Meteorol. Soc.*, vol. 128, no. 585, pp. 2511–2525, 2002.

[8] G. Deblonde and S. English, “One-dimensional variational retrievals from SSMI/S-simulated observations,” *J. Appl. Meteorol.*, vol. 42, no. 10, pp. 1406–1420, 2003.

[9] G. Deblonde, J.-F. Mahfouf, B. Bilodeau, and D. Anselmo, “One-dimensional variational data assimilation of SSM/I observations in rainy atmospheres at MSC,” *Mon. Weather Rev.*, vol. 135, no. 1, pp. 152–172, Jan. 2007.

[10] R. M. Errico, L. Fillion, D. Nychka, and Z.-Q. Lu, “Some statistical considerations associated with the data assimilation of precipitation observations,” *Q. J. R. Meteorol. Soc.*, vol. 126, no. 562, pp. 339–359, 2000.

[11] K. F. Evans, J. Turk, T. Wong, and G. Stephens, “A Bayesian approach to microwave precipitation profile retrieval,” *J. Appl. Meteorol.*, vol. 34, no. 1, pp. 260–279, Jan. 1995.

[12] J. R. Eyre, “Inversion of cloudy satellite sounding radiances by nonlinear optimal estimation. I: Theory and simulation for TOVS,” *Q. J. R. Meteorol. Soc.*, vol. 115, no. 489, pp. 1001–1026, Jul. 1989.

[13] R. R. Ferraro, F. Weng, N. C. Grody, L. Zhao, H. Meng, C. Kongoli, P. Pellegrino, S. Qiu, and C. Dean, “NOAA operational hydrological products derived from the Advanced Microwave Sounding Unit,” *IEEE Trans. Geosci. Remote Sens.*, vol. 43, no. 5, pp. 1036–1049, May 2005.

[14] L. Fillion and R. Errico, “Variational assimilation of precipitation data using moist convective parameterization schemes: A 1D-VAR study,” *Mon. Weather Rev.*, vol. 125, no. 11, pp. 2917–2942, Nov. 1997.

[15] N. C. Grody, “Satellite-based microwave retrievals of temperature and thermal winds: Effects of channel selection and *a priori* mean on retrieval accuracy,” in *Remote Sensing of Atmospheres and Oceans*, A. Deepak, Ed. New York: Academic, 1980, pp. 381–410.

[16] T. F. Hock and L. Franklin, “The NCAR GPS dropwindsonde,” *Bull. Amer. Meteorol. Soc.*, vol. 80, no. 3, pp. 407–420, Mar. 1999.

[17] C. Kummerow, Y. Hong, W. S. Olson, S. Yang, R. F. Adler, J. McCollum, R. Ferraro, G. Petty, D.-B. Shin, and T. T. Wilheit, “The evolution of the Goddard profiling algorithm (GPROF) for rainfall estimation from passive microwave sensors,” *J. Appl. Meteorol.*, vol. 40, no. 11, pp. 1801–1820, Nov. 2001.

[18] J. Li, W. Wolf, W. P. Menzel, W. Zhang, H.-L. Hiang, and T. Achtor, “Global sounding of the atmosphere from ATOVS measurements: The algorithm and validation,” *J. Appl. Meteorol.*, vol. 39, no. 8, pp. 1248–1268, Aug. 2000.

[19] C. E. Lietzke, C. Deser, and T. H. Vonder Haar, “Evolutionary structure of the Eastern Pacific double ITCZ based on satellite moisture profile retrievals,” *J. Clim.*, vol. 14, no. 5, pp. 743–751, Mar. 2001.

[20] Q. Liu and F. Weng, “Retrieval of sea surface wind vectors from simulated satellite microwave polarimetric measurements,” *Radio Sci.*, vol. 38, no. 4, pp. 8078–8085, Jul. 2003.

[21] Q. Liu and F. Weng, “One-dimensional variational retrieval algorithm of temperature, water vapor and cloud water profiles from the Advanced Microwave Sounding Unit (AMSU),” *IEEE Trans. Geosci. Remote Sens.*, vol. 43, no. 5, pp. 1087–1095, May 2005.

[22] Q. Liu and F. Weng, “Advanced doubling-adding method for radiative transfer in planetary atmospheres,” *J. Atmos. Sci.*, vol. 63, no. 12, pp. 3459–3465, 2006.

[23] P. Lopez, “Conception et validation d’une parametrisation explicite des hydrometeors de grande-echelle, Evaluation de son potential dans les calculs adjoints,” Ph.D. dissertation, Univ. Paul Sabatier, Toulouse, France, 2001.

[24] A. C. Lorenc, “Development of an operational variational assimilation scheme,” *J. Meteorol. Soc. Jpn.*, vol. 75, no. 1B, pp. 339–346, 1995.

[25] J.-F. Mahfouf, P. Bauer, and V. Marecal, “The assimilation of SSM/I and TMI rainfall rates in the ECMWF 4D-VAR system,” *Q. J. R. Meteorol. Soc.*, vol. 131, no. 606, pp. 437–458, Jan. 2005.

[26] V. Marecal and J.-F. Mahfouf, “Variational retrieval of temperature and humidity profiles from TRMM precipitation data,” *Mon. Weather Rev.*, vol. 128, no. 11, pp. 3853–3866, Nov. 2000.

[27] V. Marecal and J.-F. Mahfouf, “Four dimensional variational assimilation of total column water vapor in rainy areas,” *Mon. Weather Rev.*, vol. 130, no. 1, pp. 43–58, Jan. 2002.

[28] F. S. Marzano, S. Di Michele, A. Tassa, and A. Mugnai, “Bayesian techniques for precipitation profiles retrieval from spaceborne microwave radiometers,” in *Proc. PORSEC*, Dec. 2000, pp. 221–228.

[29] L. M. McMillin, L. J. Crone, and T. J. Kleespies, “Atmospheric transmittance of an absorbing gas. 5. Improvements to the OPTRAN approach,” *Appl. Opt.*, vol. 34, no. 36, pp. 8396–8399, Dec. 1995.

[30] A. P. McNally, J. C. Derber, W.-S. Wu, and B. B. Katz, “The use of TOVS level-1B radiances in the NCEP SSI analysis system,” *Q. J. R. Meteorol. Soc.*, vol. 126, no. 563, pp. 689–724, Jan. 2000.

[31] S. Di Michele, A. Tassa, F. S. Marzano, P. Bauer, and J. P. V. P. Baptista, “Bayesian algorithm for microwave-based precipitation retrieval: Description and application to TMI measurements over ocean,” *IEEE Trans. Geosci. Remote Sens.*, vol. 43, no. 4, pp. 778–791, Apr. 2005.

[32] T. Mo, “Calibration of the Advanced Microwave Sounding Unit-A radiometers for NOAA-N and NOAA-N,” U.S. Dept. Commerce, Washington, DC, NOAA Tech. Rep. NESDIS 106, 2002.

[33] J.-L. Moncet, S. A. Boukabara, A. Lipton, J. Galantowicz, H. Rieu-Isaacs, J. Hegarty, X. Liu, R. Lynch, and N. Snell, “Algorithm theoretical basis document (ATBD) for the Conical-Scanning Microwave Imager/Sounder (CMIS) environmental data records,” in *Core Physical Inversion Module*, vol. 2. Lexington, MA: AER Inc., Mar. 2001. Version 1.4.

[34] E. Moreau, P. Lopez, P. Bauer, A. Tompkins, M. Janiskova, and F. Chevallier, “Variational retrieval of temperature and humidity profiles using rain rates versus microwave brightness temperatures,” *Q. J. R. Meteorol. Soc.*, vol. 130, no. 589, pp. 827–852, 2004.

[35] E. Moreau, P. Bauer, and F. Chevallier, “Variational retrieval of rain profiles from spaceborne passive microwave radiance observations,” *J. Geophys. Res.*, vol. 108, no. D16, 4521, 2003. DOI: 10.1029/2002JD003315.

[36] L. Phalippou, “Variational retrieval of humidity profile, wind speed and cloud liquid-water path with the SSM/I: Potential for numerical weather prediction,” *Q. J. R. Meteorol. Soc.*, vol. 122, no. 530, pp. 327–355, Jan. 1996.

[37] C. Prigent, A. Sand, C. Klapisz, and Y. Lemaitre, “Physical retrieval of liquid water contents in a North Atlantic cyclone using SSM/I data,” *Q. J. R. Meteorol. Soc.*, vol. 120, no. 519, pp. 1179–1207, Jul. 1994.

[38] C. Prigent, L. Phalippou, and S. English, “Variational inversion of the SSM/I observations during the ASTEX campaign,” *J. Appl. Meteorol.*, vol. 36, no. 5, pp. 493–508, May 1994.

[39] C. D. Rodgers, “Retrieval of atmospheric temperature and composition from remote measurements of thermal radiation,” *Rev. Geophys. Space Phys.*, vol. 14, no. 4, pp. 609–624, Nov. 1976.

[40] C. D. Rodgers, “Characterization and error analysis of profiles retrieved from remote sounding measurements,” *J. Geophys. Res.*, vol. 95, no. D5, pp. 5587–5595, Apr. 1990.

[41] A. A. Sinkevich and R. P. Lawson, “A survey of temperature in convective clouds,” *J. Appl. Meteorol.*, vol. 44, no. 7, pp. 1133–1145, Jul. 2005.

[42] E. A. Smith, X. Xiang, A. Mugnai, and G. Tripoli, “Design of an inversion-based precipitation profile retrieval algorithm using an explicit cloud model for initial guess microphysics,” *Meteorol. Atmos. Phys.*, vol. 54, no. 1, pp. 53–78, Mar. 1994.

[43] W. L. Smith and H. M. Woolf, “The use of eigenvectors of statistical co-variance matrices for interpreting satellite sounding radiometer observations,” *J. Atmos. Sci.*, vol. 33, no. 7, pp. 1127–1140, Jul. 1976.

[44] A. Tassa, S. Di Michele, and A. Mugnai, “Cloud model-based Bayesian technique for precipitation profile retrieval from the Tropical Rainfall Measuring Mission Microwave Imager,” *Radio Sci.*, vol. 38, no. 4, 8074, Jun. 2003. DOI: 10.1029/2002RS002674.

[45] A. Tassa, S. Di Michele, A. Mugnai, F. S. Marzano, P. Bauer, and J. P. V. P. Baptista, “Modeling uncertainties for passive microwave precipitation retrieval: Evaluation of a case study,” *IEEE Trans. Geosci. Remote Sens.*, vol. 44, no. 1, pp. 78–89, Jan. 2006.

[46] F. Weng and N. C. Grody, “Retrieval of cloud liquid water using the Special Sensor Microwave Imager (SSM/I),” *J. Geophys. Res.*, vol. 99, no. D12, pp. 2535–2551, Dec. 1994.

[47] F. Weng, Y. Han, P. Van Delst, Q. Liu, T. Kleespies, B. Yan, and J. Le Marshall, “JCSDA Community Radiative Transfer Model (CRTM),” in *Proc. 14th TOVS Conf.*, Beijing, China, 2005.

[48] F. J. Wentz and R. W. Spencer, “SSM/I rain retrievals within a unified all-weather ocean algorithm,” *J. Atmos. Sci.*, vol. 55, no. 9, pp. 1613–1627, May 1998.

[49] D. Zhou, W. L. Smith, X. Liu, J. Li, A. M. Larar, and S. A. Mango, “Tropospheric CO observed with the NAST/I retrieval methodology, analyses and first results,” *Appl. Opt.*, vol. 44, no. 15, pp. 3032–3044, 2005.

[50] H. Liebe, G. Hufford, and T. Manabe, “A model for the complex permittivity of water at frequencies below 1 THz,” *Int. J. Infrared Millim. Waves*, vol. 12, pp. 659–675, 1991.

Sid-Ahmed Boukabara (SM’06) received the Ingénieur degree in electronics and signal processing from the National School of Civil Aviation, Toulouse, France, in 1994, the M.S. degree from the National Polytechnic Institute of Toulouse, Toulouse, in 1994, and the Ph.D. degree in remote sensing from the Denis Diderot University, Paris, France in 1997.

He is currently with the I.M. Systems Group, Inc., NOAA/NESDIS/STAR, Camp Springs, MD. His principal areas of interest are atmospheric and surface radiative transfers modeling, spectroscopy, and retrieval processes.

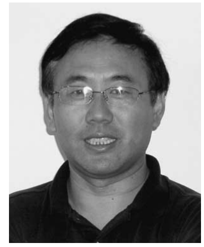

Fuzhong Weng received the Master’s degree in radar meteorology from the Nanjing Institute of Meteorology, Nanjing, China, in 1985 and the Ph.D. degree from Colorado State University, Fort Collins, CO, in 1992. AQ1

He is currently with NOAA/NESDIS/STAR, Camp Springs, MD. He is a leading expert in developing various NOAA operational satellite microwave products and algorithms such as Special Sensor Microwave Imager and Advanced Microwave Sounding Unit cloud and precipitation algorithms, land surface temperature, and emissivity algorithms. He is developing new innovative techniques to advance uses of satellite measurements under cloudy and precipitation areas in numerical weather prediction models.

Quanhua Liu received the B.S. degree from the Nanjing Institute of Meteorology, Nanjing, China, in 1981, the Master’s degree in physics from the Chinese Academy of Science, Beijing, China, in 1984, and the Ph.D. degree in marine science from the University of Kiel, Kiel, Germany, in 1991. AQ2

He is with the Joint Center for Satellite Data Assimilation. His primary interests are radiative transfer theory, retrieval methodology, and applications of the satellite data. AQ3

AUTHOR QUERIES

AUTHOR PLEASE ANSWER ALL QUERIES

AQ1 = Please specify the type of degree earned.
AQ2 = Please specify the type of degree earned.
AQ3 = Is this the current affiliation? Please provide location.

END OF ALL QUERIES

Passive Microwave Remote Sensing of Extreme Weather Events Using NOAA-18 AMSUA and MHS

Sid-Ahmed Boukabara, *Senior Member, IEEE*, Fuzhong Weng, and Quanhua Liu

***Abstract*—The ability to provide temperature and water-vapor soundings under extreme weather conditions, such as hurricanes, could extend the coverage of space-based measurements to critical areas and provide information that could enhance outcomes of numerical weather prediction (NWP) models and other storm-track forecasting models, which, in turn, could have vital societal benefits. An NWP-independent 1D-VAR system has been developed to carry out the simultaneous restitutions of atmospheric constituents and surface parameters in all weather conditions. This consistent treatment of all components that have an impact on the measurements allows an optimal information-content extraction. This study focuses on the data from the NOAA-18 satellite (AMSUA and MHS sounders). The retrieval of the precipitating and nonprecipitating cloud parameters is done in a profile form, taking advantage of the natural correlations that do exist between the different parameters and across the vertical layers. Stability and the problem's ill-posed nature are the two classical issues facing this type of retrieval. The use of empirically orthogonal-function decomposition leads to a dramatic stabilization of the problem. The main goal of this inversion system is to be able to retrieve independently, with a high-enough accuracy and under all conditions, the temperature and water-vapor profiles, which are still the two main prognostic variables in numerical weather forecast models. Validation of these parameters in different conditions is undertaken in this paper by comparing the case-by-case retrievals with GPS-dropsondes data and NWP analyses in and around a hurricane. High temporal and spatial variabilities of the atmosphere are shown to present a challenge to any attempt to validate the microwave remote-sensing retrievals in meteorologically active areas.**

***Index Terms*—Atmospheric sounding, data assimilation, dropsonde, hurricane, microwave remote sensing, retrieval algorithm.**

I. Introduction

PASSIVE microwave data measured in meteorologically active areas carry a wealth of information on the hydrometeors as well as on the temperature and water-vapor profiles. The assimilation of these space-based measurements, in either geophysical or radiometric form, could help the numerical weather prediction (NWP) models in the analysis and forecast stages by giving information about actual cloud and precipitation, thus reducing the spin-up problem that usually impacts the beginning of the forecast period [1]. The effect of the hydrometeors on the brightness temperatures measured by the microwave sensors may be negligible, significant, or something in between depending on the spectral region considered and on the type and intensity of the precipitation, making these millimeter-wave sensors an ideal tool to probe the active areas. This effect also depends, in certain cases, on the thermodynamic temperature as this changes the dielectric properties and, therefore, the absorption of the water, and on the atmospheric water vapor, above and within the active area, as this has a screening effect on the sensitivity to cloudy layers, all of which advocate for having a consistent treatment of the atmospheric profiles of temperature, water vapor, and hydrometeors. For this purpose, a physical retrieval algorithm has been developed based on a radiance assimilation-type technique to invert simultaneously the vertical profiles of temperature, water vapor, nonprecipitating cloud, and liquid and frozen precipitating hydrometeor parameters. The surface boundary layer is also treated dynamically by including the surface-emissivity spectrum and the skin temperature as part of the control-parameter vector. Optionally, the inversion of surface pressure could also be triggered under certain conditions, otherwise obtained from the background (fixed value). The information content in the radiances is however limited. This is alleviated by performing the retrieval in a mathematically reduced space which stabilizes the retrieval significantly. However, stability of the retrieval does not eliminate the null space: existence of multitude solutions that fit equally well the radiances. In other words, including the hydrometeors in the retrieved state vector increases the number of degrees of freedom in the solution-finding process. It is important to note that these degrees of freedom are also due to the limited number of channels available. Adding hypothetical channels would theoretically put additional constraints on the solution finding and reduce these degrees of freedom.

This null space is the main reason why the stated goal of this study is primarily the sounding of temperature and humidity and, to a lesser degree, the surface sensing under extreme weather events. The cloud and precipitating parameters are part of the retrieval process mainly to absorb the effects they have on the raw measurements.

The microwave sensors AMSU and MHS onboard NOAA-18, which contain a combination of semiwindow and sounding channels, will be used to test this retrieval algorithm.

Manuscript received June 1, 2006; revised February 8, 2007. The views expressed here are those of the authors and do not necessarily represent those of the National Oceanic and Atmospheric Administration.

S.-A. Boukabara is with the I.M. Systems Group, Inc. at NOAA/NESDIS/STAR, Camp Springs, MD 20746 USA (e-mail: Sid.Boukabara@noaa.gov).

F. Weng is with NOAA/NESDIS/STAR, Camp Springs, MD 20746 USA (e-mail: Fuzhong.Weng@noaa.gov).

Q. Liu is with QSS Group Inc. at NOAA/NESDIS/STAR, Camp Springs, MD 20746 USA (e-mail: Quanhua.Liu@noaa.gov).

Color versions of one or more of the figures in this paper are available online at http://ieeexplore.ieee.org

Digital Object Identifier 10.1109/TGRS.2007.898263

Note that the approach will sometimes be purposefully labeled assimilation and sometimes retrieval across the remainder of this paper. Assimilation of radiances amounts indeed to a retrieval, the retrieved parameters being the control parameters. The difference resides in the reliance on an existing analysis used as first guess and background to which the retrievals are constrained (or assimilated). But, it is important to state at this stage that no NWP information is used in this system (forecast or analysis). As will be described later, the background constraints will be built offline based on climatology. On the radiance level, all channels are used simultaneously in order to obtain a retrieval that satisfies all measurements together. This study should be viewed as an attempt to treat the whole geophysical state vector, including hydrometeors in a consistent fashion, but relying on the radiometric signal only, as we do not use the cloud/convective schemes either to generate hydrometeors from the temperature and the water vapor as other studies chose to do [5], [9], [27]. Nonprecipitating cloud and hydrometeors are thus treated from a pure radiometric-signal stand, just like the water vapor, temperature, emissivity, and skin temperature.

The next section reviews the previous studies that dealt with assimilating rain-impacted microwave measurements either within an NWP context or not, followed by Section III describing the retrieval system used in this paper. The latter also briefly describes the different components used within the 1D-VAR system, including the forward radiative operator. Section IV focuses on describing the instrumental configuration, while Section V takes a look at the expected performances in a simulation setting. Section VI deals with describing the real data that we will be using, including the GPS-dropsondes, and lays out the validation results.

II. Review of Rainy Data Assimilation and Retrieval

Microwave-based assimilation of radiance measurements is not new; NWP centers have routinely or experimentally assimilated the clear-sky radiometric data as well as the microwave-retrieved products and have more recently directly assimilated the radiances measured in cloudy and precipitating conditions [5], [9], [30].

Microwave measurements have also been used extensively for the retrieval of cloud, rain, and other precipitating parameters, either with relatively simple regression-based algorithms or with more physically based algorithms, similar to those used in NWP assimilation. Numerous sensors have been used for measuring cloud and precipitation: SSM/I, TRMM/TMI, AMSU/MHS, and AMSR-E are among them [13], [17], [48]. Improvements have recently been made in this field of assimilating the cloud- and rain-impacted microwave radiances into NWP models as well as in the microwave remote sensing of cloud and hydrometeor parameters. These two problems are, in fact, similar in nature. The former (NWP assimilation) attempts to fit the impacted radiances by adjusting the temperature and water-vapor profiles and, along the way, generates the cloud/hydrometeor parameters (usually, by incorporating the cloud and convective schemes). The latter (hydrometeors retrieval) is based also on finding the hydrometeors (or integrated amount) that fit the radiances either through an Look-Up-Table (LUT) search or through a variational technique and, along the way, need to account, somehow, for the temperature and water-vapor profiles. The physical inversion approach was found to be superior in retrieving quantities (such as rainfall rate) using the regression-based algorithms. One obvious reason is that a physical retrieval can adapt dynamically to the particular circumstance and is more likely to distinguish the precipitation signal from the water vapor and temperature signals. We exclusively focus on the physical approaches in this review.

A. *Classification via Handling the Ill-Posed Nature*

The inversion of cloudy/rainy radiances into the geophysical space is a notoriously ill-posed problem. Several physical approaches have been tried in the past to add external constraints and, therefore, stabilize the problem. Some approaches are based on precomputation of hydrometeor profiles and their corresponding radiances. The retrieval, thus, becomes a residual minimization procedure which aims at finding the closest precomputed profile to match the measurements [17], [31], [44]. Others rely on the NWP forecast outputs and associated cloud and convective schemes to constrain the temperature and water vapor as well as their relationship to the cloud and hydrometeor parameters [5], [9], [26], [27], [35]. As mentioned earlier, the present study employs the empirically orthogonal-function (EOF) decomposition technique to all vertical profiles, including the hydrometeors as well as to the surface emissivity vector, in order to constrain the inversion problem. The use of background covariances, which are computed offline and independently from the NWP forecast data, constitutes an additional constraint to the problem, in addition to introducing physical consistency between the retrieved parameters.

B. *Bayesian Approach*

Tassa *et al.* [44] developed a Bayesian algorithm to retrieve surface precipitation and cloud profiles over the ocean. The training is done using a combination of outputs from a mesoscale microphysical model and a 3-D radiative transfer model (RTM). This method is similar to that adopted by Evans *et al.* [11], Kummerow *et al.* [17], and Marzano *et al.* [28]. In these algorithms, the retrieval is done by selecting, among the precomputed profiles, those that minimize the residuals with the measurements at hand. This strongly depends on the cloud/radiation database and does not account for the local variabilities of temperatures, water-vapor profiles, and surface emissivity that could equally impact the brightness temperatures. This method typically applies to the cloudy/rainy conditions. The clear-sky case is screened out in the preprocessing stage. Preclassification of precipitating events based on the nature (stratiform/convective) or intensity (moderate/intense) is usually performed. In [45], the important parameters that do impact the brightness temperatures, but are not part of the searched parameters, are used to generate a sensitivity matrix which is used as an upper threshold limit to the residual minimization process. These factors include size distribution, density, shape, and phase for the hydrometeors. This matrix could also be used in variational analyses but was not in that study. Di Michele *et al.* [31] developed a Bayesian retrieval algorithm named Bayesian algorithm for microwave precipitation retrieval (BAMPR) that they compared to the Goddard profiling (GPROF) algorithm. Despite the similar approaches between the retrieval approaches, they found that their results differ, and those differences were attributed mainly to the training datasets and the cloud classification.

C. *1D-VAR Approach*

Eyre [12] used a variational technique (labeled equivalently estimation-theory solution) for atmospheric sounding which he applied to the microwave and infrared data from TIROS Operational Vertical Sounder (TOVS). Besides temperature and moisture, cloud amount and top pressure were also retrieved. Surface pressure, temperature, and emissivity were also allowed to vary. A damping term was introduced in the solution for certain parameters to stabilize the retrieval process after an oscillatory behavior was noticed. This consisted of a diagonal matrix with unity values except for those parameters causing the instability, amounting to an effective reduction of their variances. Eyre [12] studied the effect of assuming a single layer cloud model by simulating the mixed clouds. He found that the system was able to find an effective cloud amount and vertical location to compensate for the mixed cloud nature. It is interesting to highlight that he reported also that the effects of the effective cloud-parameter retrieval had little impact on the temperature and humidity profiles.

The standard use of 1D-VAR algorithms for the inversion of microwave data relies on using a background covariance matrix. This was shown to have limitations in the case of cloud and rain, as their variances will inevitably be large which would amount to an absence of constraint [37], [38]. In this latter study, a physical retrieval of moisture, cloud, wind speed, and rain was applied to SSM/I, and a spatial smoothing was adopted, attributing the horizontal variability exclusively to cloud structures.

In their 1996 study, Phalippou *et al.* introduced a 1D-VAR algorithm for the clear and cloudy skies for an SSM/I configuration and highlighted its potential for the NWP. It later became operational at ECMWF. The integrated amount of cloud liquid was made to vary as a scaling factor for the retained vertical structure (the output of the ECMWF cloud scheme was assumed). This approach cannot easily be extended to sounding configurations as the cloud structure severely alters the vertical weighting functions [21]. Moreover, the absorption of the cloud is also dependent, through the dielectric constant, on the temperature of the cloudy layer [50] which places some importance on the location of the cloud within the vertical temperature profile. An error in the temperature location is likely to translate into an error in the resulting liquid total amount. Chevallier *et al.* [7] demonstrated the proof of concept of a 1D-VAR algorithm that could be used to assimilate clouds data. A fast RTM was developed along with its adjoint operator. It was applied to the advanced TOVS data. Deblonde and English [8] also used a variational algorithm for the cloudy but nonprecipitating conditions, similar to that of [36], except that an alternative method was tested where the total-water-content profile was retrieved and, then, split into humidity and liquid using an empirical function. A higher rate of divergence was reported using this approach particularly in the clear-sky cases, but improved temperature retrieval performances were found using this method in cloudy skies.

Liu and Weng [21] more recently proposed a multistep variational algorithm that retrieved temperature, moisture, and cloud profiles in all-weather conditions. NCEP forecasts were used as background, and regression-based algorithms were used to produce the first guess for temperature and humidity profiles. Surface wind and pressure were also taken from the NCEP-forecast data. The integrated amount of cloud liquid was found to be consistent with the original value but that the profile presented differences due to the limited information content. To constrain the problem and make the retrieval more stable, hydrometeor profiles were modeled in an oversimplified fashion. The present study could be viewed as an upgrade to the study of Liu and Weng where the stability and information-content issues are handled through the EOF decomposition which also removed the need to have a multistep approach.

D. *1D-VAR + Cloud Models Approach*

Cloud models have started recently to become part of the 1D-VAR schemes to force consistency between the temperature and humidity profiles on one hand and the cloud and other hydrometeor profiles on the other hand. Direct measurements of brightness temperatures in rainy conditions started being assimilated, first, at ECMWF [5] where low-frequency SSM/I channels were assimilated and, then, experimentally at MSC [9]. The first step in these two stage approach (1D-VAR + 4DVAR) consists of a 1D-VAR algorithm that incorporates moist physical schemes in its forward operator, which computes the hydrometeor profiles (cloud, ice, rain, and snow) from the profiles of temperature and water vapor.

Moreau *et al.* [35] developed a 1D-VAR algorithm to retrieve the rain profiles with ECMWF model outputs used to produce the first guess for temperature and humidity and a cloud/convective scheme used to relate them to hydrometeors. However, frozen hydrometeors were excluded in their experiment which was mitigated by the choice of low-frequency channels only.

Moreau *et al.* [34] compared the performances of two 1D-VAR-based retrievals of temperature and humidity profiles from the passive TRMM and SSM/I data measured in rainy areas. The first uses classically retrieved rainfall rate as input, while the second uses directly the brightness temperatures. Both use, besides an RTM, simplified convective and large-scale condensation parameterization. They found that problems with the convergence arise when background precipitation is generated through convection and not by large-scale processes.

Bauer *et al.* [3] studied the performances of the cloud retrieval using the European Global Precipitation Mission configuration. They used the ECMWF short-term forecast profile of temperature and humidity for the initialization of the first guess. The hydrometeor first guess and background combines the temperature and humidity profiles with cloud and convective model schemes, following a similar approach implemented in [35]. In their study, surface emissivity and temperature were fixed to climatologic values and not part of the control vector. The temperature and water vapor were not part of the control vector either, as the purpose was to assess the accuracy of hydrometeor retrieval only. For this reason, the forward operator consisted of an RTM only (no convective or cloud scheme). Deblonde *et al.* [9] incorporated the ECMWF approach into the Canadian 1D-VAR assimilation system of the SSM/I retrieved rainfall rates or brightness temperatures. The resulting integrated water-vapor amount is assimilated in a 4DVAR assimilation scheme.

E. On the Use of Cloud and Convective Schemes in 1D-VAR

For it to work in a 1D-VAR context, the cloud and convective schemes employed need to be simplified and made less nonlinear which raises the question of their accuracy. Their adjoint model needs also to be developed and incorporated. This can be computed analytically (usually, for the simplified schemes) or by finite difference (usually, for the full moist physical schemes). The RTM would need to be coupled with the cloud schemes, and therefore, their uncertainties need to be accounted for. Deblonde *et al.* [9] questioned the usefulness of using a deep-convection scheme for the assimilation of cloudy/rainy radiances because of its high nonlinearity. The equivalent error was found to have a very large spread in cases where deep convection dominated. The inputs also need to be simplified as cloud models do normally depend also on time trends of radiation and vertical diffusion produced by the dynamical and other physical processes. In the same study, it was highlighted that using shallow convective scheme to produce cloud water content in the 1D-VAR actually degraded the comparison with the algorithm of Weng and Grody [46]. It was further shown that the deep convective scheme deteriorated the fit between the modeled and observed brightness temperatures, which shows that the cloud model schemes are far from being accurate, and their corresponding errors need to be accounted for in the 1D-VAR assimilation when used, along with the RTM errors. Contrary to RTMs, cloud models are very different and produce nonsimilar results in most cases. If these differences and impacts of linearization and simplifications are accounted for, the resulting errors that a 1D-VAR must use might amount to not constraining the retrieval. Moreover, cloud schemes have been documented to be sometimes locally biased, in need of tuning, and are by no means accurate in their relationship between the temperature (T) and humidity (Q) profiles on one hand and the cloud (C) and hydrometeor (H) profiles on the other. Their use carries a set of uncertainties that would need to be accounted for in the error covariance matrix, which would defeat, at least partially, the purpose of using them as a means to constraint the retrieval.

III. Retrieval/Assimilation System

A. Suggested Approach

In this paper, we have adopted an approach that relies exclusively on the direct-impact signatures of hydrometeors on the brightness temperatures. The natural correlations between the cloud and hydrometeor parameters are included in the system, through the development of a covariance matrix that puts constraints on the independence of these parameters, between themselves across the layers as well as between the parameters. Separate retrievals treating parameters independently cannot, for obvious reasons, ensure that these retrieved parameters will be consistent, all at once, with the measured radiances [37], [38]. For this reason, in the approach adopted, all channels, including window and sounding channels, are used simultaneously in order to retrieve all parameters together. The use of sounding channels was shown to present many advantages in precipitation probing, including their lesser sensitivity to surface emittance and their ability to slice the cloud profile vertically [3].

The effects of clouds could potentially improve the temperature retrieval of the cloudy layer rather than degrade it, due to the increased absorption in that layer and, therefore, increased sensitivity. Eyre [12] argues that retrievals that remove the effects of clouds in preprocessing stages only degrade the retrievals. This all-channel–all-parameter approach allows an optimal extraction of information from the measurements. It is also beneficial to use all channels together with sensitivity to a wider range of precipitation amount [1] rather than a selective channel set. The retrieval of cloud and hydrometeors in a profile form presents some nice features, including avoiding in carrying the cloud top and thickness in the state vector which usually presents some instability, when these values cross the vertical-level boundaries. It can also provide information about the multilayer nature of the cloud. Frozen and liquid profiles are both retrieved in profile form, which means that at any given layer, it is possible that we could get a mixture of these phases. This, of course, would assume that we have enough radiometric signal to distinguish them without ambiguity. With this approach: 1) Reliance on a moist physics model to relate the temperature and water vapor to the cloud and hydrometeor profiles is avoided, which allows 2) saving time by using only the RTM to project the geophysical space into the radiance space; 3) derivatives are all computed through the RTM adjoint, and no derivation of the cloud model is needed with its additional cost; 4) measurement errors, which are essential for the 1D-VAR, need only to be estimated for the instrumental noise and the RTM uncertainty. Uncertainties associated with the cloud physics modeling are therefore avoided; 5) dependence of the resulting retrievals on NWP-specific information (forecast) and/or convection scheme is also avoided. It is recognized that the cause-to-effect type of relationship between the T and Q profiles on one hand and the C and H profiles on the other is no longer hard coded through a cloud scheme coupled with the RTM such as in the studies aforementioned. These constraints are however indirectly present, although loosely, through the background covariance matrix to ensure consistency, the same way that the temperature layers are being constrained to produce a physically realistic temperature profile overall without a direct scheme that relates each layer temperature to the others. This mechanism can take advantage of known relationships between the hydrometeor formation and the nonatmospheric variables. We emphasize that the retrieved cloud and hydrometeor profiles should be viewed as an effective product that, radiometrically, represent the effects of a conglomerate of parameters that have been reported to have significant impacts on brightness temperatures. These include the following:

1) beam-filling effect;
2) shape of the particles and droplets;
3) their orientation;
4) their density;
5) volume mixture rate of liquid and frozen matters;
6) particle size distribution;
7) vertical distribution of all of the above [6];
8) 3-D cloud and rain effects or nonvalidity of plane-parallel assumption;
9) differences between the air temperature and the frozen/liquid water phases temperatures.

Using these effective profiles in the retrieval is a result of the recognition that we cannot realistically claim to be able to retrieve accurately so many parameters with the available number of channels, without too heavily relying on the external data. We will call this handling of precipitation parameters, for the purpose of retrieving temperature and humidity, a *precip-clearing* procedure, as it effectively amounts to clearing the effects of these precipitation parameters from the retrievals of temperature and moisture profiles. We emphasize that this *precip-clearing* is highly nonlinear as it accounts for the effects of precipitation, not at the radiance level, but by accounting for the hydrometeors themselves as part of the retrieved state vector within the retrieval iterations.

B. Description

The 1D-VAR system used in this paper is labeled the microwave integrated retrieval system (MIRS). The retrieval of the precipitating and nonprecipitating cloud parameters is done in a profile form as said before, along with the temperature and humidity profiles. A 100-layer pressure grid is used ranging from 1050 to 0.1 mbar. Layers below the surface are disabled before the retrieval is triggered and do not play any role. The humidity, cloud, and hydrometeor parameters are actually retrieved in the natural logarithm space. This has the advantages of 1) avoiding the nonphysical negative values and 2) making their probability density functions (pdfs) more Gaussian, which is a necessary mathematical condition, as will be described later. To alleviate the limited information content available in the instruments at hand, the inversion is performed in a reduced eigenvalue space as mentioned before, which makes the retrieval process stable and mathematically consistent; the number of EOFs used in the retrieval is less or equal to the number of channels available.

C. Mathematical Basis

The mathematical basis of MIRS is a proven and widely used variational approach described in [39]. We will briefly review it here for the purpose of showing that it is valid in precipitating conditions as well. We will follow the probabilistic approach as it will highlight the only three important assumptions made for this type of retrievals, namely, the local linearity of the forward problem, the Gaussian nature of both the geophysical state vector and the errors associated with the forward model and the instrument noise, and finally, that the measurements and the forward operator are nonbiased to each other. It is important to keep in mind that the variational, Bayesian, optimal estimation theory, and maximum probability are all the same solutions (if the same assumptions are made), although reached through different paths. The following will link the probabilistic approach to the variational solution which seeks to minimize a cost function. Intuitively, the retrieval problem amounts in finding the geophysical vector X which maximizes the probability of being able to simulate the measurement vector Y^{m} using X as an input and using Y as the forward operator. This translates mathematically into maximizing $P(X|Y^{\mathrm{m}})$.

The Bayes theorem states that the joint probability $P(X,Y)$ could be written as

$$P(X,Y) = P(Y|X) \times P(X) = P(X|Y) \times P(Y).$$

Therefore, the retrieval problem amount to maximizing

$$P(X|Y^{\mathrm{m}}) = \frac{P(Y^{\mathrm{m}}|X) \times P(X)}{P(Y^{\mathrm{m}})}.$$

X is assumed to follow a Gaussian distribution

$$P(X) = \exp\left[-\frac{1}{2}(X - X_0)^T \times B^{-1} \times (X - X_0)\right]$$

where X_0 and B are the mean vector (or background) and covariance matrix of X, respectively. Ideally, the probability $P(Y^{\mathrm{m}}|X)$ is a Dirac-Delta function with a value of zero except for X. Modeling errors and instrumental noises all influence this probability. For simplicity, it is assumed that the pdf of $P(Y^{\mathrm{m}}|X)$ is also a Gaussian function with $Y(X)$ as the mean value (i.e., the errors of modeling and instrumental noise are nonbiased), which could be written as

$$P(Y^{\mathrm{m}}|X) = \exp\left[-\frac{1}{2}(Y^{\mathrm{m}} - Y(X))^T \times E^{-1} \times (Y^{\mathrm{m}} - Y(X))\right].$$

E is the measurement and/or modeling error covariance matrix. Maximizing $P(X|Y^{\mathrm{m}})$ is a minimization of $-\log(P(X|Y^{\mathrm{m}}))$ which could be computed from the previous equations as

$$J(X) = \left[\frac{1}{2}(X - X_0)^T \times B^{-1} \times (X - X_0)\right] + \left[\frac{1}{2}(Y^{\mathrm{m}} - Y(X))^T \times E^{-1} \times (Y^{\mathrm{m}} - Y(X))\right].$$

$J(X)$ is called the cost function which we want to minimize. The first right term J_{b} represents the penalty in departing from the background value (*a priori* information), and the second right term J_{r} represents the penalty in departing from the measurements. The solution that minimizes this two-term cost function is sometimes referred to as a constrained solution. The minimization of this cost function is also the basis for the variational analysis retrieval. In theory, one could also find another optimal cost function for a non-Gaussian distribution and nonlinear problems. It is just not as a straightforward problem. The solution that minimizes this cost function is easily found by solving for

$$\frac{\partial J(X)}{\partial X} = J^{'}(X) = 0$$

and assuming local linearity around X, which is generally a valid assumption if there is no discontinuity in the forward operator

$$Y(X_0) = Y(X) + K[X_0 - X].$$

K, in this case, is the Jacobian or derivative of Y with respect to X. This results into the following departure-based solution:

$$\begin{aligned}(X - X_0) &= \Delta X \\ &= \left\{(B^{-1} + K^T E^{-1} K)^{-1} K^T E^{-1}\right\} \\ &\quad \times \left[Y^{\mathrm{m}} - Y(X_0)\right].\end{aligned}$$

If the previous equations are ingested into an iterative loop, each time assuming that the forward operator is linear, we end up with the following solution to the cost-function minimization process:

$$\begin{aligned}\Delta X_{n+1} = &\left\{\left(B^{-1} + K_n^T E^{-1} K_n\right)^{-1} K_n^T E^{-1}\right\} \\ &\times \left[(Y^{\mathrm{m}} - Y(X_n)) + K_n \Delta X_n\right]\end{aligned}$$

where n is the iteration index. The previous solution could be rewritten in another form after matrix manipulations

$$\begin{aligned}\Delta X_{n+1} = &\left\{B K_n^T \left(K_n B K_n^T + E\right)^{-1}\right\} \\ &\times \left[(Y^{\mathrm{m}} - Y(X_n)) + K_n \Delta X_n\right].\end{aligned}$$

The latter is more efficient as it requires the inversion of only one matrix. At each iteration n, we compute the new optimal departure from the background given the derivatives as well as the covariance matrices. This is an iterative-based numerical solution that accommodates moderately nonlinear problems or/and parameters with moderately non-Gaussian distributions. This approach to the solution is generally labeled under the general term of physical retrieval and is also employed in the NWP assimilation schemes along with the horizontal and temporal constraints. The whole geophysical vector is retrieved as one entity, including the temperature, moisture, and hydrometeor atmospheric profiles as well as the skin surface temperature and emissivity vector, ensuring a consistent solution that fits the radiances.

D. Forward Model

This type of inversion of cloudy/rainy radiances supposes the use of a forward operator that can simulate the multiple scattering effects due to ice, rain, snow, graupel, and cloud liquid water at all microwave frequencies and generate the corresponding Jacobians for all atmospheric and surface parameters. The forward operator used in this paper is the community RTM (CRTM) developed at the Joint Center for Satellite Data Assimilation (JCSDA) [47]. CRTM produces radiances as well as Jacobi, for all geophysical parameters. It is valid in clear, cloudy, and precipitating conditions. Derivatives are computed using K-matrix developed by tangent linear and adjoint approaches. This is ideal for retrieval and assimilation purposes. The different components of CRTM briefly are the optical-path-transmittance (OPTRAN) fast atmospheric absorption model [29], the NESDIS microwave emissivity model [20], and the advanced doubling adding radiative transfer solution for the multiple-scattering modeling [22].

E. Covariance Matrix and Background

The covariance matrix plays an important role in variational algorithms. Lopez [23] estimated an error covariance matrix of cloud and rain from the French global model ARPEGE. Chevallier *et al.* [7] simply defined an empirical covariance matrix of clouds with large errors. Moreau *et al.* [35] used the regular covariance matrix of temperature and humidity which they convolved with moist convection and large-scale condensation schemes to produce an ensemble of rain water and cloud profiles. This covariance was computed for each grid point. In this paper, the part of the covariance matrix B related to temperature and humidity is based on a set of globally distributed radiosondes (known as the NOAA-88 set) containing more than 8000 individual profiles, mostly over islands. The impact of using a different covariance has not been tested, but we expect that a more representative dataset could improve the retrieval performances. The exact formula used to compute these covariances is given as

$$\sigma_{ij}^2 = \frac{1}{N} \sum_{i=1}^{N} \sum_{j=1}^{N} (x_i - \overline{x_i}) \times (x_j - \overline{x_j})$$

where σ_{ij} is one of the elements of the matrix corresponding to row i and column j. N is the number of profiles used, and $\overline{x}$ is the average value along the row or along the column.

The part related to the cloud parameters is, for practical reasons, also built independently offline. These statistics are generated from a multitude runs (three time-consecutive fields) based on the fifth generation mesoscale model (MM5) simulations, corresponding to hurricane Bonnie (1998), with 4-km resolution and 23 vertical levels, which are extrapolated to the internal pressure grid of MIRS (100 layers).

The ability of these runs to represent the hydrometeors' global variability is not fully established, but this is believed to be accurate enough for the case of hurricanes and tropical storms. Impact studies (not shown) were also performed and showed that the system is able to reach convergence (therefore, a radiometric solution) in many conditions that are independent from the set that was used to generate these covariances. Given the high dimensionality of the covariance matrix, it is technically not feasible to include the actual values of this matrix in this paper. The matrix file is however readily available to interested parties. The background is coming from the same climatology used for building the covariance matrix, not from the NWP forecasts. Because the climatology we used is neither geographically nor time varying, the background fields are simply a mean value computed from a set of NOAA radiosondes in the case of the nonprecipitating parameters and from a number of MM5 runs for the precipitating parameters. These average background values are used everywhere, which means that the background field (to use data-assimilation terminology) is a constant field with only one value: the mean climatic value.

F. EOF Decomposition

The retrieval in MIRS is performed in EOF space through projections back and forth, at each iteration, between the original geophysical space and the reduced space. This method has been routinely used in operational centers as a standard transform approach of control variables [24]. It has also been used in the context of retrieval of trace gases, sounding, and surface properties [20], [33], [43], [49]. Applying it in the context of our 1D-VAR retrieval is therefore not very original except may be for its extension to cloud and precipitation profiles which is, to our knowledge, new. Only a limited number of eigenvectors/eigenvalues are kept in this reduced space. The selection of how many EOFs to use for each parameter is somehow subjective but depends on the number of channels available that are sensitive to that parameter. Other approaches exist such as in [36], which suggested an objective way of choosing which parameters will be included in the control parameters, using the ratio between the background covariance matrix and the *a posteriori* covariance (ratio of diagonal elements). This ratio, however, depends on the Jacobian which is only known at the end of the iterative process, unless the problem is purely linear (not the case when cloud and precipitation as well as the high-frequency channels are involved). Advantages of performing the retrieval in EOF space are the following: 1) handling the strong natural correlations that sometimes exist between parameters which usually create a potential for instability (or oscillation) in the retrieval process (small pivot), which is reduced significantly by performing the retrieval in an orthogonal space and 2) time saving by manipulating and inverting smaller matrices. The projection in EOF space is performed by diagonalizing the *a priori* covariance matrix

$$B \times L = L \times \Theta$$

where L is the eigenvector matrix, which is also called the transformation matrix, and Θ is the eigenvalue diagonal matrix which contains the independent pieces of information. The retrieval could therefore be performed using the original matrices B, ΔX, K_n as stated before (retrieval in original space), or, alternatively, it could be done using the matrices/vectors Θ, $\overline{\Delta X}$, $\overline{K_n}$ (retrieval in reduced space). The transformations back and forth between the two spaces are done using the transformation matrix L. It is important to note that, at this level, no errors are introduced in these transformations. It is merely a matrix manipulation. However, the advantage of using the EOF space is that the diagonalized covariance matrix and its corresponding transformation matrix could be truncated to keep only the most informative eigenvalues/eigenvectors. By doing so, we are bound to retrieve only the most significant features of the profile and leaving out the fine structures. How much truncation depends on how much information the channels contain. In the AMSU configuration, six EOFs are used for temperature, four for humidity and surface emissivity, one for skin temperature, one for nonprecipitating cloud, and two for both rain and frozen precipitation (a total of 20).

G. Convergence Criterion and Other Important Details

Several criteria have been reported for deciding on the convergence of variational methods, among which are the following: 1) testing that the increment of the parameter values at a given iteration is less than a certain threshold (usually, a fraction of the associated error of that particular parameter); or 2) testing that the cost-function $J(X)$ decrease is less than a preset threshold; or 3) checking that the obtained geophysical vector X at a given iteration produces radiances that fit the measurements within the noise level impacting the radiances. We have chosen the last criterion as it maximizes the radiance signal extraction. A convergence criterion based on $J(X)$, while mathematically correct, would produce an output that carries more ties to the background and, therefore, would be more inclined to present artifacts due to it. The convergence criterion adopted is when

$$\varphi^2 = \left\lfloor \left(Y^{\mathrm{m}} - Y(X)\right)^T \times E^{-1} \times \left(Y^{\mathrm{m}} - Y(X)\right) \right\rfloor \le N$$

where N is the number of channels used for the retrieval process. This mathematically means that the convergence is declared reached if the residuals between the measurements and the simulations at any given iteration are less or equal than one standard deviation of the noise that is assumed in the radiances.

Note that fitting the radiances within the noise level is necessary but not a sufficient condition. We should note here that the convergence criteria do not alter the balance of weights given to the radiances (or to the background) in the cost function that the 1D-VAR minimizes.

The evolution of the humidity profile is monitored for supersaturation in the iterative process. A maximum of 130% relative humidity is allowed. Currently, it is set in an *ad hoc* fashion at each step. This has the potential to steer nonlinearly the convergence from its mathematical path and should, in general, be avoided, but our experience has shown that this has not increased the divergence rate in a significant way.

H. Rationale for Precip-Clearing

By *precip-clearing*, we mean the inclusion of cloud and hydrometeor profiles in the retrieval state vector, not so much for the sake of their retrieval (whose accuracy is hindered by the significant null space as mentioned before) but to account for all their effects on the radiances, as well as to account for the effects of those related parameters that are not varied in the retrieval process and instead assumed constant inside the radiative transfer operator. This allows a more accurate retrieval of the other parameters, namely, the temperature and humidity profiles and the surface parameters. This is driven essentially by the limited number of channels available or, mathematically speaking, the limited number of EOFs affordable, which translates into a lack of sensitivity to fine vertical structures. The integrated values of the cloud and hydrometeor parameters (roughly represented by one or two EOFs) are however deemed accurate from simulation runs.

IV. Instrumental Configuration

In this paper, we will focus on the imaging/sounding channels of the NOAA-18 microwave sensors AMSU and MHS. This platform was launched on May 21, 2005. The main purpose of the microwave sensors is the atmospheric sounding of temperature and moisture, but other products are being produced routinely that include the rain rate, ice water path, land surface temperature and emissivity, cloud liquid amount, and total precipitable water [13], [21]. AMSU has two modules (A-1 and A-2) with channels operating at centimeter and millimeter wavelengths corresponding to frequencies ranging from 23.8 to 89 GHz and thirty scan positions per scanline. MHS on the other hand probes at millimetric frequencies between 89 and 183 GHz with a higher spatial resolution (90 scan positions per scanline). AMSU and MHS channels are unpolarized at nadir and mix-polarized off-nadir. Both sensors have a cross-track swath, scanning angles between nadir and 48.33°, corresponding to zenith angles reaching 58°.

V. Assessment of the Performances in Simulation

This section deals with the simulation results aimed at assessing the performances of the retrieval system in clear and cloudy/rainy conditions. This assessment is hard to do using the real data due to the lack of certainty about the true measure of the geophysical state. Because the system is applied in all conditions, we want first to assess its performances in the clear-sky conditions. We, then, want to know what is the advantage (if any) of using a multiple-scattering model rather than a pure absorption model. These questions will be answered in the following two subsections for an individual profile. The AMSU/MHS configuration is used. The radiances are first simulated using the forward model described in Section III-D, then the retrieval is applied after randomly impacting the radiances by a Gaussian noise whose standard deviation corresponds to the advertised NedT of the respective channels. These values were found to be consistent with those computed from the real data using the methodology of Mo [32]. In both cases, the simulated radiances were performed with a nadir-looking configuration. The background data used for these simulated retrievals are the same as used previously in Section III-E.

A. Assessment in Nonprecipitating Conditions

Fig. 1 shows the evolution of the retrieved parameters during the iterative process for a single profile where neither cloud nor precipitation was included. It shows that the retrieved parameters are all reaching the true value within three iterations. The convergence metric is plotted in the top panel, showing that the measurements were fitted within the noise level. The first guess for the cloud and hydrometeors was chosen to be nonzero, and the values reached in the final iteration were all zero, as expected. This gives us confidence that the system will produce cloud-free retrievals when applied to the truly clear-sky cases. Even if this is shown for one particular profile only, it was tested under other configurations, and similar results were obtained (not shown here).

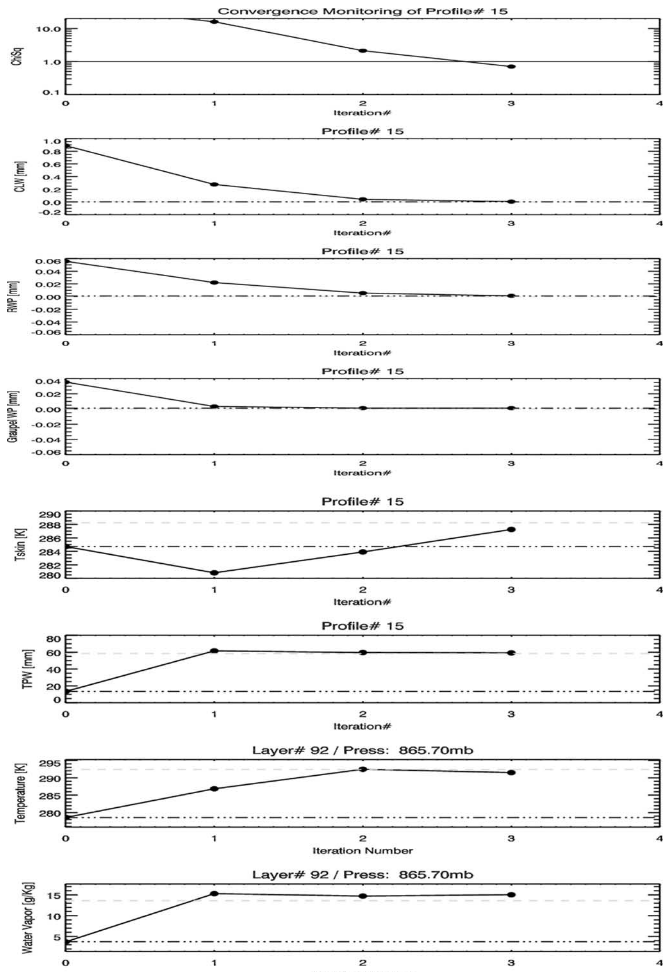

Fig. 1. Evolution of a sample of the retrieved state vector during the iterative process for an individual profile. The parameters monitored are (from top to bottom) the convergence metric, the vertically integrated cloud amount, the rain water path, the graupel-size ice amount, the skin temperature, the total precipitable water, the atmospheric temperature in layer corresponding to a pressure of 865 mbar, and, finally, the water-vapor mixing ratio in the same layer. The solid line is the retrieved quantity, the dashed line represents the truth, and the dotted-dashed line corresponds to the first guess and background values.

B. Assessment in Precipitating Conditions

Figs. 2 and 3 show the retrieval of one cloudy and rainy profile from an MM5 output run using two approaches. The radiances have been fully impacted by the extinction (absorption and scattering) effect of cloud, rain, and ice droplets during the forward simulation. The first approach (Fig. 2) consisted

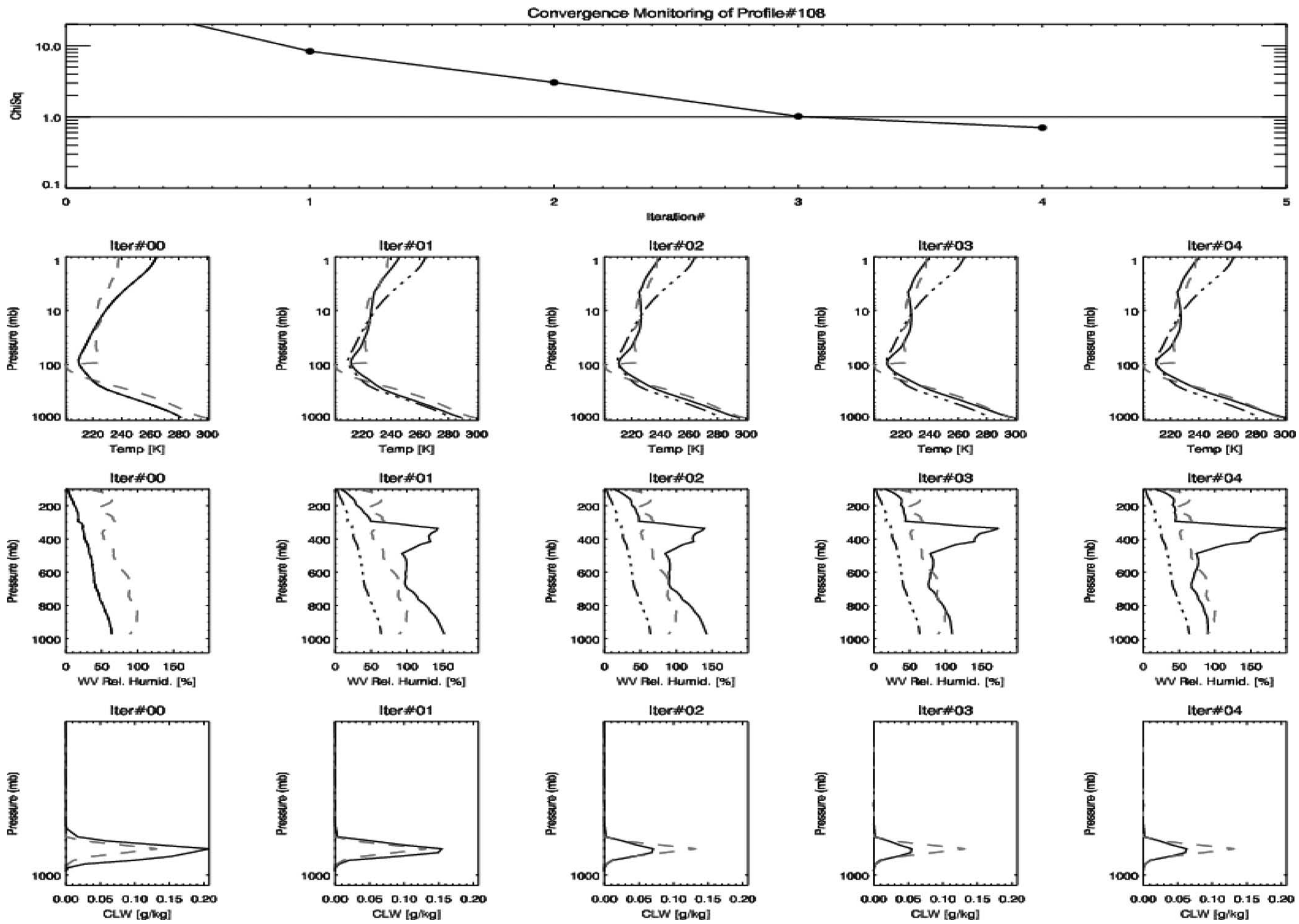

Fig. 2. Evolution, iteration-by-iteration of (from top to bottom) convergence metric, vertical profiles of temperature, moisture, and cloud amount. This is a cloudy/rainy sky (dashed lines represent true values), and the retrieval (represented by solid lines) was made assuming a purely absorbing RTM (multiple scattering turned off). Dotted-dashed lines represent the first guess and background.

of assuming that only absorption is happening; therefore, only temperature, moisture, and nonprecipitating cloud amount are retrieved, and the multiple scattering is turned off in the forward operator of the 1D-VAR. The major effect this has on the retrieval is the significant amount of supersaturation that the water vapor is experiencing to compensate for the effect of scattering, up to 200% relative humidity. This phenomenon is consistent with the previous studies that actually took advantage of this feature to estimate the amount of ice in the profile by looking at the water-vapor profile [19]. Note that this particular profile has perfectly converged within four iterations. The same radiances are inverted in Fig. 3, but, this time, by turning the scattering on, the rain and the graupel-size ice are both retrieved simultaneously with temperature, moisture, and cloud liquid amount. We notice that the water-vapor supersaturation is much reduced. There is a sort of *precip-clearing* of the radiances that allows a better retrieval of the moisture profile. The temperature profile is not much altered. The apparent discontinuity in the original temperature profile is because it is a combination of an MM5-produced profile up to 100 mbar (so that temperature, cloud, and hydrometeors are consistent) and climatology above that level. Despite the nonphysical transition of the original temperature profile at 100 mbar, which is simulated in the radiances, the retrieval is able to accommodate to a certain extent, given the shape of the background that constrains its departures. This is an example of how the variational technique is balancing *a priori* information and radiance-provided information. We also notice the degree of nullspace; the hydrometeors are not reaching the true values, and yet, the retrieval has converged within three iterations. This demonstrates that with the degrees of freedom at hand, one needs more independent radiances to constrain the problem. As a reminder, our primary goal here is to sound temperature and moisture in the cloudy/precipitating conditions, not so much the sounding of hydrometeors themselves. The integrated amounts, however, are expected to be reasonably accurate.

VI. Validation Using GPS-Dropsondes

Microwave imaging and sounding data from the NOAA-18 satellite were used to validate the retrieval system described previously in both clear cases as well as under extreme weather conditions, in the eye and within the eyewall of hurricane Dennis in the summer of 2005. This was done by comparing the retrievals of temperature and humidity profiles to the measurements made by GPS-dropsondes. Before the retrieval is performed, the brightness temperatures of the two sensors are collocated and corrected of any bias when compared to

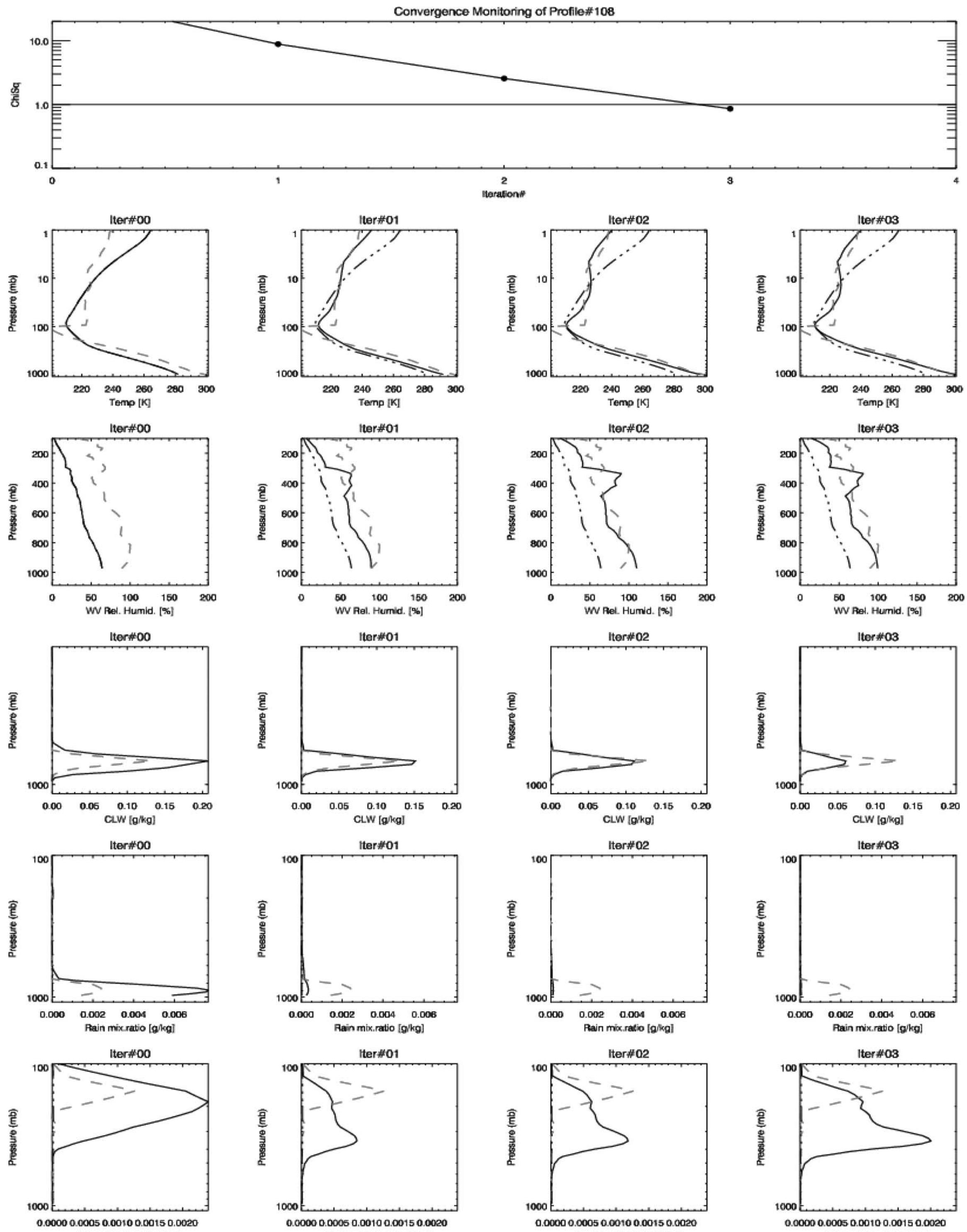

Fig. 3. Same as Fig. 2, except that the vertical profiles of rain and graupel-size ice are added. This is a cloudy/rainy sky (dashed lines represent true values), and the retrieval (represented by solid lines) was made with the full RTM where multiple-scattering effects are accounted for. The supersaturation of water vapor is much reduced compared to Fig. 2. The apparent discontinuity in the original temperature profiles is caused by their combination of the MM5-produced profiles up to 100 mbar and climatology above that level.

the forward-model simulations. The collocation is done in two different ways: 1) An averaging is performed of 3×3 MHS footprints to fit the AMSU spatial coverage (low resolution) or 2) assume the AMSU footprint valid within all the subpixel MHS footprints (high resolution). In this latter case, the subpixel heterogeneity is computed from the MHS footprints and translated into the AMSU channels but only for those that are sensitive to the same geophysical parameters, namely, channels 23.8, 31.4, 50.3, and 89 GHz. The bias removal is performed by simulating the brightness temperatures over ocean using the NCEP Global Data Assimilation System (GDAS) analyses as inputs. These biases were found to be scan dependent.

The instrumental/modeling error covariance matrix E is also built partly during this process by using the variances of the same comparisons. These variances are subjectively scaled down to account for the uncertainties in the GDAS inputs and collocation errors. The diagonal elements (in standard deviation, in Kelvin) of the modeling error matrix E for the AMSU+MHS channels (from #1 to #20) are the following: 1.9, 1.7, 1.2, 0.6, 0.3, 0.2, 0.3, 0.4, 0.4, 0.3, 0.8, 0.0, 0.0, 0.0, 2.1, 2.2, 1.4, 1.6, 1.3, and 1.1. Channels 12, 13, and 14 peak above the maximum altitude reported by GDAS, so the comparison to GDAS simulation is not terribly meaningful, therefore, the variances for these channels were deemed unreliable, and the channels were disabled. These modeling errors are used on top of the instrumental errors (NEDT values) which are computed exclusively from the raw AMSU/MHS Level-1B data, which are available from NOAA using the approach of [32]. For window channels, modeling errors are dominant over instrumental errors. These values are slightly lower than those found in the previous studies [9], [36]. They allow, however, a stable convergence in most cases. Note that these modeling errors are computed over ocean in the clear-sky conditions. The same values are used over the cloudy/rainy conditions.

A. Dropsondes Data

It is critical that one gets a clear sense of how accurate the so-considered truth measurements are before interpreting any differences between them and the retrievals. In our case, measurements are made in the cloudy/rainy conditions (typically, during hurricanes and tropical storms) by high-velocity descending GPS-dropsondes. They were obtained from the Hurricane Research Division (HRD), Miami, FL, where they were quality-controlled using the Hurricane Analysis and Processing System. They operate at altitudes up to 24 km with a descent time of about 12 min. The measurements are made every half second which allows a high vertical resolution. Along with the temperature and moisture, the vertical wind-speed profile is also measured by using the GPS-based Doppler signal, which is down to 4–10 m above the surface. The validation of these dropsondes was assessed by a comparison with standard radiosondes, radars, buoys as well as by a human visualization of clouds for the saturation check. For a full description of these measurements, see [16]. In their study, the inherent accuracy of the temperature measurement was assessed to be 0.2 °C, but a lag error correction exceeding 1 °C was applied for layers above 500 mbar. The humidity accuracy was assessed to be less than 5%, but up to 15% dry bias correction was sometimes applied (S. Feuer, personal communication, 2006). As for the wind, an accuracy of 0.5–2 m/s was estimated.

B. Limitations of the Validation in Extreme Weather Events

Traditional approach in validating the retrievals by statistical comparison with ground-truth data collected around the measurement's time/space location is not optimal in the case of hurricane conditions. The main reason is the fast-moving features involved. A category 2 storm, for instance, has an average forward speed of 30 mi/h (or 48 km/h), therefore, even

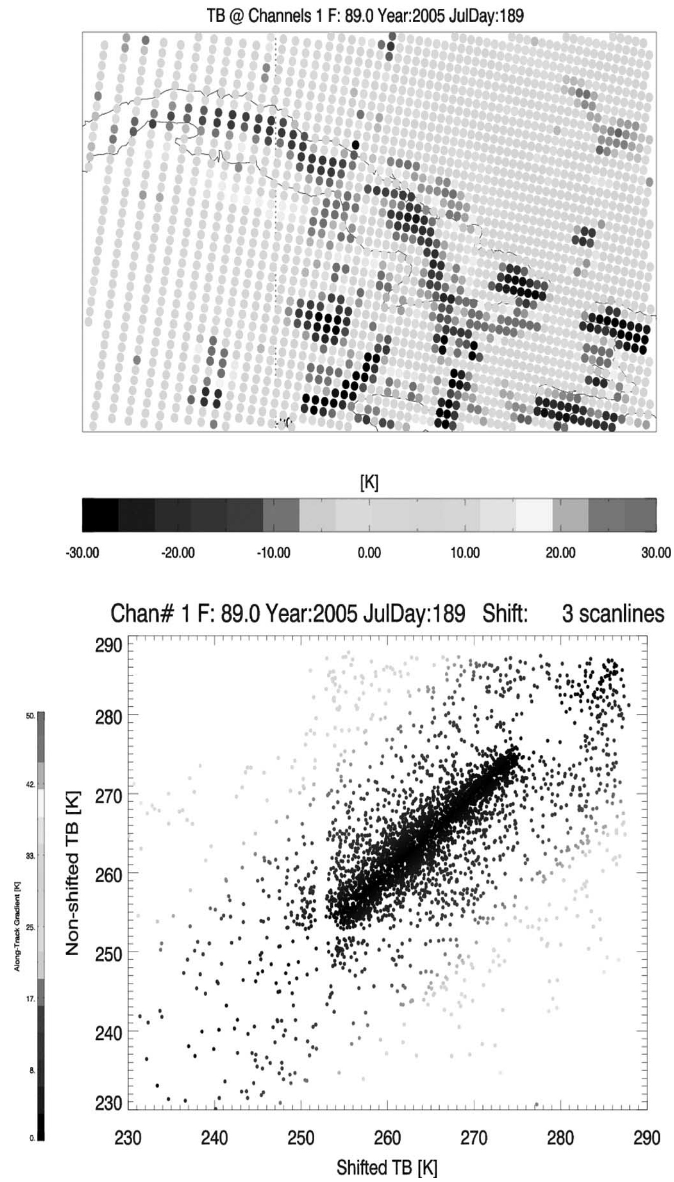

Fig. 4. Impact of shifting the field of brightness temperature by three scanlines (here 89-GHz channel) that is measured during July 2005 hurricane Dennis to simulate the effect of collocation errors in time and space. The map represents the difference of the two fields (shifted and nonshifted). In the scatterplot, the colors are modulated by the heterogeneity of the original TBs field. The darker the dot is, the smoother is the area around the measurement. Areas where the field is very heterogeneous, (green-red dots on lower panel), have differences exceeding 30 K.

if the storm features are all the same, a displacement caused by a collocation criterion of 2 h would cause a 90-km shift (~6 scanlines of MHS). For illustration, Fig. 4 shows the effect of a modest shift of three scanlines on a field of brightness temperatures, assuming the geometry of the depicted storm did not change between the shifted and the nonshifted fields. The differences between the shifted and nonshifted fields reach very high values that could make the comparison meaningless.

In reality, it is even worse: storm intensifies, fades down, hydrometeor structures change, particles form/fall, the shift is multidirectional, etc. Collocation errors are therefore expected to be dominant in very active areas. Very strict criteria must therefore be used for the validation of hydrometeor retrieval

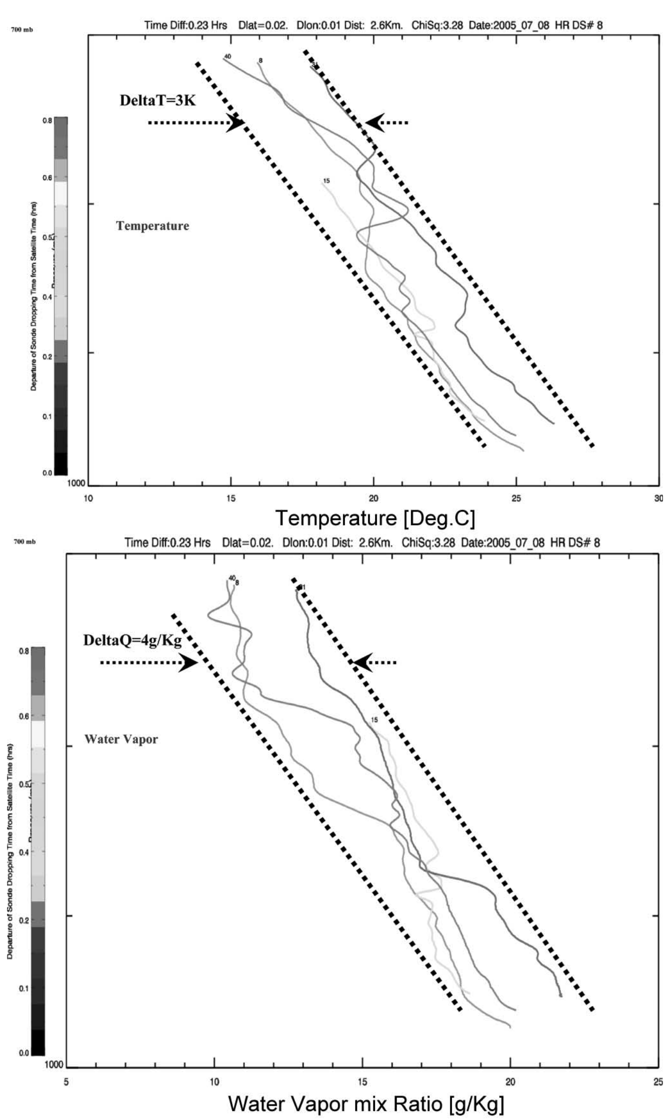

Fig. 5. Intravariability of dropsonde measurements in terms of temperature and moisture profiles, which are made within an average of 10 min from each other and within a radius of 10 km. Note that the descent time is roughly 12 min.

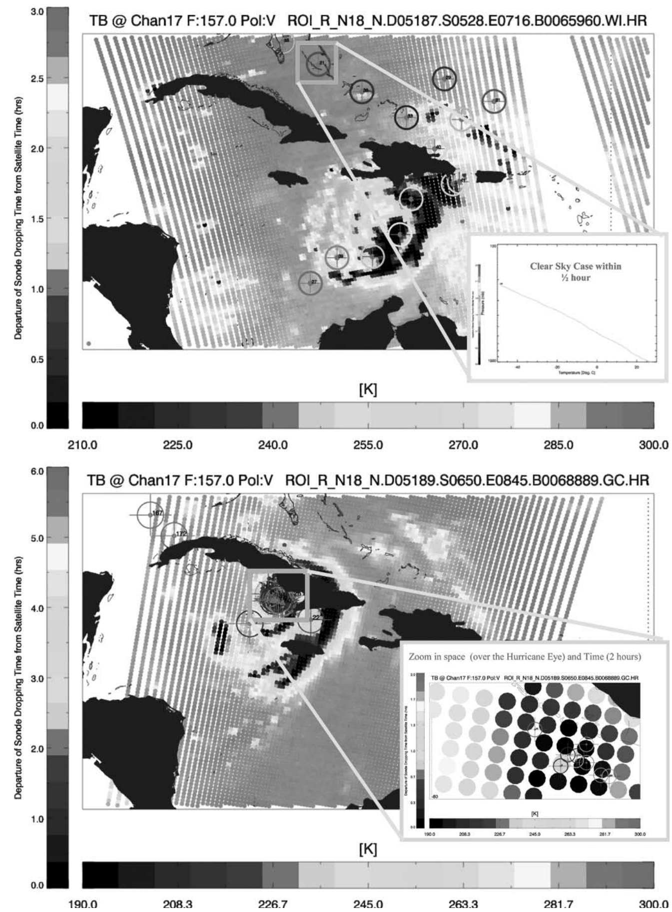

Fig. 6. Field of 157-GHz brightness temperatures taken during hurricane Dennis on (top) July 6, 2005 and (bottom) July 8, 2005. Overlaid are the circles centered around the location where the GPS-dropwindsonde was launched from the aircraft. The horizontal color bar refers to the brightness-temperature value. The vertical color bar represents the difference between the satellite-measurement time and the sonde launch time. Collocations highlighted in the upper and lower panels will serve as the validation in clear and precipitating conditions, respectively.

given their highly changing nature. Additionally, atmospheric temperature in the rain and cloud might be different from the air temperature. Sinkevich and Lawson [41] performed an assessment of the accuracy of temperature measurements in convective clouds and reported that temperature-excess amount between in-cloud and out-of-cloud areas depends on the stage of the life of the cloud and varied between 0.2 °C and up to 8 °C over ocean. Over land, an even greater temperature excess was noticed. For all these reasons, there is a need to have an almost perfect collocation in these active conditions, in order for the comparison to be meaningful. Stringent time and space criteria must therefore be used, which obviously dramatically reduces the total number of coincident collocations. This, in turn, renders the empirical assessment statistically meaningless at best or practically unfeasible at worst. Note that the tight time and space collocation must be between coincident satellite measurements, hurricane events, and ground truth such as dropsondes.

Fig. 5 shows the measurements of four dropsondes that were launched within the core of the hurricane (within and around the eye) with an average of 10-min interval and within 10 km distance. Differences in temperature up to 4 K and in moisture mixing ratio of up to 4 g/kg are noticed. These differences are inherent to collocation–coregistration. Although this is an almost perfect collocation between the dropsondes themselves (no retrieval involved), because the hurricane active features are moving fast, even a few minute interval and a few kilometer distance can make the sensor (in this case, the ground measurement) see a different signal. The descent time is by itself a limiting factor. By the time the dropsonde descends, it might be sampling the different parts of vertical profiles that are significantly different. The verticality of the retrieved and the ground-measured profiles is also an issue and adds to the overall uncertainty. The dropsonde presents the potential of drifting, while the retrieved profile's verticality depends on the viewing angle of the measurements where it was extracted from. If these latter are nadir viewing, then the retrieved profile is vertical. If, however, the channels are off-nadir viewing, then the retrieved profiles are slant. This clearly puts an upper limit to the expectations that one can have when comparing the retrievals with

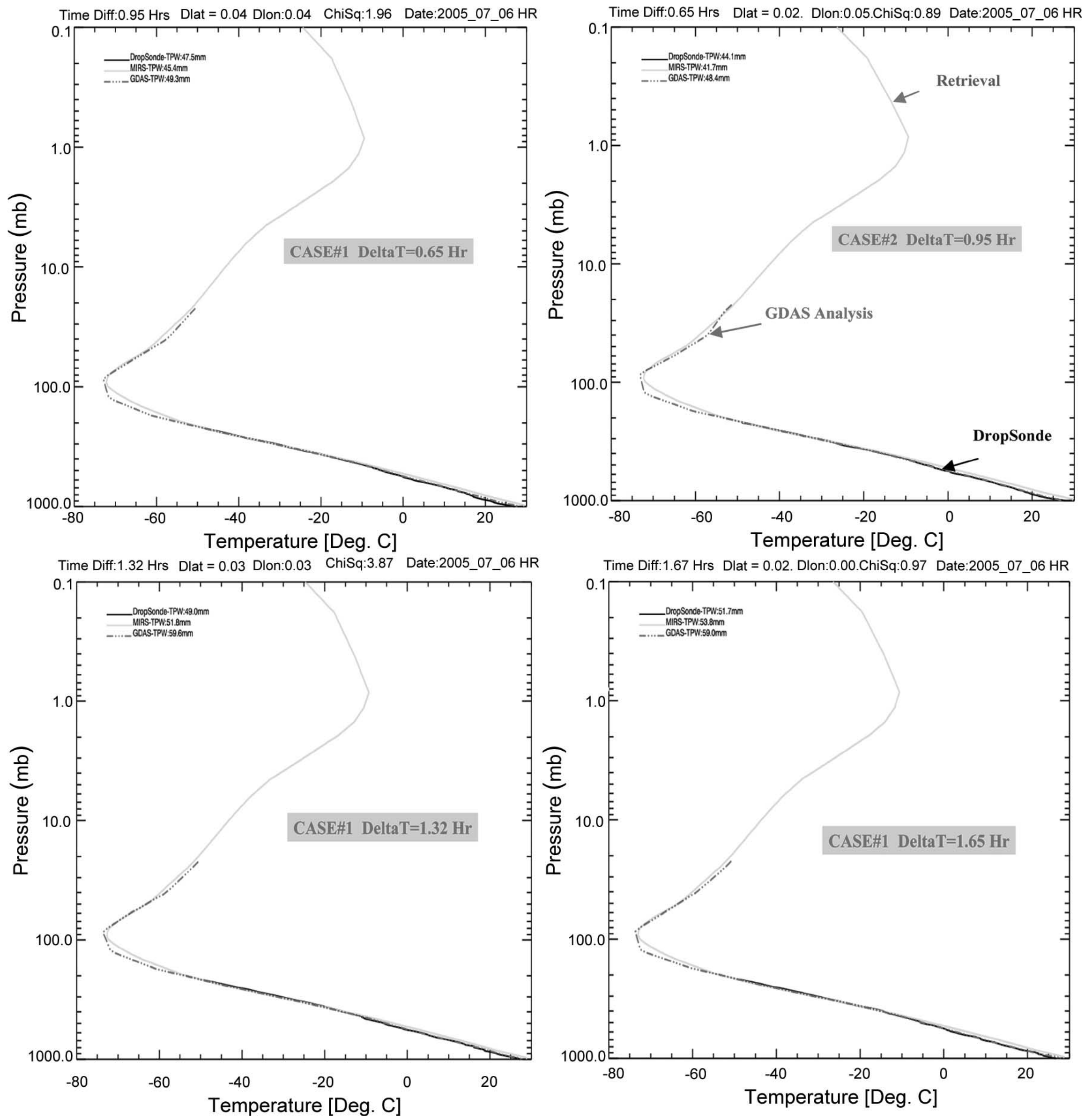

Fig. 7. Individual comparisons between dropsondes, MIRS retrievals, and GDAS. Note that all three have different pressure grids and different cloud tops. The four dropsondes represented have different time differences. The collocations are outside the inner core of the hurricane, as shown in Fig. 6 (upper panel).

the dropsonde measurements. Another type of limitation that one should be aware of is what other studies called representativeness error which relates to the fact that dropsonde measurements are point measurement and do not necessarily represent what the sensor is measuring within the field of view. This latter is around 15 km for MHS, at nadir, but more than 45 km wide at certain off-nadir viewing positions. Unfortunately, the number of dropsondes collocated with satellite measurements is limited, and therefore, the luxury of averaging within the footprint to mitigate the representativeness errors (or around the time of the measurement) cannot be afforded.

C. Case-by-Case Validation

Given the limitations discussed previously, and for the purpose of the validation, it was critical to find the as-perfect–as-possible collocation between the satellite measurements and the GPS-dropsondes. We focused on the hurricane Dennis which occurred on July 2005. Fig. 6 shows two days of that hurricane timeframe, July 6 and 8. The field of 157-GHz MHS brightness temperature is shown because of its sensitivity to cloud, rain, and ice. The dropsonde launch location is also highlighted by circles. The color of those circles indicates how far (red) or how close (dark) in time they are from when the closest satellite measurement was taken. The upper panel contains a number of decent dropsonde/satellite collocations (in space and time) that appear free of any impact of rain or ice (seems to be the same signal as the surface background). These will serve for the validation of our retrievals in a clear-sky condition. The lower panel on the other hand presents some interesting cases of dropsondes in the eye and within the eyewall of the hurricane (see close-up figure) that are very close in time to the satellite measurements. These will serve for the validation of the retrievals in the extreme conditions.

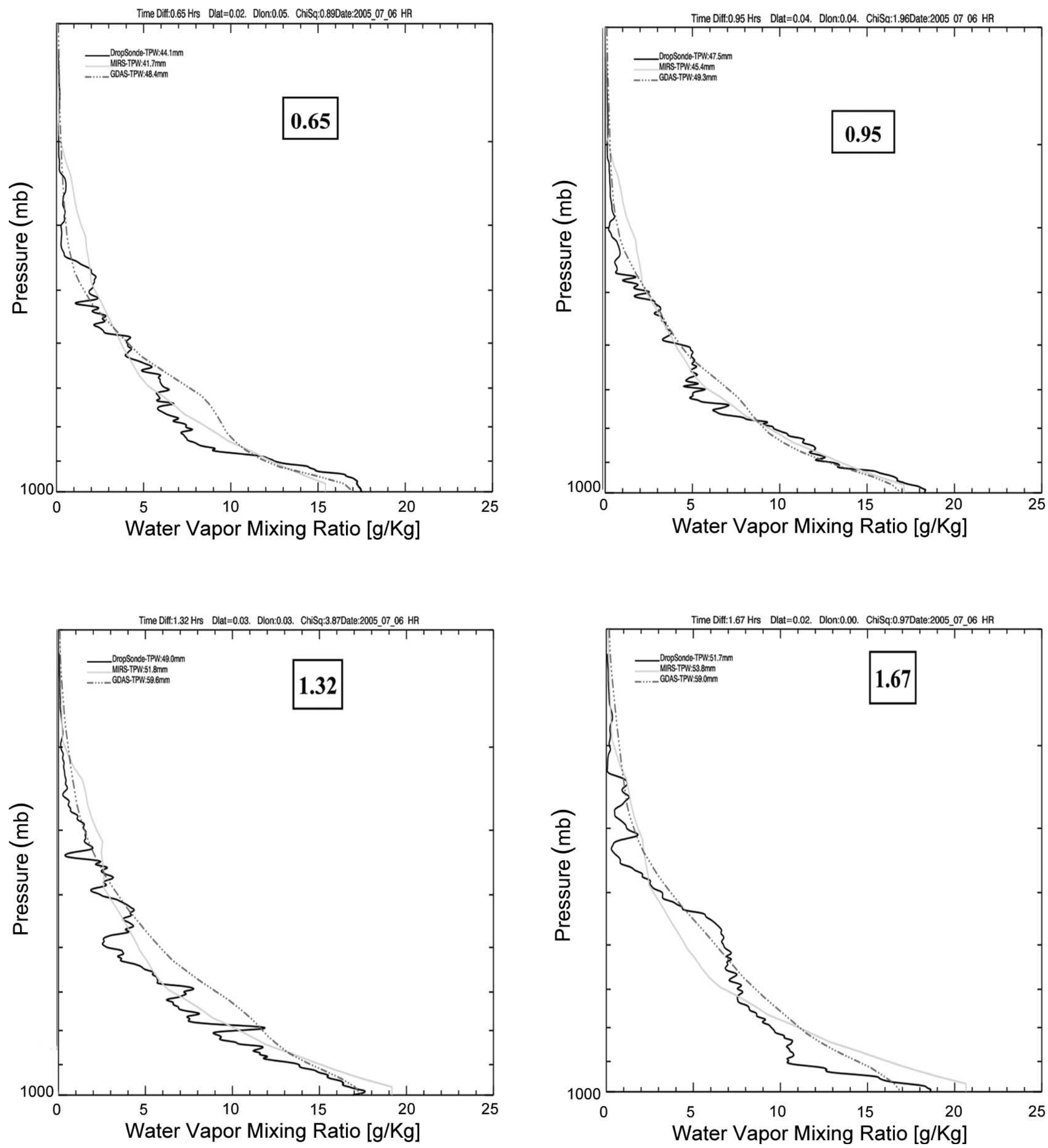

Fig. 8. Same as the previous figure, except that the water-vapor retrievals are represented. Retrievals were performed at the higher spatial resolution (MHS). Differences are higher when the retrieval is done at the lower resolution (not shown). No NWP external data were used for these retrievals.

D. Clear-Sky Conditions

Figs. 7 and 8 show four individual dropsondes that were identified above as clear sky along with the MIRS retrievals and the GDAS analysis (included for reference). They correspond to temperature and water vapor, respectively. The time difference is highlighted in the different panels. For temperature, errors are typically less than 1 K with a maximum of 3 K in the low altitudes. Note that the retrieval goes up to 0.1 mbar, while the dropsonde for this particular aircraft goes only to 200 mbar and GDAS to 20 mbar. The relatively large differences in the lower altitude might signal that the brightness temperatures for the low-peaking and window channels have some local residual bias that is hard to remove using the global approach we used. The water-vapor comparisons show a rather good agreement between the dropsonde measurements and the retrievals, except for the fine structures that the dropsonde is able to report while the retrieval is not detecting. This is not surprising given the vertically broad weighting functions of the 183-GHz channels and the horizontal size of the radiometric pixel which covers a much wider area than that of the point measurements. The latter are sensitive to subpixel horizontal variability. It is interesting also to note that, as one might expect, differences between the retrieval and dropsonde measurements tend to increase with larger time differences (displayed in the squares inside the plots). These retrievals were performed using the high-resolution footprint matching described earlier. Tests were done to see the impact of performing the retrievals in low resolution and were found higher due to the larger representativeness error. Note that in a relative sense, the differences are within the 10%–30% margin in the vertical region between the surface and 500 mbar.

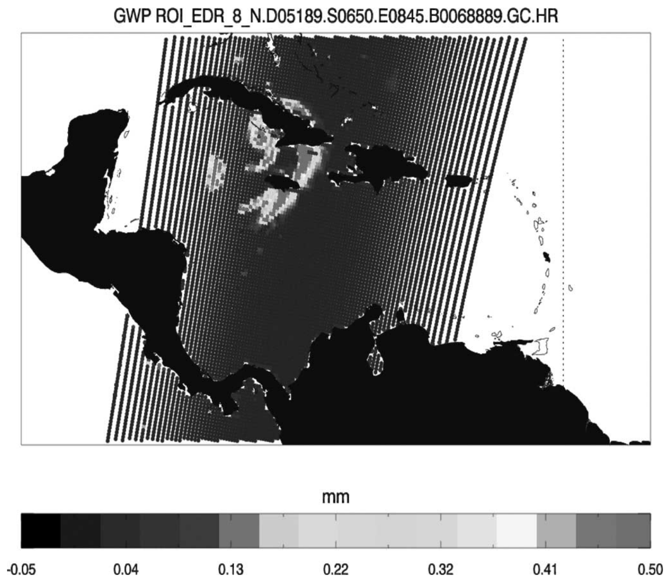

Fig. 9. Retrieval of graupel-size ice content using MIRS. Note that the output of MIRS is an actual profile. The figure above represents the vertical integration (which is performed in the postprocessing stage). Hurricane Dennis 2005 passing through the Cuba Island. Retrievals are done at MHS resolution (roughly 20 km).

E. Hurricane Conditions

Fig. 9 shows the vertically integrated graupel-size ice amount [Graupel-size ice water path (GWP)] computed from the retrieved profile. This is shown as a qualitative validation. Although the retrieval is done in profile form, the resulting integrated value displays physically plausible features and values. The retrieval corresponds to the same Dennis hurricane on July 8, 2005 (same descending orbit shown before). First, where no activity is present (from the 157-GHz brightness temperatures (TBs), the retrieval is reporting no ice or rain, even if the first guess used is actually a nonzero profile (the same used everywhere). This confirms the conclusion reached in a simulation setting (see Section V) that the system is able to produce zero amounts when the signal in the TBs indicates so, even when starting from the nonzero first guesses. Second, the large values of GWP are concentrated in the middle of the active area and decreasing gradually at the edges. One can even see that, in what seems to be the eye of the hurricane, the value of the integrated ice amount is actually very small compared to the surrounding pixels.

Figs. 10 and 11 show the comparison of MIRS retrievals to a few selected sondes that were dropped within the eye and eyewall of the hurricane. The ones closest in time and space were selected (highlighted in Fig. 6, bottom). GDAS is also represented for reference. These figures correspond to temperature and moisture, respectively. Both time difference and distance between the space-based measurement and the dropsonde are shown on the plots. Note that the vertical extent goes to 700 mbar only for this particular aircraft that dropped the sondes. GDAS and MIRS are still reporting retrievals up to 20 and 0.1 mbar. It is found that these comparisons show a rather good agreement between MIRS and the dropsondes, at least for temperature. The differences are indeed well within the intravariability of the sonde measurements themselves described previously. On top of the intravariability and the representativeness issues reported before, the vertical descent of the sonde seems to tend to drift horizontally more drastically within very active regions (see the blue curves on the figures). In contrast, the descent is almost vertical in clear-sky cases. Therefore, although the reported distance at launch location is reported to be 2.6 km for the first sonde for instance, we can see that when reaching the surface, the distance became around 10 km. Again, in fast-moving features like hurricanes, this factor could make a significant difference. For the closest collocation (less than 12 min and less than 3 km in distance), the difference in water vapor is actually also within the previously reported intravariability. When time and distance differences are larger, the moisture differences are larger. But, the errors of representativeness and the vertical drift of the sonde could at least, in part, explain the remaining differences. It is worth mentioning that NCEP GDAS does ingest the dropsonde measurements themselves within its assimilation cycle but not the rain-impacted AMSU/MHS radiances. It is interesting to notice in this case that GDAS analyses are exhibiting similar differences with the dropsondes than the MIRS retrieval does, although this latter is based solely on microwave radiances measured from AMSU and MHS.

VII. Conclusion

We have used cloud- and rain-impacted brightness temperatures in a variational retrieval, using NOAA-18 AMSU and MHS sensors. This was made possible owing to the CRTM forward model, which produces both radiances in all-weather conditions and the corresponding Jacobi for all parameters, including the cloud and hydrometeor parameters. The CRTM is incorporated into a microwave-dedicated retrieval system at NOAA/NESDIS, which is called the MIRS. The MIRS methodology described here is based on treating, in a consistent fashion, all parameters that do impact the measurements. It is also independent from the NWP-related information. The ill-posed nature of the inversion is handled through the use of the eigenvalue decomposition technique which makes the inversion very stable, and a high convergence rate is obtained. It was shown, in an ideal simulation case, that the null space is a limiting factor. This translates into cases where the retrieval process reaches a solution that satisfies the measurements, but that is different from the original in terms of hydrometeor and cloud profiles. Because of this and the limited information content of the radiances, the aim of this retrieval was essentially to target the temperature and moisture profiles as well as the surface parameters in very active regions. The hydrometeor vertical amount profiles help account for the effects they and the other parameters not accounted for explicitly, produce on the measurements (*precip-clearing*). Improvement in the cloud and hydrometeor profiling is however expected, if temperature and moisture profiles are provided externally from accurate NWP forecasts for instance. Designing the retrieval of cloud and hydrometeors in profile form presents a number of advantages, including the avoidance to account explicitly for the cloud top pressure and the cloud thickness, which could, in certain cases, cause instability or oscillation. The

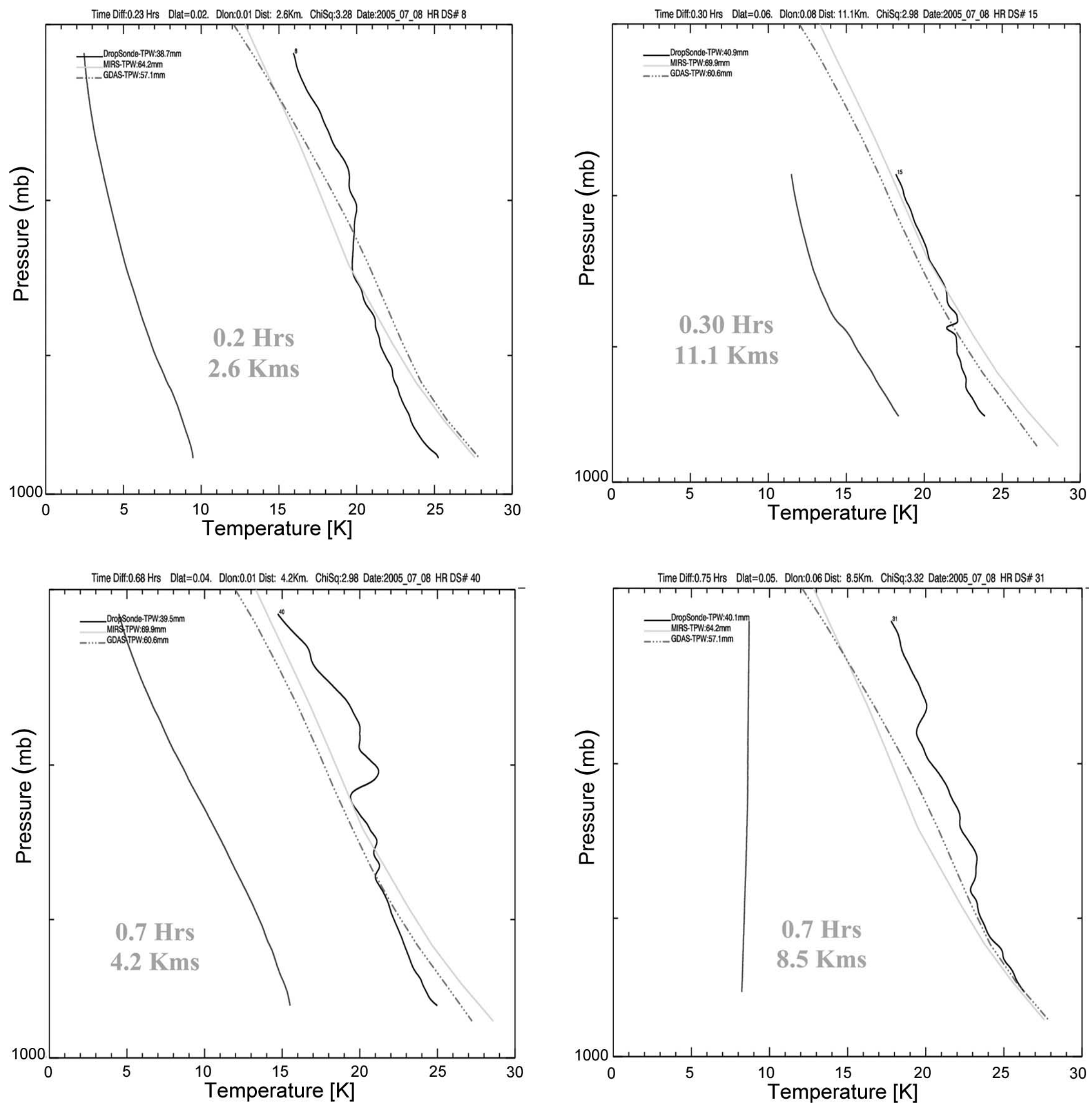

Fig. 10. Case-by-case comparison of temperature profile between 700 mbar and the surface, between (green line) MIRS retrievals, (red line) GDAS analyses, and (black line with fine vertical structures) GPS-dropsonde measurements. The blue line on the left represents the profile of the dropsonde distance drift with respect to the location of the closest satellite measurement. The collocations are within the inner core of the hurricane, as shown in Fig. 6 (lower panel).

designed system could also, in theory, give information about the multilayer nature of the clouds and mixture of phases within the cloud/precipitating layers, provided that enough information in the radiances exists. The retrieval system is used in clear, cloudy, and precipitating conditions. It was shown in simulation and confirmed with the real data that the performances, when applied to clear skies, are not degraded and that the retrieval algorithm is able to reach a zero-amount solution for all the cloud and hydrometeor parameters if the radiances indicate so.

A validation was undertaken in both clear and extremely active conditions by a controlled comparison to measurements by the aircraft GPS-dropsondes, which are taken in the vicinity of hurricane Dennis. We first showed that extreme care must be exercised when attempting validation in these weather events, as very contrasted atmospheric features are moving fast, and therefore, any collocation error in space and/or time could have enormous impact on the comparison between the retrievals and the ground-truth data. The collocation error, which is coupled with the inherent descent time of the dropsondes, thus sampling different parts of separate vertical profiles, would, in fact, be the dominant source of error. This led us to use very strict collocation criteria which, in turn, advocated doing the validation by individual comparisons rather than by computing statistical metrics. Another obvious major source of error is the representativeness error. If the same sensor is looking at different pieces of the atmosphere and this latter is very contrasted with moisture, rain, cloud, falling frozen precipitation, etc., the measurements could be very different. These differences are not due to any retrieval or calibration issues, but simply to inherent to 4-D variations of the atmosphere within the timeframe of the measurements and within the area sampled by these point measurements. Intravariability of the dropsondes themselves was assessed using four individual sondes dropped within

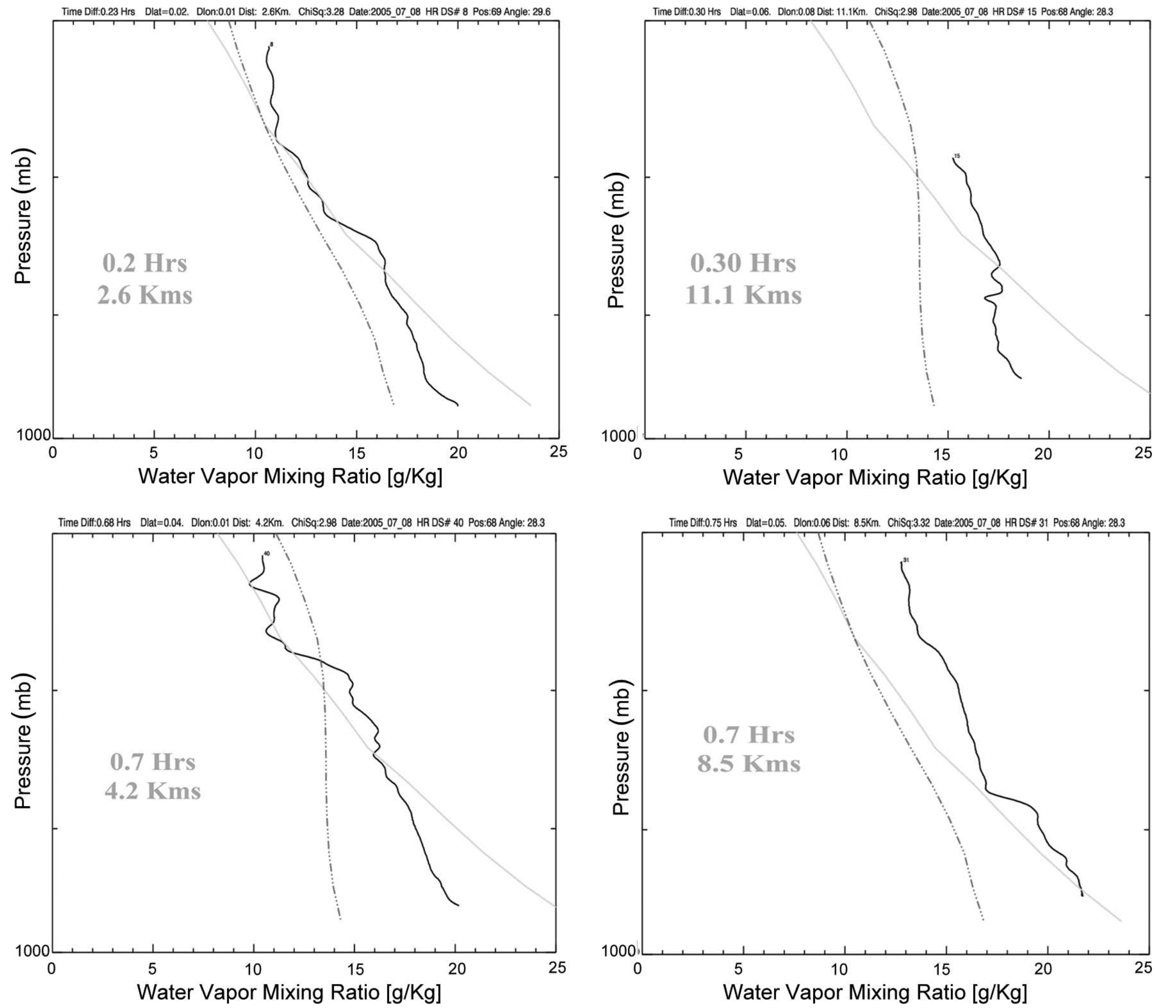

Fig. 11. Same as Fig. 10 except for the water-vapor profile.

10 min and a few kilometers from each other, which gave us an estimate of the lower limit of the differences that we must expect when validating the results.

We also hinted to the importance of the spatial resolution of the measurements which plays a key role in these active areas. To stabilize the sensor gain, the microwave radiometric measurements need to be averaged within an integration time period to reduce the noise level (NedT). This has the effect of reducing the horizontal spatial resolution. It is however acknowledged that this instrument noise is actually buried under other sources of errors such as the modeling error. It is therefore preferable from an assimilation or retrieval stand to have at least, in remote sensing of highly contrasted events (such as hurricanes and coastal boundaries), a higher horizontal spatial resolution with a higher noise rather than a lower spatial resolution with a reduced noise.

For the comparison between the MIRS retrieval and the dropsondes, we focused on two days of hurricane Dennis, corresponding to July 6 and 8, 2005. Results in the clear sky showed that the differences in temperature and water vapor were minimal. The finer vertical structures measured with the dropsondes are, for obvious reasons, not expected to be picked by the retrieval given the broad weighting functions of the sounders. The performances in the eye and the eye wall of the hurricane were shown to be largely within the intravariability of the reference measurements. These performances were comparable to those of GDAS analyses that ingested the dropsondes themselves. The MIRS-retrieved temperature and moisture profiles and the emissivity parameters, in active areas, are expected to produce positive impacts in the subsequent 4DVAR assimilations, the object of a future study. We, indeed, envision that our 1D-VAR, which considers the hydrometeor parameters as part of the retrieved vector instead of hooking it with a cloud model, could be ported into an assimilation system and used in the first part of a 1D-VAR+4DVAR assimilation process.

ACKNOWLEDGMENT

The authors would like to thank S. Feuer and M. L. Black from the HRD of the NOAA Atlantic Oceanographic and Meteorological Laboratory for kindly providing the dropsondes data. The authors would also like to thank the JCSDA CRTM team (Q. Liu, Y. Han, and P. Van Delst) for providing an early version of the radiative transfer model CRTM, and T. Zhu from NOAA/NESDIS for providing the MM5 runs for hurricane Bonnie.

REFERENCES

[1] E. Andersson *et al.*, "Assimilation and modeling of the atmospheric hydrological cycle in the ECMWF forecasting system," *Bull. Amer. Meteorol. Soc.*, vol. 86, no. 3, pp. 387–402, Mar. 2005.

[2] N. L. Baker, T. F. Hogan, W. F. Campbell, R. L. Pauley, and S. D. Swadley, "The impact of AMSU-A radiance assimilation in the U.S. Navy's operational global atmospheric prediction system (NOGAPS)," Naval Research Lab., Washington, DC, NRL/MR/7530–05-8836, 2005.

[3] P. Bauer, E. Moreau, and S. Di Michele, "Hydrometeor retrieval accuracy using microwave window and sounding channel observations," *J. Appl. Meteorol.*, vol. 44, no. 7, pp. 1016–1032, Jul. 2005.

[4] P. Bauer, E. Moreau, F. Chevallier, and U. O'Keeffe, "Multiple-scattering microwave radiative transfer for data assimilation applications," *Q. J. R. Meteorol. Soc.*, vol. 131, no. 617, pp. 1–999, Apr. 2005.

[5] P. Bauer, P. Lopez, A. Benedetti, D. Salmond, and E. Moreau, "Implementation of 1D + 4D-VAR assimilation of microwave radiances in precipitation at ECMWF, Part I: 1D-VAR," *Q. J. R. Soc. Meteorol.*, 2006. submitted for publication.

[6] R. Bennartz and G. W. Petty, "The sensitivity of microwave remote sensing observations of precipitation to ice particle size distributions," *Q. J. R. Meteorol. Soc.*, vol. 40, no. 3, pp. 245–364, Mar. 2001.

[7] F. Chevallier, P. Bauer, J.-F. Mahfouf, and J. J. Morcrette, "Variational retrieval of cloud profile from ATOVS observations," *Q. J. R. Meteorol. Soc.*, vol. 128, no. 585, pp. 2511–2525, 2002.

[8] G. Deblonde and S. English, "One-dimensional variational retrievals from SSMI/S-simulated observations," *J. Appl. Meteorol.*, vol. 42, no. 10, pp. 1406–1420, 2003.

[9] G. Deblonde, J.-F. Mahfouf, B. Bilodeau, and D. Anselmo, "One-dimensional variational data assimilation of SSM/I observations in rainy atmospheres at MSC," *Mon. Weather Rev.*, vol. 135, no. 1, pp. 152–172, Jan. 2007.

[10] R. M. Errico, L. Fillion, D. Nychka, and Z.-Q. Lu, "Some statistical considerations associated with the data assimilation of precipitation observations," *Q. J. R. Meteorol. Soc.*, vol. 126, no. 562, pp. 339–359, 2000.

[11] K. F. Evans, J. Turk, T. Wong, and G. Stephens, "A Bayesian approach to microwave precipitation profile retrieval," *J. Appl. Meteorol.*, vol. 34, no. 1, pp. 260–279, Jan. 1995.

[12] J. R. Eyre, "Inversion of cloudy satellite sounding radiances by nonlinear optimal estimation. I: Theory and simulation for TOVS," *Q. J. R. Meteorol. Soc.*, vol. 115, no. 489, pp. 1001–1026, Jul. 1989.

[13] R. R. Ferraro, F. Weng, N. C. Grody, L. Zhao, H. Meng, C. Kongoli, P. Pellegrino, S. Qiu, and C. Dean, "NOAA operational hydrological products derived from the Advanced Microwave Sounding Unit," *IEEE Trans. Geosci. Remote Sens.*, vol. 43, no. 5, pp. 1036–1049, May 2005.

[14] L. Fillion and R. Errico, "Variational assimilation of precipitation data using moist convective parameterization schemes: A 1D-VAR study," *Mon. Weather Rev.*, vol. 125, no. 11, pp. 2917–2942, Nov. 1997.

[15] N. C. Grody, "Satellite-based microwave retrievals of temperature and thermal winds: Effects of channel selection and *a priori* mean on retrieval accuracy," in *Remote Sensing of Atmospheres and Oceans*, A. Deepak, Ed. New York: Academic, 1980, pp. 381–410.

[16] T. F. Hock and L. Franklin, "The NCAR GPS dropwindsonde," *Bull. Amer. Meteorol. Soc.*, vol. 80, no. 3, pp. 407–420, Mar. 1999.

[17] C. Kummerow, Y. Hong, W. S. Olson, S. Yang, R. F. Adler, J. McCollum, R. Ferraro, G. Petty, D.-B. Shin, and T. T. Wilheit, "The evolution of the Goddard profiling algorithm (GPROF) for rainfall estimation from passive microwave sensors," *J. Appl. Meteorol.*, vol. 40, no. 11, pp. 1801–1820, Nov. 2001.

[18] J. Li, W. Wolf, W. P. Menzel, W. Zhang, H.-L. Hiang, and T. Achtor, "Global sounding of the atmosphere from ATOVS measurements: The algorithm and validation," *J. Appl. Meteorol.*, vol. 39, no. 8, pp. 1248–1268, Aug. 2000.

[19] C. E. Lietzke, C. Deser, and T. H. Vonder Haar, "Evolutionary structure of the Eastern Pacific double ITCZ based on satellite moisture profile retrievals," *J. Clim.*, vol. 14, no. 5, pp. 743–751, Mar. 2001.

[20] Q. Liu and F. Weng, "Retrieval of sea surface wind vectors from simulated satellite microwave polarimetric measurements," *Radio Sci.*, vol. 38, no. 4, pp. 8078–8085, Jul. 2003.

[21] Q. Liu and F. Weng, "One-dimensional variational retrieval algorithm of temperature, water vapor and cloud water profiles from the Advanced Microwave Sounding Unit (AMSU)," *IEEE Trans. Geosci. Remote Sens.*, vol. 43, no. 5, pp. 1087–1095, May 2005.

[22] Q. Liu and F. Weng, "Advanced doubling-adding method for radiative transfer in planetary atmospheres," *J. Atmos. Sci.*, vol. 63, no. 12, pp. 3459–3465, 2006.

[23] P. Lopez, "Conception et validation d'une parametrisation explicite des hydrometeors de grande-echelle, Evaluation de son potential dans les calculs adjoints," Ph.D. dissertation, Univ. Paul Sabatier, Toulouse, France, 2001.

[24] A. C. Lorenc, "Development of an operational variational assimilation scheme," *J. Meteorol. Soc. Jpn.*, vol. 75, no. 1B, pp. 339–346, 1995.

[25] J.-F. Mahfouf, P. Bauer, and V. Marecal, "The assimilation of SSM/I and TMI rainfall rates in the ECMWF 4D-VAR system," *Q. J. R. Meteorol. Soc.*, vol. 131, no. 606, pp. 437–458, Jan. 2005.

[26] V. Marecal and J.-F. Mahfouf, "Variational retrieval of temperature and humidity profiles from TRMM precipitation data," *Mon. Weather Rev.*, vol. 128, no. 11, pp. 3853–3866, Nov. 2000.

[27] V. Marecal and J.-F. Mahfouf, "Four dimensional variational assimilation of total column water vapor in rainy areas," *Mon. Weather Rev.*, vol. 130, no. 1, pp. 43–58, Jan. 2002.

[28] F. S. Marzano, S. Di Michele, A. Tassa, and A. Mugnai, "Bayesian techniques for precipitation profiles retrieval from spaceborne microwave radiometers," in *Proc. PORSEC*, Dec. 2000, pp. 221–228.

[29] L. M. McMillin, L. J. Crone, and T. J. Kleespies, "Atmospheric transmittance of an absorbing gas. 5. Improvements to the OPTRAN approach," *Appl. Opt.*, vol. 34, no. 36, pp. 8396–8399, Dec. 1995.

[30] A. P. McNally, J. C. Derber, W.-S. Wu, and B. B. Katz, "The use of TOVS level-1B radiances in the NCEP SSI analysis system," *Q. J. R. Meteorol. Soc.*, vol. 126, no. 563, pp. 689–724, Jan. 2000.

[31] S. Di Michele, A. Tassa, F. S. Marzano, P. Bauer, and J. P. V. P. Baptista, "Bayesian algorithm for microwave-based precipitation retrieval: Description and application to TMI measurements over ocean," *IEEE Trans. Geosci. Remote Sens.*, vol. 43, no. 4, pp. 778–791, Apr. 2005.

[32] T. Mo, "Calibration of the Advanced Microwave Sounding Unit-A radiometers for NOAA-N and NOAA-N," U.S. Dept. Commerce, Washington, DC, NOAA Tech. Rep. NESDIS 106, 2002.

[33] J.-L. Moncet, S. A. Boukabara, A. Lipton, J. Galantowicz, H. Rieu-Isaacs, J. Hegarty, X. Liu, R. Lynch, and N. Snell, "Algorithm theoretical basis document (ATBD) for the Conical-Scanning Microwave Imager/Sounder (CMIS) environmental data records," in *Core Physical Inversion Module*, vol. 2. Lexington, MA: AER Inc., Mar. 2001. Version 1.4.

[34] E. Moreau, P. Lopez, P. Bauer, A. Tompkins, M. Janiskova, and F. Chevallier, "Variational retrieval of temperature and humidity profiles using rain rates versus microwave brightness temperatures," *Q. J. R. Meteorol. Soc.*, vol. 130, no. 589, pp. 827–852, 2004.

[35] E. Moreau, P. Bauer, and F. Chevallier, "Variational retrieval of rain profiles from spaceborne passive microwave radiance observations," *J. Geophys. Res.*, vol. 108, no. D16, 4521, 2003. DOI: 10.1029/2002JD003315.

[36] L. Phalippou, "Variational retrieval of humidity profile, wind speed and cloud liquid-water path with the SSM/I: Potential for numerical weather prediction," *Q. J. R. Meteorol. Soc.*, vol. 122, no. 530, pp. 327–355, Jan. 1996.

[37] C. Prigent, A. Sand, C. Klapisz, and Y. Lemaitre, "Physical retrieval of liquid water contents in a North Atlantic cyclone using SSM/I data," *Q. J. R. Meteorol. Soc.*, vol. 120, no. 519, pp. 1179–1207, Jul. 1994.

[38] C. Prigent, L. Phalippou, and S. English, "Variational inversion of the SSM/I observations during the ASTEX campaign," *J. Appl. Meteorol.*, vol. 36, no. 5, pp. 493–508, May 1994.

[39] C. D. Rodgers, "Retrieval of atmospheric temperature and composition from remote measurements of thermal radiation," *Rev. Geophys. Space Phys.*, vol. 14, no. 4, pp. 609–624, Nov. 1976.

[40] C. D. Rodgers, "Characterization and error analysis of profiles retrieved from remote sounding measurements," *J. Geophys. Res.*, vol. 95, no. D5, pp. 5587–5595, Apr. 1990.

[41] A. A. Sinkevich and R. P. Lawson, "A survey of temperature in convective clouds," *J. Appl. Meteorol.*, vol. 44, no. 7, pp. 1133–1145, Jul. 2005.

[42] E. A. Smith, X. Xiang, A. Mugnai, and G. Tripoli, "Design of an inversion-based precipitation profile retrieval algorithm using an explicit cloud model for initial guess microphysics," *Meteorol. Atmos. Phys.*, vol. 54, no. 1, pp. 53–78, Mar. 1994.

[43] W. L. Smith and H. M. Woolf, "The use of eigenvectors of statistical co-variance matrices for interpreting satellite sounding radiometer observations," *J. Atmos. Sci.*, vol. 33, no. 7, pp. 1127–1140, Jul. 1976.

[44] A. Tassa, S. Di Michele, and A. Mugnai, "Cloud model-based Bayesian technique for precipitation profile retrieval from the Tropical Rainfall Measuring Mission Microwave Imager," *Radio Sci.*, vol. 38, no. 4, 8074, Jun. 2003. DOI: 10.1029/2002RS002674.

[45] A. Tassa, S. Di Michele, A. Mugnai, F. S. Marzano, P. Bauer, and J. P. V. P. Baptista, "Modeling uncertainties for passive microwave precipitation retrieval: Evaluation of a case study," *IEEE Trans. Geosci. Remote Sens.*, vol. 44, no. 1, pp. 78–89, Jan. 2006.

[46] F. Weng and N. C. Grody, "Retrieval of cloud liquid water using the Special Sensor Microwave Imager (SSM/I)," *J. Geophys. Res.*, vol. 99, no. D12, pp. 2535–2551, Dec. 1994.

[47] F. Weng, Y. Han, P. Van Delst, Q. Liu, T. Kleespies, B. Yan, and J. Le Marshall, "JCSDA Community Radiative Transfer Model (CRTM)," in *Proc. 14th TOVS Conf.*, Beijing, China, 2005.

[48] F. J. Wentz and R. W. Spencer, "SSM/I rain retrievals within a unified all-weather ocean algorithm," *J. Atmos. Sci.*, vol. 55, no. 9, pp. 1613–1627, May 1998.

[49] D. Zhou, W. L. Smith, X. Liu, J. Li, A. M. Larar, and S. A. Mango, "Tropospheric CO observed with the NAST/I retrieval methodology, analyses and first results," *Appl. Opt.*, vol. 44, no. 15, pp. 3032–3044, 2005.

[50] H. Liebe, G. Hufford, and T. Manabe, "A model for the complex permittivity of water at frequencies below 1 THz," *Int. J. Infrared Millim. Waves*, vol. 12, pp. 659–675, 1991.

Sid-Ahmed Boukabara (SM'06) received the Ingénieur degree in electronics and signal processing from the National School of Civil Aviation, Toulouse, France, in 1994, the M.S. degree from the National Polytechnic Institute of Toulouse, Toulouse, in 1994, and the Ph.D. degree in remote sensing from the Denis Diderot University, Paris, France in 1997.

He is currently with the I.M. Systems Group, Inc., NOAA/NESDIS/STAR, Camp Springs, MD. His principal areas of interest are atmospheric and surface radiative transfers modeling, spectroscopy, and retrieval processes.

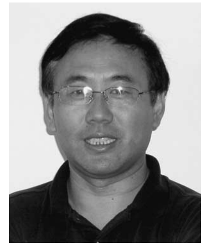

Fuzhong Weng received the Master's degree in radar meteorology from the Nanjing Institute of Meteorology, Nanjing, China, in 1985 and the Ph.D. degree from Colorado State University, Fort Collins, CO, in 1992.

He is currently with NOAA/NESDIS/STAR, Camp Springs, MD. He is a leading expert in developing various NOAA operational satellite microwave products and algorithms such as Special Sensor Microwave Imager and Advanced Microwave Sounding Unit cloud and precipitation algorithms, land surface temperature, and emissivity algorithms. He is developing new innovative techniques to advance uses of satellite measurements under cloudy and precipitation areas in numerical weather prediction models.

Quanhua Liu received the B.S. degree from the Nanjing Institute of Meteorology, Nanjing, China, in 1981, the Master's degree in physics from the Chinese Academy of Science, Beijing, China, in 1984, and the Ph.D. degree in marine science from the University of Kiel, Kiel, Germany, in 1991.

He is with the Joint Center for Satellite Data Assimilation. His primary interests are radiative transfer theory, retrieval methodology, and applications of the satellite data.

AUTHOR QUERIES

AUTHOR PLEASE ANSWER ALL QUERIES

AQ1 = Please specify the type of degree earned.
AQ2 = Please specify the type of degree earned.
AQ3 = Is this the current affiliation? Please provide location.

END OF ALL QUERIES